ANOVA STUDY OF CORROSION UNDER CONTROLLED CONDITONS OF HEAT TRANSFER

A Thesis

Submitted to the College of Engineering

of Nahrain University in Partial Fulfillment

of the Requirements for the Degree of

Master of Science

in

Chemical Engineering

by

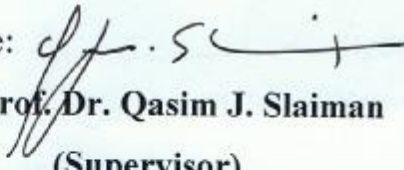**Lina Nael Saleem**

(B.Sc. in Chemical Engineering 2005)

Muharram	**1430**
January	**2009**

Certification

I certify that this thesis entitled **"ANOVA Study of Corrosion under Controlled Conditions of Heat Transfer"** was prepared by **"Lina Nael Saleem"** under my supervision at Nahrain University/College of Engineering in partial fulfillment of the requirements for the degree of Master of Science in Chemical Engineering.
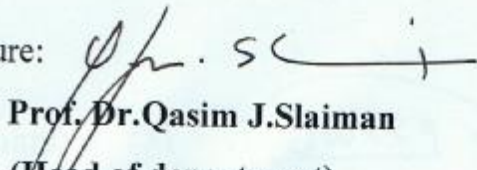
Signature:

Name: **Prof. Dr. Qasim J. Slaiman**

(**Supervisor**)

Date: 18 / 2 / 2009

Signature:

Name: **Prof. Dr. Qasim J.Slaiman**

(**Head of department**)

Date: 18 / 2 / 2009

Certificate

We certify, as an examining committee, that we have read this thesis entitled **"ANOVA Study of Corrosion under Controlled Conditions of Heat Transfer"** examined the student **" Lina Nael Saleem "** in its content and found it meets the standard of thesis for the degree of Master of Science in Chemical Engineering .

Signature:

Name:Prof.Dr.Qasim J. Slaiman
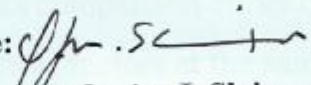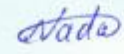
(Supervisor)

Date: 18 / 2 / 2009

Signature:

Name:Assi. Prof. Dr.Sami I. Al-Rubaiey

(Member)

Date: 15 / 02 / 2009

Signature:

Name: Dr.Sarmad T.Najim

(Member)

Date: 8 / 02 / 2009

Signature:

Name: Prof.Dr.Nada B.Nakkash

(Chairman)

Date: 18 / 2 / 2009

Approval of the College of Engineering

Signature: M. J. Jweeg

Name: Prof. Dr. Muhsin J. Jweeg

(Dean)

Date: 4 / 3 / 2009

Abstract

The aim of present work is to use the analysis of variance (ANOVA) to study the effects of several variables on the corrosion process at different conditions of different metals under isothermal and heat transfer conditions. A study was carried out to investigate the effect of hydrodynamic variables as well as temperature and heat flux on corrosion of copper and iron metals.

Two hydrodynamic geometries were investigated: cylinder in cross flow and rotating cylinder system under different ranges of temperature, Reynolds number and heat flux. The analysis of variance is used which involves comparison either of several different treatments or the influence of two or three factors at the same time.

The data obtained from different electrochemical techniques were analyzed to determine the influence of Reynolds number, temperature and heat flux on cathodic region. The responses considered are limiting current density, mass transfer coefficient, heat transfer coefficient, and interfacial (skin) temperature.

It was found that the limiting current density of carbon steel is influenced by flow more than temperature and therefore by a diffusion component of oxygen while the anodic limiting current density of copper is affected by temperature more than velocity under isothermal conditions. It is also shown that limiting current density of carbon steel and copper under heat transfer conditions is influenced by velocity followed by heat flux and then temperature to different extents at 0.01 and 0.05 significant levels.

The mass transfer coefficient is basically flow dependent, because it increases as the rotation rate or Re increases under isothermal conditions. Its value on copper in the anodic region is almost equally affected by hydrodynamics and temperature. It was found that mass transfer coefficients

under heat transfer conditions are also basically influenced by velocity more than other variables.

The heat transfer coefficients are influenced by bulk temperature followed by heat flux and then rpm or Re; it increases as temperature increases. The interfacial (skin) temperature is influenced basically by bulk temperature more than other variables, i.e., heat flux and velocity. These influences are dictated by ANOVA statistical analysis.

Under isothermal conditions, the thickness of hydrodynamic boundary layer decreases as Re or (rpm) increases at constant temperature, also it decreases with increasing temperature at constant Re or (rpm). Diffusion boundary layer decreases as Re or (rpm) increases at constant temperature. On the other hand it increases with increasing temperature at a given Re or (rpm). The ratio between hydrodynamic and diffusion boundary layers is not affected by Re or (rpm), but it decreased with increasing temperature. Under heat transfer conditions, hydrodynamic and thermal boundary layer decrease as temperature increases at constant Re or (rpm). Also they decrease with increasing Re or (rpm) at constant temperature. Diffusion boundary layer increases with increasing temperature at constant Re or (rpm) and it decreases with Re or (rpm) increasing at constant temperature. The ratio of thermal boundary layer to diffusion boundary layer is higher than one, which shows that thermal boundary layer is always greater than diffusion boundary layer.

As the diffusion boundary layer is appreciably smaller than the hydrodynamic boundary layer, this indicates a negligible convection within the diffusion layer. This means that in the major part of the hydrodynamic layer, motion of liquid completely levels concentration gradients and suppresses diffusion, but not perhaps within the thermal layer which may induce some convection in the diffusion layer and hence higher corrosion rates.

List of Contents

Chapter Three: Corrosion with Mass and Heat Transfer

Chapter Four: Results and Calculations

Chapter Five: Discussion

Chapter Six: Conclusions and Recommendations

Notations

Symbols

A_e Cross sectional area of an electrolyte.

c   Number of columns.

C_b Bulk concentration, $mole/m^3$.

C_i Concentration of species I , $mole/m^3$.

C_p Specific heat, $kJ/Kg.^oC$

C_s Surface concentration, $mole/m^3$.

d   Pipe diameter, m.

D   Diffusion coefficient ,m^2/s

D_o diffusivity of pure water , m^2/s

DF   Degree of Freedom

E, E_o Electrode potential, mV.

f   Friction factor.

F   Faradays constant (96500 Columb/equivelent).

g   Number of groups.

h   Heat transfer coefficient, $W/m^2.K$.

$i_{reaction}$ Anodic or cathodic current, A/m^2.

i_c Corrosion current density, A/m^2.

i_L Limiting current density, A/m^2.

i_o Exchange current density, A/m^2.

$J_i(y)$ Flux of species i ,$mol/m^2.s$

k_m Mass Transfer Coefficient, m/s.

k_T Thermal conductivity, $W/m.^oC$.

L_e Resistance path (i.e. separation distance between electrodes).

n   Number of participating electron.

N	Number of total observation.
Nu	Nusselt number.
Pr	Prandtl number.
Q	Heat transfer rate, Watt.
q	Heat flux, W/m^2.
r	Number of rows.
R	Gas constant.
Re	Reynolds number.
Sc	Scmhidt number.
Sh	Sherwood Number.
SS	Sum of squares.
T	Temperature, ^{o}C or K.
T_c	Total for each column.
T_r	Total for each row.
T_g	total for each group
T_{cr}	Total for each column –row combination.
T_{rg}	Total for each row –group interaction.
T_{cg}	Total for each column-group interaction.
T_i	Interfacial temperature, ^{o}C or K.
T_s	Surface temperature , ^{o}C or K.
T_r	Total for each row.
T_{crg}	Total for each column –row-group interaction.
X	Each observation.
$V(Y)$	Fluid velocity ,m/s
$\frac{\partial T}{\partial X}$	Temperature gradient.

$\dfrac{\partial \Theta(Y)}{\partial Y}$ Electrode potential gradient

$\dfrac{\partial Ci(Y)}{\partial Y}$ Concentration gradient.

Greek Symbols

δ_H	Hydrodynamic boundary layer thickness, m.
δ_D	Diffusion boundary layer thickness, m.
δ_t	Thermal boundary layer thickness, m.
μ	Viscosity, $Kg/m.sec^2$.
μ_s	Viscosity at surface temperature, $Kg/m.sec^2$.
ν	Kinematics viscosity , m^2/s.
η	Polarization overpotential, mV.
η_a	Activation overpotential, mV.
η_c	Concentration overpotential, mV
η_r	Resistance overpotential, mV.
η_T	Total overvoltage, mV.
$\eta_{reaction}$	$E_{applied} - E_{eq.}$
ρ	Density, kg/m^2.
$\beta_{reaction}$	Charge transfer barrier or symmetry coefficient for the anodic or cathodic reaction.
S	Conductivity of the electrolyte solution.

Abbreviations

ANOVA	Analysis of variance.
lim.	Limiting current density.
MANOVA	Multivariance analysis of variance.

MS	Mean Square.
MSR	Mean Square Ratio .
r.p.m	Revolution per minute.
r.d.s	Rate determine step.
RCE	Rotating cylinder electrode.
ppm	Part per million.

Subscripts

a	Activation polarization.
c	Concentration polarization.
Lim	Limiting current condition.
T	Total over voltage.
o	Exchange current density.

List of Tables

XVII

XVIII

List of Figures

Chapter One

Introduction

1.1 Introduction

Corrosion of metal is the degradation of materials by chemical or electrochemical reactions. It is most commonly seen on metals in the form of oxide films. However, similar processes also occur in non-metals, such as plastic, concrete and ceramics but the process is not corrosion [1].

Corrosion robs industry of million of dollars annually through loss or contamination of products, replacement cost and overdesign of equipment, reductions in efficiency and waste of valuable resources [2] .A recent survey on the costs of corrosion showed that the direct cost of corrosion was $276 billion in the United States for the year 2002, which is approximately 4% of their Gross National Product [3].

From an economical viewpoint, some of the corrosion damage cannot be completely avoided. However, many losses can be reduced. This can be accomplished through programs that promote public awareness and further development in mitigation technologies. Corrosion takes on two basic forms: uniform corrosion and localized corrosion. Uniform corrosion is characterized by corrosive attack that takes place evenly over the entire surface area or a large fraction of the total area of a metal surface. In contrast, localized corrosion has some selectivity, which often occurs in small areas or zones on a metal surface in contact with corrosive media. Some of the more common forms of localized corrosion are pitting corrosion, crevice corrosion, galvanic corrosion and erosion-corrosion [4].

Compared to uniform corrosion, localized corrosion is more problematic since it is very difficult to detect, predict and design against. This is because localized corrosion morphologies are typically small in size and the

locations of corrosion (e.g., pit or crevice) are often covered with corrosion products. In addition, localized corrosion is difficult to measure quantitatively by any instrument [4].

The analogy of mass transfer with heat transfer has led to successful methods regarding the mass transport interaction with fluid flow, since the behavior of heat is in many ways similar to mass transport depending as it does on a driving force, i.e., the temperature gradient may be regarded as analogous to concentration gradient. Most of the experimental studies showed that there is a relation exists between heat (or mass) transfer and skin friction. The determination of this relationship, both theoretically and experimentally, has been the concern of many investigators in the field of fluid flow, heat transfer and mass transfer. A thorough knowledge of relationship would allow prediction of rate of heat (or mass) transfer from friction loss data [5].

The study of controlled mass transfer electrochemical and corrosion process is of fundamental importance that allows the provision of the corrosion data for various metals in a process plant.However, many industrial chemical processes usually involve heat input or extraction from the chemical plant components such as power plant installations, refrigeration units and oil and gas recovery units. Here, the presence of heat transfer will play an important role in choosing the appropriate metals and assessing the plant life. Although the knowledge of the complicated problem of the interaction between mass, heat transfer and corrosion is fragmentary, the corrosion process in these units is likely to be under the influence of the combined action of the mass and heat transfer [6].

In many corrosion problems, there is strong evidence that the rate of uniform corrosion is controlled by the rate of mass transfer. This is true whether the corrosion fluid remains static or in fast motion with respect to the metal surface. However, molecular diffusion is not the only factor which

influences the rate of corrosion. In addition, in turbulent fluids, the rate of transport of eddy diffusion appears to participate in the control of the over-all transfer rate. It is only in situations where both anodic and cathodic processes are activation controlled that will be unaffected by the relative movement between surface and environment [5].

In equipments such as cooling towers and heat exchangers, a cold fluid is preferred for removing unusable heat from the process stream or reducing the temperature of the hot fluid. Hence, these equipments are usually subjected to different conditions of heat transfer .Metals; and especially tubes, due to their high cost are the most critical components of these units. They are usually chosen so that they have a high resistance to general corrosion to secure a high rate of heat transfer and gives better heat transfer characteristics [7].

Removing unwanted heat from heat transfer surface is carried out by using cooling fluid. Water is commonly used as cooling fluid in industry. Because water is one of the most common heat transfer fluids, it is not surprising that most of the problems associated with corrosion and deposits are water related [7].

Carbon Steel is the most commonly used as engineering material. It is cheap; available in wide range of standard form and sizes; can be easily worked and welded; and it has good mechanical properties like good tensile strength and ductility [5].

Copper alloys are widely used in many fields, especially for marine applications, such as seawater valves and heat exchangers. As a comparatively noble metal, copper has good resistance to corrosion in most cases. However, it still will undergo corrosion in such forms as pitting, crevice and stress corrosion cracking, and its alloys are subject to selective

leaching [8]. Among these types of corrosion, crevice corrosion is of particular interest to copper since valves are connected to piping systems with flanges and they contain numerous internal crevices.

1.2 The Aim of Present Work

The aim of this work is to analyze theoretically the relative influences of Reynolds number (or velocity), temperature, and heat flux on corrosion rate is used (copper and iron) metals under different conditions .Use the analysis of variance to show the effects and interactions between various variables and factors according to the world of heat and mass transfer and fluid flow.

Chapter Two
Corrosion

2.1 Introduction

Corrosion is the degradation of a metal by chemical or electrochemical reaction with its environment [9,10], or it is an interaction of a metal with its surroundings [11,12]. Corrosion in aqueous environment and atmospheric environment is an electrochemical process because corrosion involves the transfer of electrons between a metal surface and an aqueous electrolyte solution. It results from the overwhelming tendency of metals to react electrochemically with oxygen, water, and other substances in the aqueous environment [13].

Corrosion is a natural process, just like water flows to the lowest level, all natural processes tend toward the lowest possible energy states.Thus, for example, iron and steel have a natural tendency to combine with other chemical elements to return to their lowest energy states .In order to return to lowest energy states, iron and steel frequently combine with oxygen and water, both of which are present in most natural environments, to form hydrated iron oxides(rust).,similar in chemical composition to the origin of iron ore. Figure 2.1 illustrates the corrosion life cycle of a steel product [14].
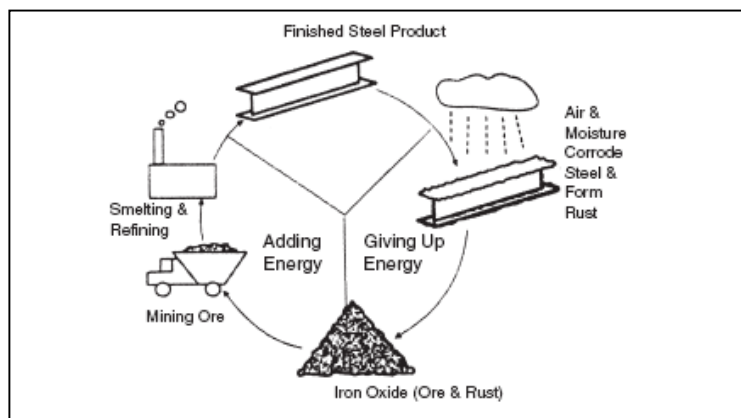
Fig. 2-1 The corrosion cycle of steel [14].

2.2 Importance of Corrosion

The importance of corrosion studies is threefold. The first area of significance is economic including the objective of reducing material losses resulting from the corrosion of piping, tanks, metal components of machines, ships, bridges, marine structures, and so on. The second area is improved safety of operating equipment which, through corrosion, may fail with catastrophic consequences. Examples are pressure vessels, boilers, metallic containers for toxic materials, turbine blades and rotors, bridges, airplane components, and automotive steering mechanisms. Third is conservation, applied primarily to metal resources, the world's supply of these is limited, and the wastage of them includes corresponding losses of energy and water reserves associated with the production and fabrication of metal structures[1].

2.3 Electrochemistry of Corrosion

The metallic surface exposed to an aqueous electrolyte usually possesses sites for an oxidation (an anodic chemical reaction) that produces electrons in the metal, and a reduction (or cathodic reaction) that consumes the electrons produced by the anodic reaction .These sites together make up a corrosion cell. The anodic reaction is the dissolution of a metal to form either soluble ionic products or an insoluble compound of the metal, usually an oxide. Several cathodic reactions are possible depending on what reducible species are present in the solution. Because these anodic and cathodic reactions occur simultaneously on a metal surface, they create an electrochemistry cell.

The sites where the anodic and cathodic reactions take place, the anodes and the cathodes of the corrosion cell, are determined by many factors: they

are not necessarily fixed in location, they can be adjacent or widely separated so that, for example, if two metals are in contact, one metal can be the anode and other the cathode leading to galvanic corrosion of the more anodic metal ,there can exist variations over the surface of oxygen concentration in the environment that results in the establishment of an anode at those sites exposed to the environment containing the lower oxygen content ,i.e., differential aeration or similarly , variations in the concentration of metal ions or other species in the environment, arising because of the spatial orientation of the corroding metal and gravity ,or finally variations in the homogeneity of the metal surface, due to the presence of inclusions leading to the establishment of anodic and cathodic sites.

The process occurring at the anodic sites is the dissolution of a metal as metallic ions in the electrolyte or the conversion of these ions to insoluble corrosion products such as rust [1].

2.4: Corrosion Reactions

2.4.1 Anodic Reactions of Corrosion

The anode is that portion of the metal surface that is corroded. It is the point at which metal dissolves, or goes into solution. When metal dissolves, the metal atom loses electrons and is oxidized.

Equation (2.1) represents the generalized anodic reaction that corresponds to the rate-determining step of atmospheric corrosion.

$$M \rightarrow M^{n+} + ne^{-} \qquad\qquad ….. (2.1)$$

The reaction for iron is:

$$Fe \rightarrow Fe^{+2} + 2e^{-} \qquad\qquad ….. (2.2)$$
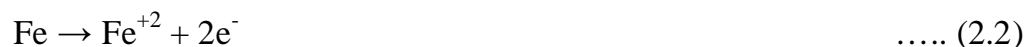
The iron ion goes into solution and two electrons are left behind in the metal. The formation of corrosion products, the solubility of corrosion

products in the surface electrolyte, and the formation of passive films affect the overall rate of the anodic metal dissolution process and cause deviations from simple rate equations [4].

2.3.2 Cathodic Reactions of Corrosion

In cathodic reduction of hydrogen ions and oxygen molecules, these species must be adsorbed on the metal surface in order to react .Thus the hydrogen ions and oxygen molecules must be transported from the bulk solution up to the metal/solution interface .The transport occurs by the process of diffusion and convection, and in the case of hydrogen ions electromigration.As the potential of the metal is made more negative in the Tafel region, the rate of reduction of hydrogen ions and oxygen molecules may increase to such an extent that it exceeds the rate at which these species can be transported to the metal surface. Then the rate of transport of the reducible species controls the rate of reduction. The cathodic current density attains a limiting value equivalent to the rate of transport and independent of potential .This is termed the limiting diffusion current density and its magnitude increased with increasing concentration of the reducible species and increasing movement of the solution [12].

The transport of oxygen from the atmosphere to the metal/solution interface involves the following steps [15]:

1. Transport of oxygen across the atmosphere /solution interface.
2. Transport through the solution (by diffusion and by natural and forced convection) to the diffusion layer.
3. Transport across the static solution at the metal /solution interface (the diffusion layer δ_D) by diffusion.
4. Proceeding chemical and electrochemical reactions.

All of previous steps are fairly rapid compared with step three which is the rate determining during the process.

The reaction occurs on this mechanism:

$$(O_2)_{aq} \iff (O_2)_{ads} \quad\quad\quad\quad .....(2.3)$$

$$2H_2O \iff 2H^+ + 2OH^- \quad\quad\quad\quad .....(2.4)$$

$$(O_2)_{ads} + H^+ + e \xrightarrow{\;\;r.d.s\;\;} (H_2O)_{ads} \quad\quad\quad\quad .....(2.5)$$

$$(HO_2)_{ads} + H^+ + e \iff (H_2O_2)_{ads} \quad\quad\quad\quad .....(2.6)$$

$$(H_2O_2) + 2e \iff 2OH^- \quad\quad\quad\quad .....(2.7)$$
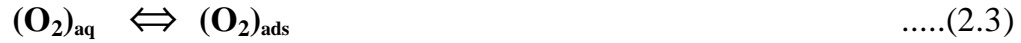
2.5 Corrosion of Iron and Steel

Stainless steels continue to be one of the most widely applied alloy systems for the chemical industry. Total tonnage in the United States has leveled off in recent years; world-wide consumption continues to increase. Stainless steel technology continues to be broad, complex, and ever-expanding. The majority of the developments are in applications of stainless steels in handling chemicals. Corrosion resistance continues to be the primary attribute of stainless steels and studies on the resistance of these alloys to specific environments are reported.

Stainless steels are economical materials of construction only if they can provide a useful and predictable service life. The factors which tend to produce unpredictability are constantly under study. Under certain conditions stainless steels may fail by selective attack. These forms of corrosion, usually sudden, are among the most important areas of investigation. Much effort is

also being expended to determine those services where an economical service life is possible even though general attack is being experienced. Such service information is vitally important to the chemical industry since it makes the task of proper selection of materials much simpler [16].

Bare iron and steel are liable to rust in most environments but the extent of the corrosion depends upon a number of factors, the most important of which are the composition and surface condition of the metal, the corrosive medium itself and the local conditions.

In pure dry air at normal temperatures a thin protective oxide film forms on the surface of polished mild steel. Unlike that formed on stainless steels it is not protective in the presence of electrolytes and usually breaks down in air, water and soil. The anodic reaction is:

$$Fe \rightarrow Fe^{2+} + 2e^{-} \qquad \text{E=0.44V} \qquad \qquad ..... (2.2)$$
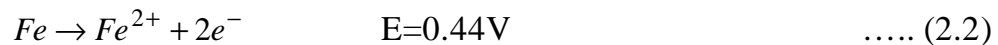
In de-aerated solutions, the cathodic reaction is

$$2H^{+} + 2e^{-} \rightarrow H_2 \qquad \text{E=0.0V} \qquad \qquad ..... (2.8)$$

This occurs fairly rapidly in acids but very slowly in alkaline and neutral solutions. In the presence of oxygen the following reaction occurs in slightly alkaline and neutral solutions:

$$O_2 + 2H_2O + 4e^{-} \rightarrow 4OH^{-} \qquad \text{E=0.401V} \qquad \qquad ..... (2.9)$$
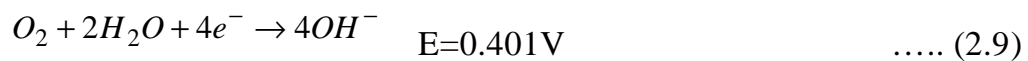
This is the common form of cathodic reaction in most environments. The OH^{-} ions react with Fe^{2+} ions to form ferrous hydroxide

$$Fe^{2+} + 2OH^{-} \rightarrow Fe(OH)_2 \qquad \qquad ..... (2.10)$$

This is oxidized to ferric hydroxide Fe (OH) $_3$, which is a simple form of rust. The final product is the familiar reddish brown rust Fe_2O_3, .H_2O [16].

2.6 Corrosion of Copper

The purest grade of copper commercially available, and that with the highest electrical conductivity, is oxygen-free high-conductivity copper .The minimum copper content required by some specifications is 99.99%, and the method of manufacture is such that no residual deoxidant is present.

Copper occurs in combined state in nature and is relatively easily obtained by the reduction of its compounds. It is not very active chemically and oxidizes only very slowly in air at ordinary temperatures.

In the electrochemical series of elements, copper is near the noble end and will not normally displace hydrogen, even from acid solutions. Indeed, if hydrogen is bubbled through a solution of copper salts, copper is slowly deposited (more rapidly if the process is carried out under pressure).

As copper is not an inherently reactive element, it is not surprising that the rate of corrosion, even if unhindered by films of insoluble corrosion products, is usually low. Nevertheless, although the breakdown of a protective oxide film on copper is not likely to lead to such rapid attack as with a more reactive metal such as, say, aluminum, in practice the good behavior of copper (and more particularly of some of its alloys) often depends to a considerable extent on the maintenance of a protective film of oxide or other insoluble corrosion product [16].

2.7 Polarization

Since the corrosion reactions involve the transfer of electrons and ions between the metal and the solution the rates are equivalent to electric currents. The rates of these reactions depend on the potential difference between the metal and the solution.As the potential of the metal becomes more positive than equilibrium potential , the rates of anodic reactions increase and the

rates of cathodic reactions decrease .The converse effect on the reaction rates occurs as the potential of the metal becomes more negative than equilibrium potential, as electrode is no longer at equilibrium when a net current flows to or from its surface .The measured potential of such an electrode is altered to an extent that depends on the magnitude of the external current and its direction [13] .The direction of potential changes always opposes the shift from equilibrium and hence opposes the flow of current, whether the current is impressed externally or is of galvanic origin. When current flows in a galvanic cell, for example, the anode always becomes more cathodic in potential and the cathode always becomes more anodic, the difference of potential becoming smaller .The extent of potential change caused by net current to or from an electrode, measured in volts, is called polarization. Polarization can be conveniently divided into three different types; activation, concentration and IR drop [1].

2.7.1 Activation Polarization

This is polarization caused by a slow electrode reaction. The general representation of the polarization of an electrode is given by the Bulter-Volmer [17] equation (2.11)

$$i_{reaction} = i_o \left[\exp\left(\frac{b_{reaction} nF}{RT} h_{reaction} \right) - \exp\left(-[1 - b_{reaction}] \frac{nF}{RT} h_{reaction} \right) \right] \qquad \dots . (2.11)$$

When η reaction is anodic (i.e., positive), the second term in the Bulter-Volmer equation becomes negligible and i_a can be more simply expressed by equation (2.12) and its logarithm, Equation (2.13)

$$i_a = i_o \left[\exp\left(b_a \frac{nF}{RT} h_a \right) \right] \qquad \dots . (2.12)$$

$$h_a = b_a \log_{10}\left(\frac{i_a}{i_o} \right) \qquad \dots . (2.13)$$

12

where b_a is the Tafel slope coefficient that can be obtained from the slope of a plot of η against log i ,with the intercept yielding a value for i_o

$$b_a = 2.303 \frac{RT}{bnF}$$ ..... (2.14)

Similarly, When η reaction is cathodic (i.e., negative), the first term in the Bulter-Volmer equation becomes negligible and i_c can be more simply expressed by equation (2.15) and its logarithm, equation (2.16), with b_c obtained by plotting η versus log i equation (2.17):

$$i_c = i_o \left[-\exp\left(-(1-b_c)\frac{nF}{RT}h_c \right) \right]$$ ...... (2.15)

$$h_c = b_c \log_{10}\left(\frac{i_c}{i_o} \right)$$ ...... (2.16)

$$b_c = -2.303 \frac{RT}{bnF}$$ ..... (2.17)

2.7.2 Concentration Polarization

Concentration polarization refers to electrochemical reactions that are controlled by the diffusion in the electrolyte [4].Concentration polarization changes are not a problem with the anodic reaction. However concentration polarization is a factor in determining the rate of cathodic reaction [10].

At very high reduction rates, the region adjacent to the electrode surface will become depleted of ions. If the reduction rate is increased further, a limiting rate will be reached which is determined by the diffusion rate of ions to the electrode surface. This limiting rate is the limiting diffusion current density i_L. It represents the maximum rate of reduction possible for a given system; the expressing of this parameter is

$$i_l = \frac{DnFC_b}{d_D}$$ ..... (2.18)

where i_L is the limiting diffusion current density, D is the diffusion coefficient of the reacting ions, C_b is the concentration of the reacting ions in the bulk solution, and δ_D is the thickness of the diffusion layer. The limiting current density is a function of diffusion coefficient, the concentration of the reacting ions in solution, and the thickness of the diffusion layer.

By combining the laws governing diffusion with Nernest equation:

$$E = E_o + 2.303\frac{RT}{nF}\log\frac{a_{oxid}}{a_{red}} \qquad\qquad \text{...... (2.19)}$$

the following expression can be developed :

$$E - E_0 = h_c = \frac{2.303RT}{nF}\log\left(1 - \frac{i}{i_l}\right) \qquad\qquad \text{..... (2.20)}$$

This equation is shown in Fig. 2.2
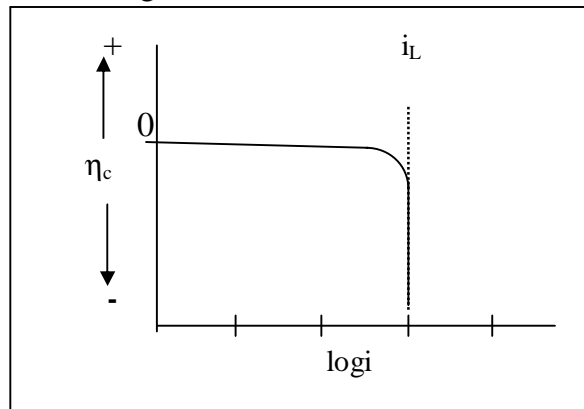
Fig. 2-2 Concentration polarization curve (reduction process) [4].

2.7.3 Combined Polarization

Both activation and concentration polarization usually occur at an electrode. At low reaction rates, activation polarization usually controls, whereas at higher reaction rates concentration polarization becomes controlling. The total polarization of an electrode is the sum of the contribution of activation polarization and concentration polarization [4]:

$$\eta_T = \eta_a + \eta_C \qquad \qquad \text{..... (2.21)}$$

where η_T is total overvoltage. During anodic dissolution, concentration polarization is not a factor and the equation of kinetics of anodic dissolution is given by:

$$h_{dissolution} = b \log \left(\frac{i}{i_o} \right) \qquad \qquad \text{..... (2.22)}$$

During reduction process such as hydrogen evolution or oxygen reduction, concentration polarization becomes important as the reduction rate approaches the limiting diffusion current density. The overpotential for reduction process is given by combining equation (2.16) and (2.20) with appropriate sings:

$$\eta_{red} = -b \log \left(\frac{i}{i_o} \right) + 2.303 \frac{RT}{nF} \log \left(1 - \frac{i}{i_L} \right) \qquad \qquad \text{..... (2.23)}$$

equation (2.13) is graphically illustrated in Fig. 2.3.

The importance of equation (2.22) and (2.23) cannot overemphasized since they are the basic equation of all electrochemical reaction equation (2.23) applies to any reduction reaction, and equation (2.22) applies to almost all anodic dissolution reactions. Exceptions to equation (2.22) are metals which demonstrate active-passive behavior. Using only three basic parameters namely, b , i_o, and i_L the kinetics of virtually every corrosion process can be precisely described [4].
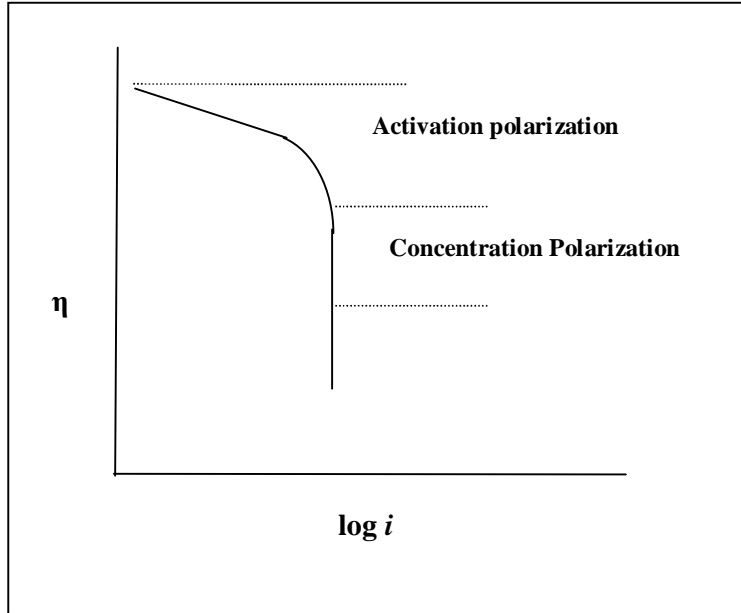
Fig. 2-**3** Combined Polarization [4].

2.7.4 Resistance Polarization

Polarization measurement includes a so–called ohmic potential drop through a portion of the electrolyte surrounding the electode, through a metal-reaction product film on the surface, or both. This contribution to polarization is equal to IR [15, 1]

$$R = \frac{L_e}{sA_e}$$
….. (2.24)

2.8 Nernest Boundary Layer

One of the first approaches to mass transfer in electrode processes was given by Nernest in 1904[18]. He assumed a stationary thin layer of solution in contact with electrode. Within this layer it was postulated that diffusion alone controlled the transfer of substances to the electrode. Outside the layer, diffusion was negligible and concentration of electro-active material was maintained at the value of bulk concentration by convection. This

16

hypothetical layer has become known as "Nernst diffusion layer (δ_D)". Fig. (2.4) gives a schematic diagram of this layer. Nernst assumed that the concentration varied linearly with distance through layer. The thickness of this layer is given by:

$$d_D = \frac{D}{k_m}$$

..... (2.25)
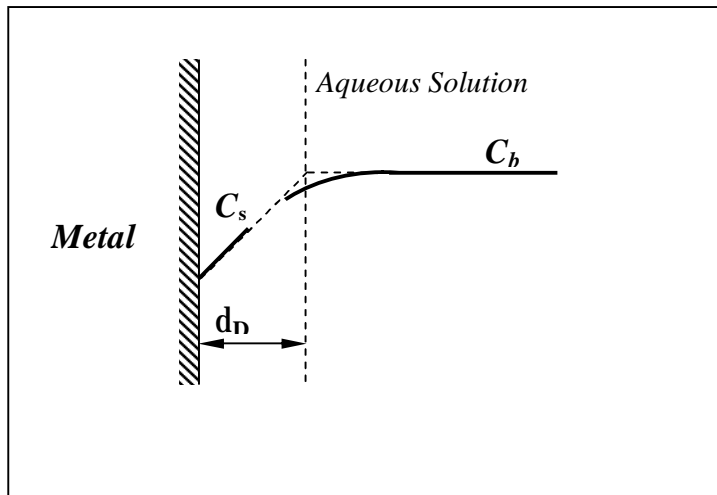
Fig. 2-4 Diffusion boundary layer [19].

The diffusion layer thickness is dependent on the velocity of the solution past the electrode surface. As the velocity increases, δ_D decreases and the limiting current density increases [10]. The time interval required to set up the diffusion layer varies with the current density and limiting diffusion rate, but it is usually of the order of 1 second while it is 10^{-4} second needed to establish the electrical double layer, which makes it possible to distinguish between η_a and η_c experimentally. The diffusion layer may reach a thickness of 100-500 μm, depending upon concentration, agitation (or velocity), and temperature [15].

2.9 Factors Effecting on Corrosion Rate

Frequently in the process industries, it is desirable to change process variables. This will usually have an effect on the corrosion rate of the metal involved.

Many factors were found to have an influence on the corrosion rate, these factors are:

1. Velocity
2. Temperature
3. Corrosive concentration
4. Heat flux
5. Galvanic coupling.

2.9.1 Effect of Velocity

The effects of velocity on corrosion rate are complex and depend on the characteristics of the metal and the environment to which it is exposed. For corrosion process is under cathodic control, then agitation or velocity increases the corrosion rate as shown in Fig. (2.5) in curve A, section 1. This effect generally occurs when an oxidizer present in very small amounts as in the case of dissolved oxygen in acids or water. If the process is under diffusion control and the metal is readily passivated, then the behavior corresponding to curve A, section 1 and 2 will be observed. That is, with increasing agitation, the metal will undergo an active-to-passive transition. Easily passivited materials such as stainless steel and titanium frequently are more carrion resistant when the velocity of the corrosion medium is high.

If corrosion processes which are controlled by activation polarization, agitation and velocity has no effect on the corrosion rate as illustrated in curve B. Some metals owe their corrosion resistance in certain medium to the

formation of massive bulk protective films on their surface. These films differ from the usual passivation film in that they are readily visible and much less tenacious. When materials such as these are exposed to extremely high corrosive velocities, mechanical damage or removal of these films can occur, resulting in accelerated attack as shown in curve C. This is called erosion corrosion [4].
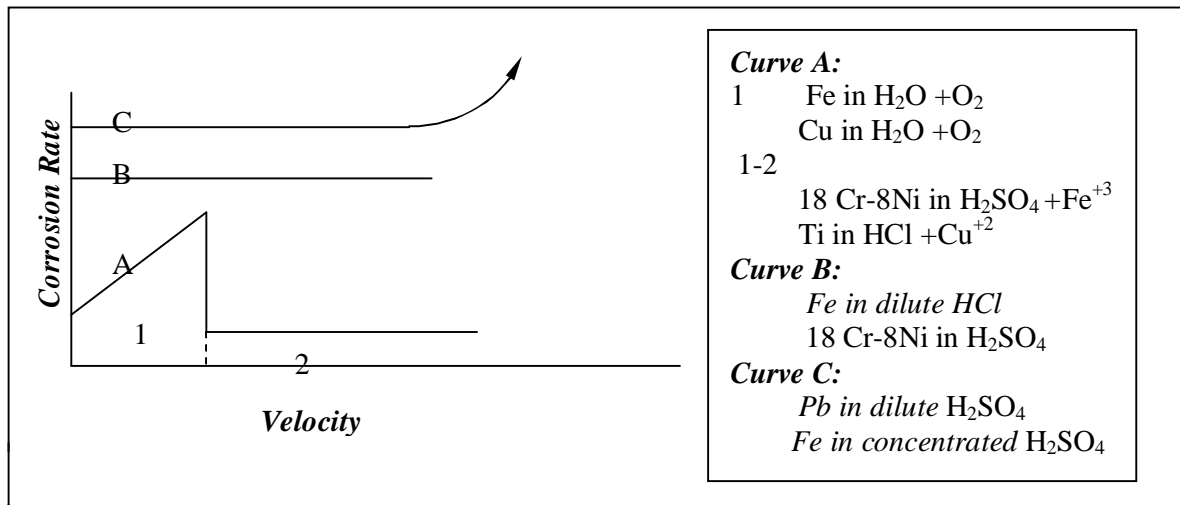
Fig. 2-5 Effect of Velocity on the Corrosion Rate [4].

2.9.2 Effect of Temperature

Temperature increases the rate of almost all chemical reactions [4]. An increase in temperature of corroding system has effect on the rate of chemical reaction is increased, the solubility of gases in solution is decreased, the solubility of reaction products may change resulting in different corrosion reaction products and viscosity is decreased and may thermal difference will result in increased circulation.

Temperature changes have the greatest effect when the rate determining step is activation process. In general, if diffusion rate is double for a certain

increase in temperature, activation process may be increased by 10-100 times, depending on the magnitude of activation energy [16].

2.9.3 Effect of Corrosive Concentration

The effect of oxidizer additions or the presence of oxygen on corrosion rate depends on both the medium and the metals involved. The corrosion rate may be increased by the addition of oxidizers, oxidizers may have no effect on the corrosion rate, or a very complex behavior may be observed. By knowing the basic characteristics of a metal or alloy and the environment to which it is exposed, it is possible to predict in many instances the effect of oxidizer additions [4].

For diffusion-controlled process, an increase in concentration of the diffusing species in the bulk of the environment increases the concentration gradient at the metal interface. The concentration gradient provides the driving force for the diffusion process. Thus the maximum rate at which oxygen can be diffused to the surface (the limiting diffusion current) would be essentially directly proportional to the concentration in solution. Fig 2. 6 is an example of the cathodic polarization diagram which is operative for this system [20].
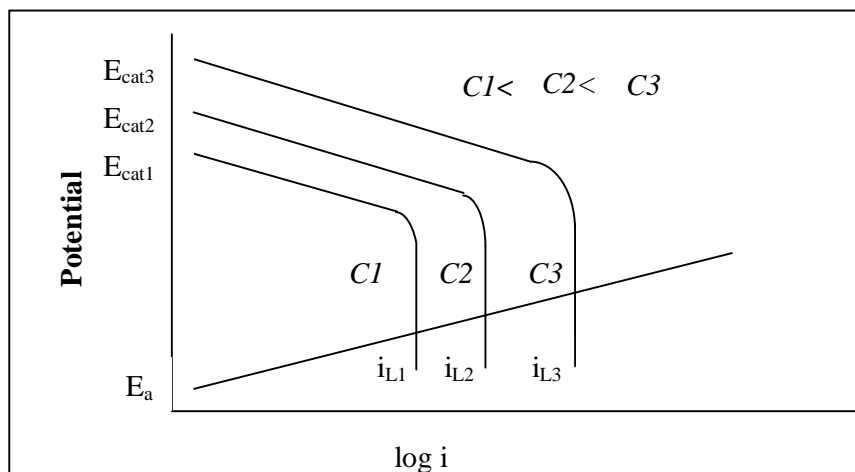
Fig. 2-6 Effect of Concentration on i_L [20].

2.9.4 Corrosion under Heat Transfer Conditions, Review of Previous Work

In the last 10 years many workers had studied the problem of corrosion in the presence of heat flux, but there had been little agreement as to whether the different corrosion rates were due to the heat flux itself, to the changed surface temperature or to some other causes such as an uneven surface.

In most cases a heat flux into the solution had been found to increase the corrosion rate but sometimes decreased attack had also been observed, particularly if an inhibitor was present. The reason for this uncertainly was that only in a few cases had the heat flux been related to the type or mechanism of corrosion although clearly this is important.

Knowledge of the controlling step would make the predication of the effect of heat flux on the overall corrosion rate much more reliable [21].

Fisher and Whitney [22] had found that the corrosion rate of cast iron and stainless steel disc under heat transfer is determined by the wall temperature. This was confirmed by Zarubin et. al. [23] for iron disc in concentrated sulfuric acid.

Kerst [24] confirmed the enhanced corrosion rates under heat flux circumstances for a series of metal and quoted rate increases between 3.5 to 8.2 times greater than the rate observed under isothermal conditions. Such increase in corrosion rate was entirely attributed to the higher metal surface temperature compared to that of solution [25].

Krzysztof [26] confirmed Ross observation and found that corrosion rates of steel in 80% H_2SO_4 during heating of steel were higher than observed under isothermal conditions at the same bulk temperature, which was ranged between 353-393K. However, corrosion rates lower than those measured

under isothermal conditions were observed with steel cooling and stated that metal surface temperature greatly affects the rate of corrosion.

Porter et al. [21] studied the rate of dissolution of Cu into 50% H_3PO_4 in the range 20-65 ^oC in the absence of heat flux and in the presence of either positive or negative heat fluxes up to 80 kW/m^2. The limiting current was found to be proportional to C_b, D, and v, such that;

$$i_L = 4.33 \times 10^5 (C_s - C_b) D^{2/3} v^{-1/6}$$
……. (2.26)

It was concluded that heat flux alters the mass transfer rate of diffusion controlled reaction mainly because it alters the surface/solution interface temperature. According to Zarubin [23], corrosion rate under heat transfer is consistent with that under isothermal conditions at some mean temperature of a given temperature drop. With the increasing liquid flow velocity this mean temperature shifts from the metal temperature to the solution temperature.

Ross [27] observed about the direction of the heat flux upon corrosion of nickel in alkaline salt solution. He showed that, with increasing heat flux, the corrosion rate was increased with metal heating and conversely was decreased with metal cooling.

Ionic mass transfer from iron pipe by free convection (stationary conditions) with simultaneous heat transfer was studied by Wragg and Nasiruddin [28]. They found that the effect of temperature gradient upon the limiting current is very clear and at maximum surface temperature an increase of some 65% above the isothermal case was observed and they showed that the higher electrode surface temperature would result in even greater mass transfer rates (thinner diffusion layers).

The corrosion rate of mild steel was monitored in oxygenated and de-oxygenated 100 ppm sodium chloride solutions at temperature between 200 and 350^oC at heat fluxes of 110-260 kW /m^2 which were studied by

Ashford et al. [29] They attributed the increase in corrosion rate to the formation of acidic solutions at the corroding surface by a mechanism analogous to the pitting corrosion mechanism at room temperature in oxygenated chloride solutions. Acidic solutions are generated at anodic sites which form particularly at heated surfaces because of the higher temperature and reduction of oxygen.

Alwash [30] studied electrochemical behavior of rotating nickel disc emitting heat in deaerated and oxygen saturated 0.01N H_2SO_4. He found that in the absence and presence of oxygen, the effect of heat transfer in increasing the reaction rates on the nickel electrode depends on the interfacial temperature.

Jaralla [31] found that the activation energy of iron dissolution in 1 N H_2SO_4 is the same under both isothermal and heat transfer condition which indicates that the mechanism of iron dissolution was unchanged in the presence of heat transfer. Besides, he showed that corrosion rates were increased with increasing temperature (that of bulk or interfacial).

Kolotyrkin et. al. [32] investigated the problem of metal corrosion under heat transfer conditions. They showed that the corrosion and electrochemical behavior of metal and alloys during heat transfer depends on all the electrochemical; hydrodynamic, heat and mass transfer conditions in the system. Besides, studies of the electrochemical behavior of iron in sulphate solutions made it possible to establish that under heat transfer the rate of the active dissolution of the metal at a constant potential depends not only on the temperature of the metal, but also on the magnitude and direction of the heat flux.

Pakhomove et. al. [33] studied the corrosion behavior of iron disc rotated in sulfate solution of varying conditions of bulk temperature, acidity,

and heat flux. They stated that the change in metal dissolution rate under heat transfer may be due to the temperature drop between metal and liquid.

Andon et. al. [34] studied the corrosion of stainless steel under controlled heat fluxes. In this investigation the corrosion of stainless steels in nitric acid test at various heat fluxes with steel surface temperature kept constant had shown that the cooler acid present at the surface under higher heat fluxes lead to slightly smaller corrosion rates than under isothermal conditions. They attributed such decrease in corrosion rate to the presence of cooler acid in contact with the metal surface as the heat flux was increased. This was confirmed by other investigators [35].

Jaralla [36] compared the variation of corrosion rates, of iron rotating discs emitting heat in water containing 200 ppm NaCl, with interfacial temperature and concluded that heat transfer stimulated the reaction more than the increase in interfacial temperature. Furthermore, the influence of heat transfer on the corrosion rate was decreased with increasing flow velocity, due to the decrease in the interfacial temperature.

Sameh [37] studied the corrosion of carbon steel rotating cylinder electrode (RCE) in 600 ppm chloride solution under controlled conditions of heat and mass transfer. She reported that the anodic dissolution of iron depends on the temperature at reaction site. She also found that higher corrosion rates were obtained under heat transfer conditions compared with those under isothermal conditions which were due to higher stimulation of the anodic dissolution and oxygen transfer rate accompanied with higher interfacial temperature.

Al-Tal [38] investigated the electrochemical behavior of rotating carbon steel cylinder in natural aerated neutral chloride/sulphate solution and performance of an inhibitor blend on the corrosion process. He found that the heat transfer from specimen to the electrolyte bulk enhances the rate of mass

transfer of oxygen towards the electrode/electrolyte interface. Hence, the limiting current density of oxygen reduction reaction increases

Atia [39] found that the heat flux increases i_L for oxygen reduction on steel plate.

Mashta [40] studied the corrosion of carbon steel cylinder in cross flow in 0.01 N NaCl solutions under controlled conditions of heat and mass transfer. He found that limiting current density under heat transfer conditions is higher than under isothermal conditions and anodic active current densities are increased when the specimen was subjected to heat transfer.

Wathiq [41] studied the corrosion of copper rotating cylinder in 0.03 N NaCl solutions under controlled conditions of heat and mass transfer. He found that copper dissolution is increased with increasing temperature and velocity. He found that heat transfer from the specimen to the electrolyte bulk with anodic limiting conditions of concentration polarization enhances the rate of mass transfer of $CuCl_2^-$ away from the electrode/electrolyte interface.

2.9.5 Effect of Galvanic Coupling

In many practical applications the contact of dissimilar materials unavoidable. In complex process streams and piping arrangements, different metals and alloys are frequently in contact with each other and the corrosive medium. The effect of galvanic coupling will be considered a piece of zinc immersed in a hydrochloric acid solution and contacted to a noble metal such as platinum show in Fig. (2.7).Since platinum is inert in the medium; it tends to increase the surface at which hydrogen evolution can occur. Further, hydrogen evolution occurs much more readily on the surface of platinum than on zinc.

These two factors increase the rate of the cathodic reaction and consequently increase the corrosion rate of zinc .Note that the effect of galvanic coupling in this instance is instances, the rate of electron consumption is increased and hence the rate of metal dissolution increases .It is important to recognize that galvanic coupling dose not always increase the corrosion rate of a given metal; in some cases it decreases the corrosion rate [4].
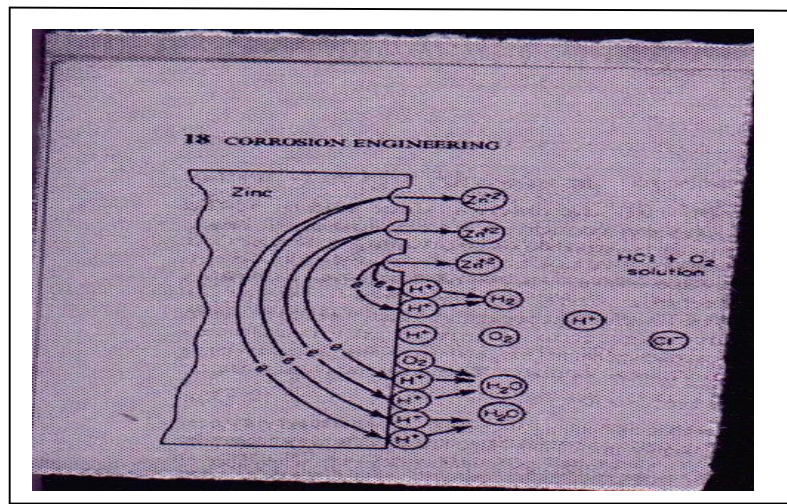
Fig. 2-7 Electrochemical reactions occurring on galvanic couple of zinc and platinum [4].

Chapter Three
Corrosion with Mass and Heat Transfer

3.1 Introduction

Most of corrosion involves some relative motion between the corroding metal and its environment. Such movement can increase or decrease process occurring under static condition.

Electrochemical measurements in flowing solution can provide data on (a) the rate of general corrosion and the possibility of other forms of attack, (b) mechanism by using the effect of flow as a diagnostic criterion, (c) the characteristic hydrodynamic parameters, e.g. the rate of mass transfer, the degree of turbulence or the surface shear stress, and (d) the composition of the solution by electro-analytically monitoring composition or measuring redox potentials, pH etc [42].

When a component of a fluid acts upon the surface of a solid, the rate of any reaction occurring is influenced by:

1. The chemical nature of the reactants, solid and fluid.
2. The physical nature of the solid surface, the state of the exterior portion of the crystal lattice.
3. The impurities present on the surface of the solid.
4. The activation energy of reactions taking place between solid and fluid phases.
5. The rate of transfer of fluid phase reactant to the surface of the solid, as influenced by: film of inert fluid, layer of solid reaction product and the diffusion coefficient of reacting fluid component through inert fluid component.

Apparatus for examining the effects of flow on corrosion is similar to that in static tests except that either the specimen (rotating discs and cylinders) or the solution must be moved, and more thought must be given to the placement of reference and counter electrode. Units with rotating electrodes in the form of discs or cylinders were to obtain reliable and producible results; they also offer practical advantages [43]:

1. Convenience based i.e. they are cheap and easy to use, small and steady state condition.

2. There are no problems of entry lengths.

3. It is easy to control accurately and the results obtained should be highly reproducible.

4. Need relatively small quantities of test fluid and ease of cleaning.

3.2 Hydrodynamic Boundary Layer

When a fluid moves past a stationary, hydraulically smooth surface, there is an implicit assumption that the fluid is stationary at that surface. That assumption is often called "no slip at the wall". In many flow configurations and especially when turbulent flow conditions prevail, the velocity profile shows an increase from 0 at the solid-fluid interface to the free stream value across a relatively short distance into the fluid. Though in the rotating cylinder the surface is moving, the fluid adjacent to that surface moves at the same velocity as the cylinder so, in effect, the fluid is stationary relative to the surface and fulfills the no slip at the wall criterion. The boundary layer thickness is independent of position on the surface meaning that the velocity profile, momentum transfer, and wall shear stress are independent of position.

The rotating cylinder electrode as traditionally constructed cannot examine situations where such uniformity does not exist without some modification. Mass transfer requires a concentration gradient between the surface and fluid bulk. Such a gradient implies that the concentration changes across some small distance between the surface and the bulk. This region is called the concentration or mass transfer boundary layer. For the large Schmidt Numbers normally encountered in liquids the fully developed mass transfer boundary layer for hydraulically smooth surfaces is much thinner than the fully developed hydrodynamic boundary layer [44].

This relationship is shown in this figure (3.1)
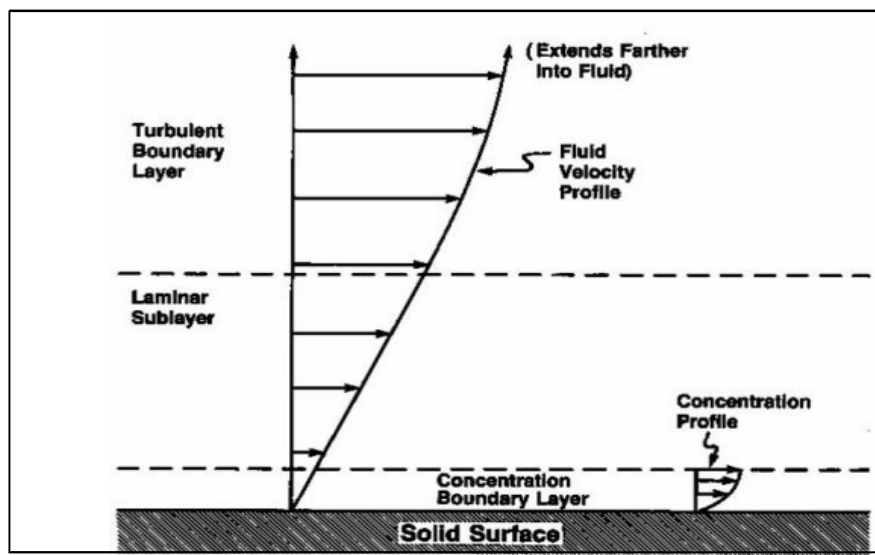
Fig. 3-1 Relationship between the hydrodynamic boundary layer and the mass-transfer boundary layer [44].

The hydrodynamic boundary layer is represented as having two sections, a viscous sub layer and a turbulent outer layer and that the fluid is moving relative to a surface. Since the flow is turbulent, the profiles are time-averaged profiles and are not drawn to actual scale. As in the case of the velocity

profile, the mass transfer boundary layer thickness is independent of position meaning that the mass transfer rate is independent of position [44].

3.3 Effect of Mass Transfer

3.3.1 Introduction

Mass transfer can result from several different phenomena. There is mass transfer associated with convection in that mass is transported from one place to another in the flow system. This type of mass transfer occurs on a macroscopic level and is usually treated in the subject of fluid mechanics. When a mixture of gases and liquid is contained such that there exists a concentration gradient of one or more of the constituents across the system, there will be a mass transfer on a macroscopic level as the result of diffusion from regions of high concentration to region of low concentration.

Not only may mass diffusion occur on a molecular basis, but also in turbulent flow system accelerated diffusion rates will occur as a result of the rapid -eddy mixing processes, just as these mixing processes created increased heat transfer and viscous action in turbulent flow [45].

3.3.2 Mass Transfer Controlled Corrosion Reactions

Mass transfer plays a big role in chemical and electrochemical dynamic process. It is the movement of materials from one location in the solution to another arises from difference in electrical or chemical potential at the two locations or from the movement of a volume element of solution.

The understanding of this process has been enhanced by the application of the basic principle of mass transfer .There are three modes of mass transfer [46]:

Migration:

This occurs when charged particles placed in an electric field. Thus a negatively charged ion is attracted towards a position electrode and vice versa. This movement is due to a gradient in the electrical potential [47].

Diffusion:

This occurs whenever a species moves from a region of high concentration to one of low concentration, thus it is movement due to concentration gradient [47].

Convection:

This occurs from a movement of the fluid by forced means (stirring, for example), or from density gradient within fluid. Generally fluid flow occurs because of natural or forced convection.

Mass transfer to an electrode is governed by the Nernest-plank equation which may be expressed [46, 48]:

$$Ji(y) = -Di\frac{\partial Ci(Y)}{\partial Y} - \frac{n_i F}{RT} DiCi\frac{\partial \Theta(Y)}{\partial Y} + CiV(Y) \qquad \dots\dots (3.1)$$

and the 1St term of equation (3.1) is diffusion term ,2nd is migration term and 3rd is convection term .

In many practical cases the cathodic reaction is under diffusion control. In this case the reaction current is governed by Fick's first law .Fick's first law states that the flux proportional to the concentration gradient:

$$Ji(y,t) = -Di\frac{\partial Ci(y,t)}{\partial y} + Xi(Jj + Ji) \qquad \dots\dots (3.2)$$

In flowing system the convection term is small compared with the diffusion term, the equation (3.2) becomes

$$Ji(y) = -Di\frac{\partial Ci(y)}{\partial y} \qquad \dots\dots (3.3)$$

The negative sign in equation (3.3) has been omitted as it indicates only that the direction of transfer from a region of high concentration to one of low concentration.

$$Ji = \frac{i}{nF} = -D_i \frac{dCi}{dy} \bigg| y = 0 \qquad \qquad \text{..... (3.4)}$$

or it is equivalent (for any species) to

$$i = nFD \frac{C_b - C_s}{d_D} \qquad \qquad \text{..... (3.5)}$$

At a given current or more exactly, at a given reaction rates, the concentration right at the electrode surface is determined by a mass transfer process. If this current is increased, the reaction rate is increased due to a faster consumption of the reactive species at the electrode, resulting in a lower interfacial concentration C_s. However ,this concentration can not, drop below zero, thus the current at which the interfacial concentration reaches zero is called the limiting current .This current is determined by setting C_s equals to zero in equation (3.5) [46] .

$$i_{lm} = nF \frac{D}{d_D} C_b \qquad \qquad \text{..... (3.6)}$$

$$i_{lm} = nFkC_b \qquad \qquad \text{..... (3.7)}$$

where : $k = D / d_D$ $\qquad \qquad \text{..... (3.8)}$

3.4 Diffusion Boundary Layer

A thin, uniform, and stationary diffusion boundary layer is important in obtaining high-quality electrodeposits. Limiting current depends on thickness of the diffusion boundary layer for a given reactant concentration .

If concentration gradient exists within a fluid flowing in a surface, mass transfer is usually created. The whole concentration gradient of the resistance to mass transfer lies within a thin layer known as diffusion boundary layer in the vicinity of the surface. Outside this layer, the concentration is maintained at its bulk value [49].

According to Nernest, the mass is transferred across this layer by diffusion alone. Following Fick's law of diffusion transfer, the mass transfer rate could be determined using concentration gradient across this layer, species diffusion coefficient and layer thickness as [46]:

$$J = \frac{D}{d_D}(C_s - C_b) \qquad \qquad \text{….. (3.9)}$$

A general expression for the thickness of the diffusion boundary layer formed on a smooth surface under turbulent flow is [44]:

$$d_D = 62 \, \text{Re}^{-0.875} \qquad \qquad \text{….. (3.10)}$$

The diffusion boundary layer thickness for rotating cylinder is given by the equation [50, 51]:

$$d_D = 12.64 \frac{d^{0.3} n^{0.344} D^{0.356}}{V^{0.7}} \qquad \qquad \text{….. (3.11)}$$

With a known concentration of ions in the solution and limiting current, the diffusion layer thickness [49]:

$$d_D = nF \frac{DC_b}{i_{lm}} \qquad \qquad \text{….. (3.12)}$$

At mass-transfer limiting condition, the mass-transfer coefficient can be expressed as

$$k = \frac{i_{lm}}{nFC_b} \qquad \qquad \text{….. (3.13)}$$

Therefore, the diffusion layer thickness in equation (3.13) may be expressed in terms of the mass-transfer coefficient and the diffusivity

$$d_D = \frac{D}{k}$$ ….. (3.14)

Therefore the thickness of diffusion boundary layer depends on the velocity or rotation (for rotating system) and it is a function of the physical properties of the system. However, under turbulent flow conditions for most aqueous solution, the thickness of the hydrodynamic layer may be related indirectly to diffusion boundary layer using [52]:

$$\frac{d_H}{d_D} = Sc^{1/3}$$ ….. (3.15)

The thickness of diffusion boundary layer depends upon the hydrodynamic flow conditions.

3.5 Mass Transfer Correlations

As shown the dimensionless analysis is a useful tool to relate the experimental variables of a diffusion-convection controlled electrochemical process. In most correlation these dimensionless groups correlated by general form for fully developed flow [44]:

Sh=f (Re, Sc) …..(3.16)

These groups are usually related to each others via the following equation:

$$Sh = a \, Re^b \, Sc^c$$

Extensive data are available on mass transfer correlations for rotating cylinder electrode and cylinder in cross flow were seen in appendix B in Tables (B.1 and B.2)

3.6 Rotating Cylinder

3.6.1 Introduction

The rotating cylinder electrode offers an interesting alternative for electrochemical studies in that it has simple construction, reproducible response and reaches the turbulent flow conditions at low Reynolds number. Its application in corrosion studies for example, permits the use of samples in the form of tubes, simulating the hydrodynamic conditions in which the material is commonly employed.

The lack of an exact mathematical solution for the turbulent flow case has been responsible for the empirical approach used to describe mass transport to a rotating cylinder electrode surface [51].Eisenberg, Tobias and Wilke [53] were the first to carry out a detailed investigation on mass transport to rotating cylinder electrode under turbulent flow .From measurement of limiting current density at a smooth Ni RCE using $Fe(CN)_6^{-3}$ /$Fe(CN)_6^{-4}$ couple in alkaline medium they obtained:

$$i_l = knCd^{-0.3}n^{-0.344}D^{0.644}U^x \qquad ..... (3.17)$$

Where k = 0.0791 and x = 0.7

Pang and Ritchi [54] minimized the end effects by installing inert ends and obtained the following equation:

$$i_l = knFCd^{-0.299}n^{-0.345}D^{0.644}U^x \qquad ..... (3.18)$$

Where k = 0.086 and x = 0.71

Gabe and Walsh [55] obtained the value x=0.74 for cupric ion electroreduction to metallic copper on a smooth cylinder and observed that x changes to 0.9 as the electrode surface becomes rougher.

3.6.2 Mass Transfer to Rotating Cylinder Electrode

Eisenberg et al. [53] were the earlier who studied the mass transfer to R.C.E. comprehensively using both chemical dissolution and limiting current density, and they suggested that in the range of Reynolds number (1000-100000), the best representive relationship can be expressed by:

$$\frac{k_m}{V} Sc^{0.644} = 0.0791 Re^{0.3} \qquad\qquad ….. (3.19)$$

Recalling that mass transfer coefficient;

$$k_m = \frac{N}{C_b - C_s} \qquad\qquad ….. (3.20)$$

For steady state to be maintained, all the reagent transport down the concentration gradient must react electrochemically giving a current:

$$\frac{i}{nF} = N \qquad\qquad ….. (3.21)$$

Therefore,

$$k_m = \frac{i}{nF(C_b - C_s)} \qquad\qquad ….. (3.22)$$

Under limiting condition, $C_s \rightarrow 0$, a limiting current density i_l is obtained, therefore:

$$k_m = \frac{i}{nFC_b} \qquad\qquad ….. (3.23)$$

Substituting equation (3.19) in equation (3.23), the following relation for the limiting current density is obtained:

$$i_l = 0.079 nFC_b V \left[\frac{Vd}{n}\right]^{-0.3} \left[\frac{n}{D}\right]^{-0.644} \qquad\qquad ….. (3.24)$$

Rearranging equation (3.22)

$$k_m = \frac{D}{d_D}$$

..... (3.25)

Therefore

$$i_l = nF\frac{D}{d_D}C_b$$

..... (3.26)

Where:

d_D was given by Eisenberg et al [50,51] to be:

$$d_D = 12.64\frac{d^{0.3}n^{0.344}D^{0.356}}{V^{0.7}}$$

..... (3.27)

Using equation (3.19) a dimensional equation was obtained:

$$Sh = 0.079\,\mathrm{Re}^{0.7}\,Sc^{0.356}$$

..... (3.28)

3.7 Effect of Heat Transfer

The transfer of heat can be found throughout industrial processing . Heat must be removed when it is generated in compressions or in chemical reaction such as found in process reactors, power plants using chemical combustion or nuclear sources, etc. Heat or other energy must be provided in purification process and is often needed in mass transfer operation such as drying and distillation .The conservation of heat in plants is important because heat loss is costly: thus in large plants one finds extensive use of heat exchangers, which are pieces of equipment to remove heat from one stream and transfer it to a second stream [45].

3.8 Thermal Boundary layer

Heat will flow between a wall and the fluid adjacent to it when a temperature gradient is established between the wall and the fluid. Near the wall the fluid velocity increases from zero at the wall to the bulk velocity, sometimes not too distant from the wall relative to the radius of curvature. Likewise, the temperature changes from that at the wall to that in the free stream. The result is that the fluid temperature adjacent to the wall is assumed to be equal to the surface temperature of the wall at the interface and is equal to the bulk fluid temperature at some point in the fluid. This distance is called the thermal boundary layer. A momentum boundary layer also is present if the fluid is flowing past the wall. The momentum (hydrodynamic) boundary layer and the thermal boundary layer can affect each other. The distances over which the velocity changes from zero to the free stream velocity and the temperature changes from the wall temperature to the free stream temperature are often different.

From a corrosion standpoint, the wall temperature or more specifically, the temperature at the wall-fluid boundary is the important parameter driving corrosion. The fluid temperature and even the average temperature in the wall could be vastly different. The two temperatures are related through an equation of the form

$$Q = kA(T_i - T_s)/d_t \qquad \text{….. (3.29)}$$

$$Q = hA(T_i - T_s) \qquad \text{….. (3.30)}$$

The science of heat transfer enables "h", the heat transfer coefficient, to be estimated from the fluid properties and fluid dynamics. Once the value of h is estimated, the interfacial temperature can be estimated (at least in principle). [44].

However, under turbulent flow conditions for most aqueous solutions, the thickness of the hydrodynamic layer may be related indirectly to d_t using [52]:

$$d_H\!\big/\!d_t = \mathrm{Pr}^{1/3} = \left[\frac{C_p m}{k_T}\right]^{1/3} \qquad \text{..... (3.31)}$$
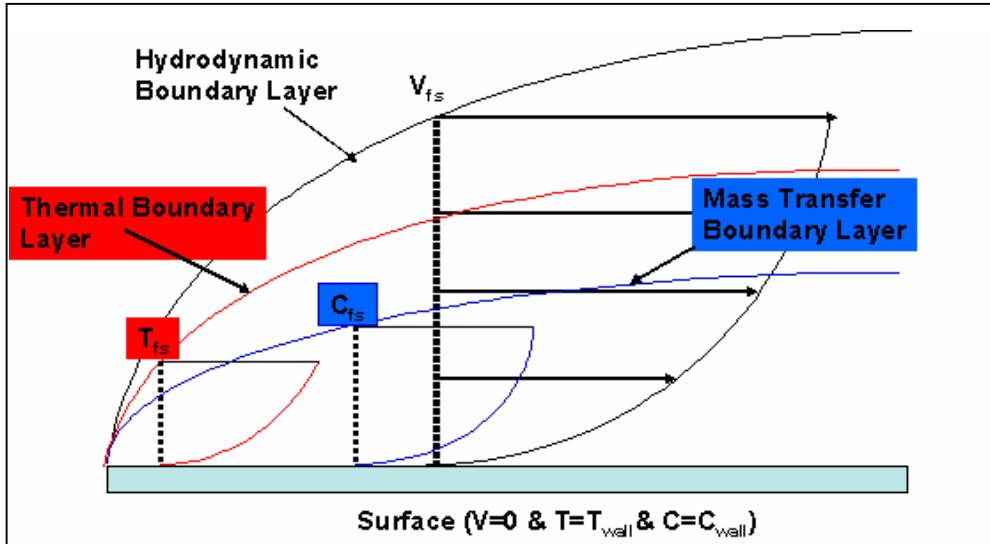
Fig. 3-2 The hydrodynamic, thermal and diffusion boundary layer [44]

3.9 Heat Transfer Correlations

In the absence of thermal or hydrodynamic entry effect. It had been seen that the heat transfer correlation is

$$\mathrm{Nu} = a\,\mathrm{Re}^b\,\mathrm{Pr}^c \qquad \text{.....(3.32)}$$

with the Nusselt number related to the Prandtl number and the mean flow velocity in the form of the Reynolds number. Some classical correlations, for turbulent pipe flow are generally available. One of the first equation developed to compute the heat transfer coefficients in pipes is the Dittus-Bolter equation [56]:

$$Nu = 0.023\,\text{Re}^{4/5}\,\text{Pr}^{0.4} \qquad\qquad\qquad\qquad\qquad\text{….. (3.33)}$$

with the coefficients 0.023 recommended by McAdams (0.0243 originally). The above equation is a slightly different version of the Colburn equation [56]:

$$Nu = 0.023\,\text{Re}^{4/5}\,\text{Pr}^{1/3} \qquad\qquad\qquad\qquad\qquad\text{….. (3.34)}$$

These equations are used for fully developed turbulent flow in smooth circular tube. For flows characterized by large property variations, a correlation determined by Seider -Tate is used [56]:

$$Nu = 0.027\,\text{Re}^{4/5}\,\text{Pr}^{1/3}\left[\dfrac{m}{m_s}\right]^{0.14} \qquad\qquad\qquad\text{….. (3.35)}$$

where μ and μ_s are the viscosities determined by the bulk and surface temperatures, respectively. In most cases, this correction term is neglected leaving just the Nusselt-Reyonold/Prandtl number relationship [56].

   Kramers [57] published analysis of heat transfer for fully developed cylinder in cross flow, was found to be correlated by the following equation:

$$Nu = 0.57\,\text{Re}^{0.5}\,\text{Pr}^{1/3} \qquad\qquad\qquad\qquad\qquad\boldsymbol{\text{…... (3.36)}}$$

   Churchill and Bernstein [58] proposed the following equation for heat transfer cylinder in cross flow:

$$Nu = 0.3 + \dfrac{0.62\,\text{Re}^{1/2}\,\text{Pr}^{1/3}}{\left[1 + \left(\dfrac{6.4}{\text{Pr}}\right)^{2/3}\right]^{1/4}} \qquad\qquad\qquad\text{….. (3.37)}$$

3.10 Presence of Heat Transfer

The presence of heat transfer between a metal wall and an aggressive medium has a significant influence on corrosion processes, changing the corrosion rate and frequently its mechanism. Despite this, as a rule constructional materials and methods of protection from corrosion for heat exchange apparatus are selected without taking into consideration the possible influence of heat transfer on corrosion. The specifics of corrosion processes, the rate of which is limited by the transport stages, are related to the possible influence of heat exchange on the hydrodynamics and mass transfer in the metal-solution system. In heat transfer the temperature distribution in the near electrode zone depends upon the hydrodynamic conditions [59].

Under heat transfer condition, the metal can be at a temperature different from the fluid bulk; this difference in temperature will affect the corrosion process. This effect may be direct or indirect .A direct effect could be that of the wall temperature on the kinetics of the reaction at the metal/solution interface. Indirect effects would include the physical and chemical changes that occur at and next to the metal /solution interface because of temperature gradients. In particular, this concerns the stability of a protective film and the solubility and transfer (i.e. diffusion coefficient) of the reactive species [12].

The discussion to date has assumed isothermal conditions, but in many practical situations corrosion reactions have to be considered when the electrode is acting as a cooler or a heater.

From various studies it is, becoming clear that in spite of a heat flux, the overriding parameter is the temperature at the interface between the metal electrode and the solution, which has an effect on diffusion coefficients and viscosity.

When film-forming reactions occur and activation control is the rate determining factor then the interfacial temperature again will determine the extent of corrosion [5, 16].

3.11 Analysis of Variances

Analysis of variance is the simultaneous testing of two or more treatment means by examination of the variances among and within groups (treatments). The t-test can test a single mean versus a hypothesized value or the difference between two means of two groups, but not more than two. Even though the ANOVA is an analysis of variances among data, its primary use is the test of differences among group means [60].

Statistically, analysis of variance (ANOVA) is a collection of statistical models, and their associated procedures, in which the observed variance is partitioned into components due to different explanatory variables.

The initial techniques of the analysis of variance were developed by Fisher's in the 1920s and 1930s and is sometimes known as Fisher's ANOVA or Fisher's analysis of variance, where F- distribution is part of the test of statistical significance.

There are a number of ways in which analysis of variance might be further extended, but the assumptions of normality and equal standard deviation still need to hold. First, perhaps the observations could be grouped according to two different categorical variables .The extension allowing for two factors is called two-way ANOVA. A second extension of one way ANOVA is when we have two dependant variables that we wish to compare simultaneously across two or more groups. This extension is called multivariate analysis of variance (MANOVA). In practice, there are several

types of ANOVA depending on the number of treatments and the way they are applied to the subjects in the experiment [61].

ANOVA is incomplete on its own if you have more than two samples. If a significant difference is found you will only know that the samples with the highest and lowest means are different. You will not know with any certainty whether the intermediates are significantly different from either of the extremes. One of the multiple comparison tests must be used for this reason. The multiple comparison tests need to be associated with ANOVA since the latter is more reliable for detecting differences. An important technique for analyzing the effect of categorical factors on a response is to perform an Analysis of Variance. An ANOVA decomposes the variability in the response variable amongst the different factors. Depending upon the type of analysis, it may be important to determine: (a) which factors have a significant effect on the response, and/or (b) how much of the variability in the response variable is attributable to each factor [62].

3.11.1 The Purpose of Analysis of Variance

In general, the purpose of analysis of variance (ANOVA) is to test for significant differences between means. Elementary Concepts provides a brief introduction into the basics of statistical significance testing. If we are only comparing two means, then ANOVA will give the same results as the t- test for independent samples (if we are comparing two different groups of cases or observations), or the t- test for dependent samples (if we are comparing two variables in one set of cases or observations) [61] .

3.12 Two Ways ANOVA

Two Way Analysis of Variance is a way of studying the effects of two factors separately (their main effects) and (sometimes) together (their interaction effect). Analyzing by two factors is often a first step in investigating whether an association is confounded or likely to be causal. Understanding the interrelated causes is very important [63].

The parameter symbols typically used in ANOVA are described below:

1. Source: The source includes the controlling factors (column, row) and the error factor, and the sum of all observations, T.

2. SS (sum of squares).SS_c, SS_r, SS_{cr}…, denote the sum of the squares of column, row, interaction; SS_e denotes the error sum of squares; SS_T denotes the total variation.

3. DF (degree of freedom): DF denotes the number of independent variables. In ANOVA table, the degree of freedom for each factor is the number of its level minus one. The total degree of freedom is the number of total variables value minus one. The error degree of freedom is the total degree of freedom minus the sum of degree of freedom of each factor.

4. Mean Square (MS): is defined as the sum of squares deduced by the total degree of freedom, i.e., $MS_i : \dfrac{SS_i}{(DF)i}$

5. F-ratio: This value is defined as the variance of each factor deduced by the error variance, i.e. $F_i = \dfrac{MS_i}{MS_e}$ (i=column, row …)

F- distribution: $F = \dfrac{s_1^2}{s_2^2}$, measures difference between two variances with the following characteristics:

i. Always positive, since variance positive

ii.Two degrees of freedom, one for s_1, one for s_2

In order to find F_{crit} which is the critical value as extracted from the f-distribution in statistical tables based on two values of degrees of freedom DF as shown in appendix C in Tables (C.27,28) .

The analysis of variance depends on the number of independent variables, and whether the experimental are carried out with replication or without replication in order to assess the presence of all degrees of interactions between variables as in the following tables:

Table 3-1 Two ways ANOVA without replication [62]

Source of variation	Sum of squares SS	Degree of Freedom DF	Mean Square MS	Mean Square Ratio
Among Columns	$\dfrac{\sum T_C^{\;2}}{nr} - \dfrac{T^2}{N}$	c-1	$\dfrac{SS}{DF}$	$\dfrac{MS_c}{MS_{residual}}$
Among Rows	$\dfrac{\sum T_r^{\;2}}{nc} - \dfrac{T^2}{N}$	r-1	$\dfrac{SS}{DF}$	$\dfrac{MS_r}{MS_{residual}}$
Residual	Total SS-all above	Total DF-all above		
Total	$\sum X^2 - \dfrac{T^2}{N}$	N-1		

Table 3-2 Two ways ANOVA with replication [62]

Source of variation	Sum of squares SS	Degree of Freedom DF	Mean Square MS	Mean Square Ratio
Among Columns	$\dfrac{\sum T_C{}^2}{nr} - \dfrac{T^2}{N}$	c-1	$\dfrac{SS}{DF}$	$\dfrac{MS_c}{MS_{residual}}$
Among Rows	$\dfrac{\sum T_r{}^2}{nc} - \dfrac{T^2}{N}$	r-1	$\dfrac{SS}{DF}$	$\dfrac{MS_r}{MS_{residual}}$
Column-row interaction	$\dfrac{\sum T_{cr}{}^2}{n} - \dfrac{T^2}{N} - SS_c - SS_r$	(c-1)(r-1)	$\dfrac{SS}{DF}$	
Residual	Total SS-all above	Total DF-all above		
Total	$\sum X^2 - \dfrac{T^2}{N}$	N-1		

3.13 Three Ways ANOVA

Computationally, the three-way ANOVA adds nothing new to the procedure for the two-way; the same basic formulae are used a greater number of times to extract a greater number of SS components from SS_{total} (eight SSs for the three-way as compared with four for the two-way). However, anytime you include three factors, you can have a three-way interaction, and that is something that can get quite complicated, as will be seen. To give a manageable view of the complexities that may arise when dealing with three factors [60]. The ANOVA table has six columns:

The first shows the source of the variability.

The second shows the sum of squares (SS) due to each source.

The third shows the degrees of freedom (DF) associated with each source.

The fourth shows the mean squares (MS), which is the ratio SS/DF.

The fifth shows the F statistics, which are the ratios of the mean squares.

Table 3-3 Three ways ANOVA [62]

Source of variation	Sum of squares SS	Degree of Freedom DF	Mean Square MS	Mean Square Ratio
Among Columns	$\sum T_C{}^2 \over nrg$ $- {T^2 \over N}$	c-1	$SS \over DF$	$MS_c \over MS_{residual}$
Among Rows	$\sum T_r{}^2 \over ncg$ $- {T^2 \over N}$	r-1	$SS \over DF$	$MS_r \over MS_{residual}$
Among Groups	$\sum Tg^2 \over ncr$ $- {T^2 \over N}$	g-1	$SS \over DF$	$MS_g \over MS_{residual}$
Column-Row Interaction	$\sum T_{Cr}{}^2 \over ng$ $- {T^2 \over N} - SS_C - SS_r$	(c-1)(r-1)	$SS \over DF$	
Column-Group Interaction	$\sum Tcg^2 \over nr$ $- {T^2 \over N} - SS_C - SSg$	(c-1)(g-1)	$SS \over DF$	
Row-Group Interaction	$\sum T_{rg}{}^2 \over nc$ $- {T^2 \over N} - SS_r - SS_g$	(r-1)(g-1)	$SS \over DF$	
Column-Row-Group Interaction	$\sum T_{crg}{}^2 \over n$ $- {T^2 \over N}$ minus all six previous sum of squares	(c-1)(r-1) (g-1)	$SS \over DF$	
Residual	Total SS minus all seven sum of squares	Total DF minus all previous DF	$SS \over DF$	
Total	$\sum X^2 - {T^2 \over N}$	N-1		

47

The results are then compared with F found in appendix C in Tables (C.27, C.28).

In the experimental having only one replication, the sum of squares of the residual is always equal to zero. This is because the residual error arises only from replicating (repeating) the experimental under the same set of conditions. This does not necessarily mean that the error term (experimental error and error involved due to some other factors unknown to the test designer) does not exist. In single replication experiments, this error term is generally lost in the interactions (column-row, column-group, row-group and column-row-group) .This is known as confounding; where certain effects cannot be distinguished from others. Hence ,the sum of squares SS of the error term (residual)and its degrees of freedom DF may be taken as the total of SS of all the interactions and the sum of their degrees of freedom respectively. This is shown in Table above (3.3).

In the single –replication experimental it is therefore not possible to estimate or to test the interaction (interaction term) for the significance. Therefore, only main effects (among column, among row, and among group) have been investigated [62].

Chapter Four
Results and Calculations

4.1 Introduction

The aim of this work to study and analyse the corrosion behavior under controlled heat and mass transfer conditions with different metals and different range of Reynolds number, temperature and heat flux. And then followed by the analysis of these data according to statistical ANOVA to identify the effect of individual factors.

A large amount of corrosion research is currently conducted in quiescent solutions. Accordingly, hydrodynamic factors are frequently ignored in the analysis of corrosion kinetics, or at best, a hydrodynamic regime is employed that does not effectively simulate that which occurs in the industrial environment of interest. However, many industrial systems involve the flow of corrosive fluids through pipes, channels, etc., at high velocities. In these cases, mass transfer and surface shear stress may have a profound effect on the rate of material degradation, either by modifying the rate of mass transport of chemical species to or from the surface or by shear-stripping films from the metal/ solution interface. As a result, an accurate simulation of corrosion phenomena that take place in the plant environments can be accomplished in the laboratory only if the hydrodynamic effects are considered [64].

Fluid motion can influence the corrosion mechanism and from that, the corrosion rate. Such influence would occur, for example, when the corrosion rates are controlled wholly or partially by mass transfer of reactant to or product from the surface, or by direct impingement of particles or occasionally the fluid itself against the surface. When the rate of mass transfer is the rate-controlling step in the corrosion process, the corrosion rate can, in

theory, be calculated from the product of the mass-transfer coefficient for that geometry and environment and the difference in concentration of the rate-limiting species between that at the surface and that which is in the environment. Oxygen is usually sparingly soluble in aqueous media [65].

A number of systems have been proposed as laboratory devices, including a stirrer housing coupons, a stirrer moving fluid relative to stationary coupons, rotating electrodes of various geometries, impinging jets, and flow loops with cylindrical spool pieces in a variety of configurations. All of these systems have some positive and some negative characteristics with respect to construction, corrosion measurement, and prediction. The rotating cylinder electrode is one such apparatus that has seen increasing popularity for examining corrosion in the presence of fluid motion. The reason is that this apparatus has a number of appealing characteristics, including the following [65]:

— defined hydrodynamics that are turbulent even at low rotation rates.

— reasonably well-defined empirical correlations that relate such quantities as mass-transfer coefficient (Sherwood number), fluid flow rate (Reynolds number), and fluid physical properties (Schmidt number).

— a uniform current and potential distribution.

— fluid characteristics independent of position on the electrode surface.

— reasonably easy assembly, disassembly, and use.

The most common type of flow conditions found in industrial processes is turbulent; however, corrosion studies in controlled turbulent flow conditions are available. With the increasing necessity to describe the corrosion of metals in turbulent flow conditions some laboratory hydrodynamic systems have been used with different degrees of success. Among these hydrodynamic systems, rotating cylinder electrodes (RCEs), pipe segments, concentric pipe segments, submerged impinging jets and close

- circuit loops have been used and have been important in the improvement of the understanding of the corrosion process taking place in turbulent flow conditions. It has been found that for a RCE enclosed in a concentric cell, the transition between the laminar and turbulent flow occurs at values of Reynolds number (Re) of 200 approximately. The RCE in corrosion laboratory studies is a useful tool for the understanding of mass transfer processes, effects of surface films, inhibition phenomena, etc., taking place in turbulent flow conditions. However, the use of the RCE has been questioned by some researchers, due to the differences found between the values of corrosion rates measured on pipe flow electrodes and on the RCE [66].

The most convenient method to present the results is to split them into three sections:

1. Corrosion of carbon steel cylinder in cross flow
2. Corrosion of carbon steel as Rotating Cylinder Electrode.
3. Corrosion of copper as Rotating Cylinder Electrode.

Each section is divided into isothermal and heat transfer conditions and each part contains cathodic region.

4.2 Corrosion of Carbon Steel Cylinder in Cross Flow

This corrosion study of carbon steel cylinder is under cross flow [40] in 0.1N sodium chloride solution. These experimental data are found at different flow rates (Re = 5000, 8000, 10000 and 12000) and different bulk temperatures (T = 30, 40, 50 °C).

Similar conditions were used under heat transfer conditions (Q = 10, 30, and 50 kW/ m^2) and different bulk temperature (T = 30, 40°C).The results

are to be split into two sections: isothermal conditions and heat transfer condition.

4.2.1 Isothermal Conditions

The limiting current densities of oxygen in 0.1N NaCl were determined from the polarization curves. Table (4.1) [40] is for isothermal conditions.

Table 4-1 The limiting current densities, A/m^2

Re	30°C	40°C	50°C
5000	2.3277	2.1978	————
8000	2.8723	2.5252	2.2595
10000	3.4050	3.1425	2.8201
12000	3.9496	3.5416	3.2118

It is clear from Table (4.1) that limiting current density at constant temperature, increases as Reynolds number increases, and limiting current density at constant Reynolds number, decreases as temperature increases.

4.2.2 Heat Transfer Conditions

The limiting current densities of oxygen in 0.1N NaCl were determined from the polarization curves with different heat fluxes. Tables (4.2-4.7) [40] show results under cross flow for heat transfer conditions with the interfacial temperatures.

Table 4-2 The limiting current density and interfacial temperature
at bulk temperature 30°C and Q =10kW/m²

Re	T_i(℃)	Limiting current density, A/m²
5000	38	2.4964
8000	36	2.9060
10000	35	3.6657
12000	34	4.0257

Table 4-3 The limiting current density and interfacial temperature
at bulk temperature 40°C and Q =10kW/m²

Re	T_i(℃)	Limiting current density, A/m²
5000	47	2.2107
8000	45	2.7448
10000	44	3.5290
12000	43	3.7230

Table 4-4 The limiting current density and interfacial temperature
at bulk temperature 30°C and Q =30kW/m²

Re	T_i(℃)	Limiting current density, A/m²
5000	43	2.8708
8000	40	3.4605
10000	38	4.7091
12000	36	5.3733

Table 4-5 The limiting current density and interfacial temperature
at bulk temperature 40°C and Q =30kW/m²

Re	T_i(℃)	Limiting current density, A/m²
5000	51	2.5862
8000	49	3.2155
10000	47	4.3535
12000	45	5.1969

Table 4-6 The limiting current density and interfacial temperature
at bulk temperature 30°C and Q =50kW/m²

Re	T_i(°C)	Limiting current density, A/m²
5000	46	3.2388
8000	44	4.3956
10000	41	4.8053
12000	39	6.1016

Table 4-7 The limiting current density and interfacial temperature
at bulk temperature 40°C and Q =50kW/m²

Re	T_i(°C)	Limiting current density, A/m²
5000	53	3.0201
8000	51	3.9466
10000	49	4.5786
12000	47.5	5.3014

It is clear from Tables (4.2, 3,4,5,6 and 7) that limiting current density at constant temperature, increases as Reynolds number increases. Also limiting current density at constant Reynolds number decreases as temperature increases. It is also shown that at constant temperature and Reynolds number, limiting current density increases as heat flux increases. The interfacial temperature decreases with the increasing Reynolds number at a given temperature and heat flux.

4.3 Corrosion of Carbon Steel Rotating Cylinder Electrode

This work presents the electrochemical kinetic results measured during the corrosion of carbon steel immersed in aqueous environments, containing 600 ppm chloride (Cl⁻) solution under turbulent flow conditions.

In order to control the turbulent flow conditions, a Rotating Cylinder Electrode (RCE) [67, 68] was used. Four different rotation rates were studied (also one under static conditions) (50,200,300 and 400) rpm and different bulk temperatures (T = 30, 40, 50 °C). Similar conditions were used under heat transfer conditions (Q =20kW/ m^2) and different bulk temperatures. The results are to be split into two sections: isothermal conditions   and heat transfer conditions.

4.3.1 Isothermal Conditions

The limiting current density of iron in 600 ppm chloride solutions were obtained from polarization curves. These results are presented in Tables (4.8-4.10) [67] for isothermal conditions.

Table 4-8 The limiting current density at 30°C

r.p.m	Re	Limiting current density, (A/m²)
0	0	0.146
50	15111.10	0.97
200	60461.40	4.87
300	90675.15	5.4
400	120897.3	8.1

Table 4-9 The limiting current density at 40°C

r.p.m	Re	Limiting current density, A/m²)(
0	0	0.341
50	17313.07	1.8
200	73601.20	5.23
300	113810.16	6.82
400	147172.40	8.3

Table 4-10 The limiting current density at 50°C

r.p.m	Re	Limiting current density, A/m²)(
0	0	0.487
50	21848.3	2.38
200	87418.0	5.36
300	131120.5	7.3
400	174799.2	8.53

It is clear from Tables (4.8, 9, and 10) that limiting current density at constant temperature, increases as velocity increases. And limiting current density at constant velocity increases as temperature increases.

4.3.2 Heat Transfer Conditions

The limiting current density of iron in 600 ppm chloride solutions were obtained from polarization curves with single heat flux (Q=20kW/m²). These results are presented in Tables (4.11-4.13) [68] for heat transfer conditions. The surface temperatures under heat transfer conditions are also shown in these tables.

Table 4-11 The limiting current density and interfacial temperature at bulk temperature 30°C and Q=20kW/m²

r.p.m	T_i(°C)	Re	Limiting current density, (A/m²)
50	56	19415.7	1.88
200	54.3	76320.30	4.97
300	50.3	116467.8	6.60
400	49.2	147374.2	8.10

Table 4-12 The limiting current density and interfacial temperature
at bulk temperature 40°C and Q=20kW/m²

r.p.m	$T_i(°C)$	Re	Limiting current density, (A/m²)
50	60	22093.3	2.20
200	56	84674.7	5.10
300	52.7	122757.9	6.70
400	51.8	160898.1	8.00

Table 4-13 The limiting current density and interfacial temperature
at bulk temperature 50°C and Q=20kW/m²

r.p.m	$T_i(°C)$	Re	Limiting current density, (A/m²)
50	68.2	24974.4	1.30
200	66.8	98540.9	3.30
300	62.6	143923.5	5.80
400	60.8	189399.9	7.40

It is clear from these Tables (4.11, 12 and 13) that limiting current density at constant temperature, increases as velocity increases. At constant velocity, it decreases generally as temperature increases. The interfacial temperature decreases with the increasing Reynolds number at a given temperature and heat flux.

4.4 Corrosion of Copper Rotating Cylinder Electrode

This corrosion study of copper rotating cylinder in 3% NaCl solution. The experimental data [41] found at different Reynolds number (r.p.m = 0,100,200,300,400) and different bulk temperatures (T = 30, 45, 60 °C). Similar conditions were used under heat transfer conditions with (Q = 15.6, 18.75, 21.87 kW/ m²).

The results are to be split into two sections: isothermal conditions and heat transfer conditions.

4.4.1 Isothermal Conditions

The limiting current densities of $CuCl_2$ were also determined from polarization curves .Tables (4.14-4.16) [41] for isothermal conditions

Table 4-14 The limiting current density at 30°C

r.p.m	Re	Limiting current density, (A/m²)
0	0	0.129
100	30137	0.157
200	60137	0.170
300	89987	0.201
400	120803	0.355

Table 4-15 The limiting current density at 45°C

r.p.m	Re	Limiting current density, (A/m²)
0	0	0.231
100	42500	0.306
200	85119	0.358
300	126901	0.486
400	170359	0.603

Table 4-16 The limiting current density at 60°C

r.p.m	Re	Limiting current density, (A/m²)
0	0	0.282
100	50821	0.335
200	101785	0.418
300	149743	0.543
400	203713	0.628

From Tables (4.14- 4.16) it is clear that limiting current density increases as velocity increases at constant temperature. At constant velocity, the limiting current density increases as temperature increases

4.4.2 Heat Transfer Conditions

The limiting current densities of $CuCl_2$ were also determined from polarization curves .Tables (4.17-4.25) [41] for heat transfer conditions. The surface temperatures under heat transfer conditions are also presented in these Tables.

Table 4-17 The limiting current density and interfacial temperature
at bulk temperature 30°C and Q =15.6kW/m²

r.p.m	T_i(℃)	Re	Limiting current density, A/m²)(
100	68	42304.168	0.325
200	65.81	84413.175	0.382
300	63.13	.00131293	0.477
400	59.1	148782.00	0.553

Table 4-18 The limiting current density and interfacial temperature
at bulk temperature 45°C and Q =15.6kW/m²

r.p.m	T_i(℃)	Re	Limiting current density, (A/m²)
100	76.12	54029.51	0.339
200	75.13	101642.11	0.415
300	72.7	152067.00	0.506
400	70.15	195426.03	0.610

Table 4-19 The limiting current density and interfacial temperature
at bulk temperature 60 °C and Q =15.6kW/m²

r.p.m	T_i(℃)	Re	Limiting current density, A/m²)(
100	86.3	59381.23	0.353
200	85.01	119593.76	0.428
300	84.22	177712.03	0.546
400	81.53	233518.74	0.630

Table 4-20 The limiting current density and interfacial temperature
at bulk temperature 30°C and Q =18.75kW/m²

r.p.m	T_i(℃)	Re	Limiting current density, (A/m²)
100	77.2	45550.24	0.342
200	74.8	90666.67	0.403
300	72.8	130579.0	0.518
400	71	175889.8	0.580

Table 4-21 The limiting current density and interfacial temperature
at bulk temperature 45°C and Q =18.75kW/m²

r.p.m	T_i(℃)	Re	Limiting current density, (A/m²)
100	83.01	52900.45	0.354
200	80.6	87781.00	0.429
300	78	153918.43	0.546
400	77.9	206104.59	0.616

Table 4-22 The limiting current density and interfacial temperature
at bulk temperature 60°C and Q =18.75kW/m²

r.p.m	T_i(℃)	Re	Limiting current density, (A/m²)
100	86.72	59544.65	0.366
200	83.8	120039.78	0.445
300	82.4	176148.58	0.552
400	80.3	231892.41	0.641

Table 4-23 The limiting current density and interfacial temperature
at bulk temperature 30°C and Q =21.87 kW/m²

r.p.m	T_i(℃)	Re	Limiting current density, (A/m²)
100	84.59	47685.8	0.368
200	83.3	95795.55	0.428
300	82.2	141864.6	0.519
400	79.8	186805.9	0.629

Table 4-24 The limiting current density and interfacial temperature
at 45°C and Q =21.87 kW/m²

r.p.m	T_i(℃)	Re	Limiting current density, (A/m²)
100	88.2	54929.83	0.381
200	86.7	110450.22	0.443
300	85.39	162855.85	0.561
400	81.81	212546.78	0.647

Table 4-25 The limiting current density and surface temperature
at 60°C and Q =21.87 kW/m²

r.p.m	T_i(℃)	Re	Limiting current density, (A/m²)
100	91.3	61163.65	0.459
200	88.7	122215.4	0.492
300	87.39	180950.9	0.567
400	84	237762.2	0.653

From Tables (4.17-4.25) it is clear that limiting current density increases as velocity increases at constant temperature. At constant velocity, the limiting current density increases as temperature increases. The interfacial temperature decreases with the increasing Reynolds number at a given temperature and heat flux. Furthermore the limiting current density increases with increasing heat flux for a given conditions of other variables.

4.5 Mass Transfer Correlations

4.5.1 Isothermal Conditions

Values of limiting current density were used to estimate the mass transfer coefficients k_m for the whole range of Re and temperature. Mass transfer studies of electrochemical system were usually conducted under limiting condition, in which case the mass transfer coefficient k_m can be expressed as:

$$k_m = \frac{i_{lm}}{nFC_b} \qquad \text{..... (4.1)}$$

The Sherwood number is a dimensionless number that expresses mass transport under forced convection flow conditions. The Sh number can be calculated according to the following equation:

$$Sh = \frac{k_m d}{D} \qquad \text{..... (4.2)}$$

Also, Schmidt number (Sc=v/D) is calculated as shown in the following Tables (4.26 - 4.34) for all the system analysed in this work. All the physical properties are found in appendix A.

Table 4-26 Mass transfer coefficients in cross flow at 30°C [40]

Re	$k_m * 10^5$,(m/s)	Sc
5000	2.5732	337.76
8000	3.1753	337.76
10000	3.7642	337.76
12000	4.3662	337.76

Table 4-27 Mass transfer coefficients in cross flow at 40°C [40]

Re	$k_m * 10^5$,(m/s)	Sc
5000	2.869	217.625
8000	3.297	217.625
10000	4.1032	217.625
12000	4.6243	217.625

Table 4-28 Mass transfer coefficients in cross flow at 50C [40]

Re	$k_m *10^5$,(m/s)	Sc
8000	3.345	155.576
10000	4.175	155.576
12000	4.755	155.576

Tables (4.26, 27 and 28) show that at a constant temperature, mass transfer coefficient increases as Reynolds number increases. At constant Reynolds number, mass transfer coefficient increases as temperature increases.

Table 4-29 Mass transfer coefficient for rotating cylinder at 30°C [67]

r.p.m	Re	$k_m *10^4$,(m/s)	Sc
50	15111.1	1.1489	305.14
200	60461.4	5.7683	305.14
300	90675.15	6.39612	305.14
400	120897.3	9.59418	305.14

Table 4-30 Mass transfer coefficient for rotating cylinder at 40°C [67]

r.p.m	Re	$k_m *10^4$,(m/s)	Sc
50	17313.07	2.19474	184.67
200	73601.2	6.3769	184.67
300	11381.16	8.3156	184.67
400	147172.4	10.12023	184.67

Table 4-31 Mass transfer coefficient for rotating cylinder at 50°C [67]

r.p.m	Re	$k_m *10^4$,(m/s)	Sc
50	21848.3	3.18277	140.68
200	87418	7.16793	140.68
300	13112.5	9.7623	140.68
400	174799.2	11.40718	140.68

Table 4-32 Mass transfer coefficient for rotating cylinder at 30°C [41]

r.p.m	Re	$k_m *10^5$,(m/s)	Sc
100	30137	1.784	715
200	60395	2.929	715
300	89987	3.877	715
400	120803	4.757	715

Table 4-33 Mass transfer coefficient for rotating cylinder at 45°C [41]

r.p.m	Re	$k_m *10^5$,(m/s)	Sc
100	42500	2.472	334
200	85119	4.054	334
300	126901	4.367	334
400	170359	6.586	334

Table 4-34 Mass transfer coefficient for rotating cylinder at 60°C [41]

r.p.m	Re	$k_m *10^5$,(m/s)	Sc
100	50821	3.286	226.5
200	101785	5.392	226.5
300	149743	7.138	226.5
400	203713	8.770	226.5

The above Tables (4.29-4.34) show that mass transfer coefficient increases as velocity increases at a constant temperature while at constant velocity, mass transfer coefficient increases as temperature increases.

4.5.2 Heat Transfer Conditions

When there is heat transfer, the value of heat transfer coefficient can be calculated according to this following equation:

$$Q = hA(T_s - T_b)$$ ….. (4.3)

and $$Pr = \frac{C_p m}{k_T}$$ ….. (4.4)

The following Tables (4.35-4.52)for all system analyzed show that at a constant temperature, mass transfer coefficient increases as velocity or (Re) increases ,while at constant velocity, it increases as temperature increases. The mass transfer coefficient increases as heat flux increases with constant temperature and velocity.

Also, the same trend and behaviors are observed regarding heat transfer coefficient as related to velocity, temperature and heat flux, as given in the following tables:

Table 4.35 Mass transfer coefficients and heat transfer coefficients for cross flow at 30°C and Q =10 kW/m² [40]

Re	k_m*10^5,(m/s)	Sc	$h(W/m^{2.}.K)$	Pr
5000	2.76	287.4	1250	4.96
8000	3.21	300.65	1666.67	5.07
10000	4.05	307.33	2000	5.13
12000	4.45	314.53	2500	5.19

Table 4-36 Mass transfer coefficients and heat transfer coefficients for cross flow at 40°C and Q =10 kW/m² [40]

Re	k_m*10^5,(m/s)	Sc	$h(W/m^{2.}.K)$	Pr
5000	2.89	194.59	1428.57	4.04
8000	3.58	202.16	2000	4.13
10000	4.60	206.10	2500	4.17
12000	4.86	214.31	3333.33	4.26

Table 4-37 Mass transfer coefficients and heat transfer coefficients for cross flow at 30°C and Q =30 kW/m² [40]

Re	k_m*10^5,(m/s)	Sc	$h(W/m^{2.}.K)$	Pr
5000	3.17	257.71	2307.69	4.69
8000	3.83	274.96	3000	4.84
10000	5.21	287.40	3750	4.96
12000	5.94	300.65	5000	5.07

Table 4-38 Mass transfer coefficients and heat transfer coefficients for cross flow at 40°C and Q =30 kW/m² [40]

Re	$k_m *10^5$,(m/s)	Sc	h(W/m²·K)	Pr
5000	3.38	180.62	2727.27	3.89
8000	4.20	187.42	3333.3	3.96
10000	5.68	194.59	4285.71	4.04
12000	6.79	202.16	6000	4.13

Table 4-39 Mass transfer coefficients and heat transfer coefficients for cross flow at 30°C and Q =50 kW/m² [40]

Re	$k_m *10^5$,(m/s)	Sc	h(W/m²·K)	Pr
5000	3.58	241.97	3125	4.54
8000	4.86	252.30	3571.43	4.64
10000	5.31	269.03	4545.45	4.79
12000	6.74	281.08	5555.56	4.90

Table 4-40 Mass transfer coefficients and heat transfer coefficients for cross flow at 40°C and Q =50 kW/m² [40]

Re	$k_m *10^5$,(m/s)	Sc	h(W/m²·K)	Pr
5000	3.94	171.06	3846.15	3.76
8000	5.15	180.62	4545.45	3.89
10000	5.98	187.42	5555.55	3.96
12000	6.92	192.76	6666.67	4.02

Table 4-41 Mass transfer coefficients and heat transfer coefficients for rotating cylinder at 30°C and Q =20 kW/m² [68]

r.p.m	Re	k_m*10^5,(m/s)	Sc	h(W/m²·K)	Pr
50	19415.7	2.222	168.93	753.30	4.067
200	76320.3	5.900	174.03	775.93	4.140
300	116467.8	7.816	184.67	964.876	4.307
400	147374.2	9.600	185.2	1029.687	4.377

Table 4-42 Mass transfer coefficients and heat transfer coefficients for rotating cylinder at 40°C and Q =20 kW/m² [68]

r.p.m	Re	k_m*10^5,(m/s)	Sc	h(W/m$^{2.}$.K)	Pr
50	22093.3	2.682	140.68	942.75	3.548
200	84674.7	6.217	155.45	1201.25	3.588
300	122757.9	8.168	156.08	1556.690	3.847
400	160898.1	9.753	157.86	1613.389	3.850

Table 4-43 Mass transfer coefficients and heat transfer coefficients for rotating cylinder at 50°C and Q =20 kW/m² [68]

r.p.m	Re	k_m*10^5,(m/s)	Sc	h (W/m$^{2.}$.K)	Pr
50	24974.4	2.566	93.20	1086.26	3.075
200	98540.9	6.5133	99.00	1165.89	3.140
300	143923.5	11.448	110.98	1583.570	3.244
400	189399.9	14.6100	118.75	1779.722	3.281

Table 4-44 Mass transfer coefficients and heat transfer coefficients for rotating cylinder at 30°C and Q =15.6kW/m² [41]

r.p.m	Re	k_m*10^5,(m/s)	Sc	h (W/m$^{2.}$.K)	Pr
100	42304.168	2.627	335.66	408.42	3.703
200	84413.175	4.284	349.57	428.93	3.722
300	131293.00	5.539	367.954	451.82	3.808
400	148782.00	6.523	399.841	477.11	3.967

Table 4-45 Mass transfer coefficients and heat transfer coefficients for rotating cylinder at 45°C and Q =15.6kW/m² [41]

r.p.m	Re	k_m*10^5,(m/s)	Sc	h (W/m$^{2.}$.K)	Pr
100	45029.51	3.407	206.03	498.71	2.756
200	101642.11	5.410	224.48	499.50	3.010
300	152067.00	6.996	235.27	548.74	3.067
400	195426.03	8.636	245.60	596.42	3.128

Table 4-46 Mass transfer coefficients and heat transfer coefficients for rotating cylinder at 60°C and Q=15.6kW/m² [41]

r.p.m	Re	k_m*10^5,(m/s)	Sc	h (W/m².K)	Pr
100	59381.23	4.126	146.4	590.11	2.458
200	119593.76	6.701	149.2	614.15	2.478
300	177712.03	8.804	151.5	628.5	2.490
400	233518.74	10.56	158.1	700	2.546

Table 4-47 Mass transfer coefficients and heat transfer coefficients for rotating cylinder at 30°C and Q =18.75kW/m² [41]

r.p.m	Re	k_m*10^5,(m/s)	Sc	h (W/m².K)	Pr
100	45550.24	2.926	282.43	396.39	3.341
200	90666.67	4.698	295.24	417.41	3.407
300	130579.0	6.052	310.82	435.05	3.507
400	175889.8	7.352	317.09	453.90	3.539

Table 4-48 Mass transfer coefficients and heat transfer coefficients for rotating cylinder at 45°C and Q =18.75kW/m² [41]

r.p.m	Re	k_m*10^5,(m/s)	Sc	h (W/m².K)	Pr
100	52900.45	3.537	196.37	485.92	2.810
200	87781.00	5.675	204.09	516.8	2.868
300	153918.43	7.336	214.85	564.24	2.937
400	206104.59	8.998	215.64	565.9	2.961

Table 4-49 Mass transfer coefficients and heat transfer coefficients for rotating cylinder at 60°C and Q =18.75kW/m² [41]

r.p.m	Re	k_m*10^5,(m/s)	Sc	h (W/m².K)	Pr
100	59544.65	4.14	145.5	685.76	2.4507
200	120039.78	6.73	147.92	726.65	2.4682
300	176148.58	8.66	155.76	846.36	2.5178
400	231892.41	10.45	161.08	917.24	2.5470

Table 4-50 Mass transfer coefficients and heat transfer coefficients for rotating cylinder at 30°C and Q =21.87kW/m² [41]

r.p.m	Re	k_m*10^5,(m/s)	Sc	h (W/m²·K)	Pr
100	47685.8	3.125	249.67	400.07	3.152
200	95795.55	5.067	255.45	407.50	3.186
300	141864.6	6.640	260.50	416.09	3.215
400	186805.9	8.003	271.78	436.34	3.280

Table 4-51 Mass transfer coefficients and heat transfer coefficients for rotating cylinder at 45°C and Q =21.87kW/m² [41]

r.p.m	Re	k_m*10^5,(m/s)	Sc	h (W/m²·K)	Pr
100	54929.83	3.703	179.63	503.93	2.6903
200	110450.22	6.001	183.89	521.11	2.7181
300	162855.85	7.824	189.38	538.46	2.7566
400	212546.78	9.322	200.66	586.14	2.8377

Table 4-52 Mass transfer coefficients and heat transfer coefficients for rotating cylinder at 60°C and Q =21.87kW/m² [41]

r.p.m	Re	k_m*10^5,(m/s)	Sc	h (W/m²·K)	Pr
100	61163.65	4.72	135.76	696.47	2.377
200	122215.4	6.904	141.09	761.67	2.418
300	180950.9	9.037	144.15	791.57	2.441
400	237762.2	10.79	151.63	905	2.495

4.6 Boundary Layer

For all systems studied, other effects such as transport and natural convection are small compared to the diffusion rate and so the overall mass transfer coefficient k_m is directly dependent on the diffusivity, the eddy diffusivity and inversely proportional to the diffusion boundary layer thickness [21]:

$$k_m = \frac{D + e_D}{d_D}$$

….. (4.5)

For cylinder in cross flow δ_D can be calculated by the above equation. In the absence of eddy diffusivity, calculate k from equation (4.1) and estimate D from appendix A .The δ_D values are calculated and given in Tables (4.53-4.61).

For rotating cylinder, δ_D can be calculated by the following equation [50, 51]:

$$d_D = 12.64 \frac{d^{0.3} n^{0.344} D^{0.356}}{V^{0.7}} \qquad \ldots.. (4.6)$$

For those cases where there is a temperature difference between the metal surface and the electrolyte a heat flux is flowing and the third boundary layer δ_t is present .Under steady heat flow conditions the rate of heat flux is dependent on the temperature gradient across the layer and the thermal conductivity of the layer. Assuming the thermal boundary layer lies entirely within the hydrodynamic boundary layer, heat is transferred across the boundary layer by conduction alone and the layer thickness is given as fellows [21]:

$$Q = hA(T_s - T_b) \qquad \ldots.. (4.7)$$

Both temperatures are known so h can be calculated and then δ_t is obtained from the following equation:

$$h = k_T / \delta_t \qquad \ldots.. (4.8)$$

where k_T : thermal conductivity.

However, under turbulent flow conditions for most aqueous solutions, the thermal boundary layer thickness and the hydrodynamic layer may be related indirectly using [52]:

$$d_H / d_t = Pr^{1/3} \qquad \ldots.. (4.9)$$

And using equation below to calculate the hydrodynamic boundary layer according to diffusion boundary layer [52] :

$$\frac{d_H}{d_D} = Sc^{1/3} \qquad\qquad \text{….. (4.10)}$$

In the present analysis of the different systems studied the thicknesses of the various boundary layers are calculated as explained above for isothermal and heat transfer conditions and presented in the following tables with the relevant values of Sc and Pr.

Table 4-53 Mass and hydrodynamic boundary layer thickness over cylinder with cross flow at 30°C [40]

Re	$\delta_D *10^5$ (m)	$\delta_H *10^4$ (m)	$Sc^{0.333}$
5000	9.216	6.418	6.964
8000	7.468	5.201	6.964
10000	6.299	4.387	6.964
12000	5.431	3.782	6.964

Table 4-54 Mass and hydrodynamic boundary layer thickness over cylinder with cross flow at 40°C [40]

Re	$\delta_D *10^5$ (m)	$\delta_H *10^4$ (m)	$Sc^{0.333}$
5000	10.524	6.330	6.015
8000	9.158	5.509	6.015
10000	7.359	4.426	6.015
12000	6.529	3.927	6.015

Table 4-55 Mass and hydrodynamic boundary layer thickness over cylinder with cross flow at 50°C [40]

Re	$\delta_D *10^5$ (m)	$\delta_H *10^4$ (m)	$Sc^{0.333}$
8000	10.64	5.722	5.378
10000	8.520	4.582	5.378
12000	7.481	4.023	5.378

Table 4-56 Mass, thermal and hydrodynamic boundary layer thicknesses over cylinder with cross flow at 30°C and Q =10 kW/m^2 [40]

Re	$\delta_D *10^5$ (m)	$Sc^{0.333}$	$\delta_T *10^4$ (m)	$Pr^{0.333}$	$\delta_H *10^4 = \delta_D \, Sc^{0.333}$ (m)	$\delta_H *10^4 = \delta_T \, Pr^{0.333}$ (m)
5000	9.225	6.599	4.912	1.704	6.107	8.370
8000	7.738	6.698	3.684	1.716	5.183	6.322
10000	6.056	6.747	3.070	1.725	4.086	5.296
12000	5.442	6.799	2.456	1.731	3.700	4.251

Table 4-57 Mass, thermal and hydrodynamic boundary layer thicknesses over cylinder with cross flow at 40°C and Q =10 kW/m^2 [40]

Re	$\delta_D *10^5$ (m)	$Sc^{0.333}$	$\delta_T *10^4$ (m)	$Pr^{0.333}$	$\delta_H *10^4 = \delta_D \, Sc^{0.333}$ (m)	$\delta_H *10^4 = \delta_T \, Pr^{0.333}$ (m)
5000	10.853	5.794	4.396	1.596	6.288	7.016
8000	8.588	5.868	3.140	1.604	5.039	5.037
10000	6.616	5.897	2.512	1.609	3.901	4.042
12000	6.134	5.973	1.880	1.620	3.663	3.046

Table 4-58 Mass, thermal and hydrodynamic boundary layer thicknesses over cylinder with cross flow at 30°C and Q =30 kW/m^2 [40]

Re	$\delta_D *10^5$ (m)	$Sc^{0.333}$	$\delta_T *10^4$ (m)	$Pr^{0.333}$	$\delta_H *10^4 = \delta_D \, Sc^{0.333}$ (m)	$\delta_H *10^4 = \delta_T \, Pr^{0.333}$ (m)
5000	8.514	6.363	2.660	1.673	5.417	4.450
8000	6.819	6.491	2.046	1.649	4.426	3.374
10000	4.892	6.598	1.637	1.704	3.228	2.789
12000	4.182	6.698	1.228	1.718	2.801	2.109

Table 4-59 Mass, thermal and hydrodynamic boundary layer thicknesses over cylinder with cross flow at 40°C and Q =30 kW/m^2 [40]

Re	$\delta_D *10^5$ (m)	$Sc^{0.333}$	$\delta_T *10^4$ (m)	$Pr^{0.333}$	$\delta_H *10^4 = \delta_D \, Sc^{0.333}$ (m)	$\delta_H *10^4 = \delta_T \, Pr^{0.333}$ (m)
5000	9.659	5.652	2.303	1.573	5.459	3.623
8000	7.619	5.722	1.884	1.582	4.359	2.980
10000	5.518	5.794	1.465	1.593	3.197	2.334
12000	4.531	5.869	1.047	1.604	2.659	1.679

Table 4-60 Mass, thermal and hydrodynamic boundary layer thicknesses over cylinder with cross flow at 30°C and Q=50 kW/m^2 [40]

Re	$\delta_D *10^5$ (m)	$Sc^{0.333}$	$\delta_T *10^4$ (m)	$Pr^{0.333}$	$\delta_H *10^4 = \delta_D \, Sc^{0.333}$ (m)	$\delta_H *10^4 = \delta_T \, Pr^{0.333}$ (m)
5000	7.633	6.231	1.965	1.656	4.756	3.254
8000	5.622	6.319	1.719	1.668	3.552	2.867
10000	4.968	6.455	1.351	1.686	3.207	2.277
12000	3.821	6.550	1.105	1.699	2.503	1.877

Table 4-61 Mass ,thermal and hydrodynamic boundary layer thicknesses over cylinder with cross flow at 40°C and Q =50 kW/m^2 [40]

Re	$\delta_D *10^5$ (m)	$Sc^{0.333}$	$\delta_T *10^4$ (m)	$Pr^{0.333}$	$\delta_H *10^4 = \delta_D \, Sc^{0.333}$ (m)	$\delta_H *10^4 = \delta_T \, Pr^{0.333}$ (m)
5000	8.513	5.550	1.632	1.555	4.725	2.538
8000	7.462	5.562	1.381	1.573	4.150	2.172
10000	5.249	5.723	1.130	1.582	3.004	1.788
12000	4.554	5.767	0.942	1.590	2.626	1.498

Table 4-62 Mass and hydrodynamic boundary layer thickness over rotating cylinder at 30°C [67]

r.p.m	$\delta_D *10^5$ (m)	$\delta_H *10^4$ (m)	$Sc^{0.333}$
50	13.736	4.059	6.732
200	5.525	1.538	6.732
300	3.946	1.158	6.732
400	3.234	0.947	6.732

Table 4-63 Mass and hydrodynamic boundary layer thickness over rotating cylinder at 40°C [67]

r.p.m	$\delta_D *10^5$ (m)	$\delta_H *10^4$ (m)	$Sc^{0.333}$
50	13.870	7.899	5.695
200	5.255	2.992	5.695
300	3.957	2.254	5.695
400	3.235	1.842	5.695

Table 4-64 Mass and hydrodynamic boundary layer thickness over rotating cylinder at 50°C [67]

r.p.m	$\delta_D * 10^5$ (m)	$\delta_H * 10^4$ (m)	$Sc^{0.333}$
50	13.540	7.042	5.201
200	5.133	2.669	5.201
300	3.865	2.010	5.201
400	1.501	0.781	5.201

Table 4-65 Mass, thermal and hydrodynamic boundary layer thicknesses over rotating cylinder at 30°C and Q =20 kW/m² [68]

r.p.m	$\delta_D * 10^5$ (m)	$Sc^{0.333}$	$\delta_T * 10^4$ (m)	$Pr^{0.333}$	$\delta_H * 10^4 = \delta_D Sc^{0.333}$ (m)	$\delta_H * 10^4 = \delta_T Pr^{0.333}$ (m)
50	12.91	5.528	0.838	1.596	7.137	1.337
200	4.90	5.583	0.812	1.606	2.736	1.304
300	3.62	5.695	0.651	1.627	2.062	1.059
400	2.89	5.699	0.609	1.636	1.647	0.996

Table 4-66 Mass, thermal and hydrodynamic boundary layer thicknesses over rotating cylinder at 40°C and Q=20 kW/m² [68]

r.p.m	$\delta_D * 10^5$ (m)	$Sc^{0.333}$	$\delta_T * 10^4$ (m)	$Pr^{0.333}$	$\delta_H * 10^4 = \delta_D Sc^{0.333}$ (m)	$\delta_H * 10^4 = \delta_T Pr^{0.333}$ (m)
50	12.70	5.200	0.679	1.525	6.604	1.035
200	4.55	5.377	0.531	1.531	2.447	0.813
300	3.46	5.384	0.408	1.567	1.863	0.639
400	2.82	5.404	0.393	1.581	1.552	0.621

Table 4-67 Mass ,thermal and hydrodynamic boundary layer thicknesses over rotating cylinder at 50°C and Q=20 kW/m² [68]

r.p.m	$\delta_D * 10^5$ (m)	$Sc^{0.333}$	$\delta_T * 10^4$ (m)	$Pr^{0.333}$	$\delta_H * 10^4 = \delta_D Sc^{0.333}$ (m)	$\delta_H * 10^4 = \delta_T Pr^{0.333}$ (m)
50	13.12	4.533	0.602	1.454	5.947	0.875
200	4.98	4.626	0.566	1.464	2.304	0.827
300	3.74	4.806	0.413	1.480	1.797	0.611
400	3.13	4.915	0.368	1.486	1.538	0.547

Table 4-68 Mass and hydrodynamic boundary layer thickness over rotating cylinder at 30°C [41]

r.p.m	$\delta_D * 10^5$ (m)	$\delta_H * 10^4$ (m)	$Sc^{0.333}$
100	6.041	5.470	9.055
200	3.682	3.334	9.055
300	2.781	2.518	9.055
400	2.266	2.052	9.055

Table 4-69 Mass and hydrodynamic boundary layer thickness over rotating cylinder at 45°C [41]

r.p.m	$\delta_D * 10^5$ (m)	$\delta_H * 10^4$ (m)	$Sc^{0.333}$
100	6.208	4.543	7.318
200	3.784	2.770	7.318
300	2.858	2.091	7.318
400	2.329	1.704	7.318

Table 4-70 Mass and hydrodynamic boundary layer thickness over rotating cylinder at 60°C [41]

r.p.m	$\delta_D * 10^5$ (m)	$\delta_H * 10^4$ (m)	$Sc^{0.333}$
100	6.433	3.922	6.096
200	2.921	1.781	6.096
300	2.962	1.806	6.096
400	2.413	1.471	6.096

Table 4-71 Mass, thermal and hydrodynamic boundary layer thicknesses over rotating cylinder at 30°C and Q =15.6 kW/m^2 [41]

r.p.m	$\delta_D * 10^5$ (m)	$Sc^{0.333}$	$\delta_T * 10^4$ (m)	$Pr^{0.333}$	$\delta_H * 10^4 = \delta_D Sc^{0.333}$ (m)	$\delta_H * 10^4 = \delta_T Pr^{0.333}$ (m)
100	6.380	6.949	1.510	1.547	4.433	2.336
200	3.819	7.044	1.432	1.549	2.690	2.218
300	2.873	7.166	1.324	1.561	2.059	2.067
400	2.328	7.367	1.157	1.583	1.715	1.832

Table 4-72 Mass, thermal and hydrodynamic boundary layer thicknesses over rotating cylinder at 45°C and Q =15.6 kW/m^2 [41]

r.p.m	$\delta_D *10^5$ (m)	$Sc^{0.333}$	$\delta_T *10^4$ (m)	$Pr^{0.333}$	$\delta_H *10^4 = \delta_D$ $Sc^{0.333}$ (m)	$\delta_H *10^4 =$ $\delta_T Pr^{0.333}$ (m)
100	6.275	5.906	1.267	1.402	3.706	1.776
200	3.911	6.077	1.226	1.444	2.377	1.770
300	2.950	6.173	1.128	1.453	1.821	1.639
400	2.397	6.262	1.024	1.462	1.501	1.498

Table 4-73 Mass, thermal and hydrodynamic boundary layer thicknesses over rotating cylinder at 60°C and Q =15.6 kW/m^2 [41]

r.p.m	$\delta_D *10^5$ (m)	$Sc^{0.333}$	$\delta_T *10^4$ (m)	$Pr^{0.333}$	$\delta_H *10^4 = \delta_D$ $Sc^{0.333}$ (m)	$\delta_H *10^4 = \delta_T$ $Pr^{0.333}$ (m)
100	6.633	5.270	1.096	1.349	3.496	1.479
200	4.035	5.304	1.042	1.353	2.140	1.409
300	3.042	5.331	1.008	1.355	1.622	1.366
400	2.475	5.407	0.896	1.365	1.338	1.223

Table 4-74 Mass, thermal and hydrodynamic boundary layer thicknesses over rotating cylinder at 30°C and Q =18.75 kW/m^2 [41]

r.p.m	$\delta_D *10^5$ (m)	$Sc^{0.333}$	$\delta_T *10^4$ (m)	$Pr^{0.333}$	$\delta_H *10^4 = \delta_D$ $Sc^{0.333}$ (m)	$\delta_H *10^4 = \delta_T$ $Pr^{0.333}$ (m)
100	6.321	6.561	1.626	1.495	4.139	2.429
200	3.842	6.659	1.541	1.505	2.557	2.318
300	2.893	6.774	1.444	1.519	1.959	2.193
400	2.355	6.819	1.411	1.524	1.605	2.148

Table 4-75 Mass, thermal and hydrodynamic boundary layer thicknesses over rotating cylinder at 45°C and Q =18.75 kW/m^2 [41]

r.p.m	$\delta_D *10^5$ (m)	$Sc^{0.333}$	$\delta_T *10^4$ (m)	$Pr^{0.333}$	$\delta_H *10^4 = \delta_D$ $Sc^{0.333}$ (m)	$\delta_H *10^4 = \delta_T$ $Pr^{0.333}$ (m)
100	6.478	5.812	1.353	1.411	3.765	1.909
200	3.942	5.888	1.270	1.421	2.321	1.805
300	2.971	5.989	1.160	1.432	1.779	1.661
400	2.420	5.997	1.147	1.436	1.451	1.647

Table 4-76 Mass, thermal and hydrodynamic boundary layer thicknesses over rotating cylinder at 60°C and Q =18.75 kW/m^2 [41]

r.p.m	$\delta_D *10^5$ (m)	$Sc^{0.333}$	$\delta_T *10^4$ (m)	$Pr^{0.333}$	$\delta_H *10^4 = \delta_D$ $Sc^{0.333}$ (m)	$\delta_H *10^4 = \delta_T$ $Pr^{0.333}$ (m)
100	6.635	5.259	0.972	1.349	3.489	1.311
200	4.038	5.289	0.917	1.351	2.136	1.239
300	3.031	5.380	0.785	1.360	1.631	1.068
400	2.472	5.441	0.723	1.366	1.345	0.988

Table 4-77 Mass, thermal and hydrodynamic boundary layer thicknesses over rotating cylinder at 30°C and Q =21.87 kW/m^2 [41]

r.p.m	$\delta_D *10^5$ (m)	$Sc^{0.333}$	$\delta_T *10^4$ (m)	$Pr^{0.333}$	$\delta_H *10^4 = \delta_D$ $Sc^{0.333}$ (m)	$\delta_H *10^4 = \delta_T$ $Pr^{0.333}$ (m)
100	6.396	6.297	1.628	1.466	4.028	2.387
200	2.893	6.345	1.597	1.472	1.836	2.351
300	2.937	6.387	1.563	1.476	1.876	2.307
400	2.377	6.477	1.487	1.486	1.539	2.209

Table 4-78 Mass, thermal and hydrodynamic boundary layer thicknesses over rotating cylinder at 45°C and Q =21.87 kW/m^2 [41]

r.p.m	$\delta_D *10^5$ (m)	$Sc^{0.333}$	$\delta_T *10^4$ (m)	$Pr^{0.333}$	$\delta_H *10^4 = \delta_D$ $Sc^{0.333}$ (m)	$\delta_H *10^4 = \delta_T$ $Pr^{0.333}$ (m)
100	6.513	5.642	1.309	1.391	3.675	1.821
200	3.961	5.687	1.265	1.396	2.253	1.766
300	2.987	5.743	1.213	1.402	1.715	1.701
400	2.428	5.854	1.121	1.416	1.421	1.587

Table 4-79 Mass, thermal and hydrodynamic boundary layer thicknesses over rotating cylinder at 60°C and Q =21.87 kW/m^2 [41]

r.p.m	$\delta_D *10^5$ (m)	$Sc^{0.333}$	$\delta_T *10^4$ (m)	$Pr^{0.333}$	$\delta_H *10^4 = \delta_D$ $Sc^{0.333}$ (m)	$\delta_H *10^4 = \delta_T$ $Pr^{0.333}$ (m)
100	6.674	5.139	0.959	1.335	3.427	1.280
200	4.055	5.206	0.876	1.342	2.110	1.176
300	3.057	5.243	0.842	1.346	1.603	1.133
400	2.480	5.332	0.735	1.356	1.322	0.997

4.7 Analysis of Variances

An important technique for analyzing the effect of categorical factors on a response is to perform an Analysis of Variance. ANOVA decomposes the variability in the response variable amongst the different factors. Depending upon the type of analysis, it may be important to determine: (a) which factors have a significant effect on the response, and/or (b) how much of the variability in the response variable is attributable to each factor [61].

4.7.1 Two ways ANOVA

When more than one factor is present and the factors are crossed, a multifactor ANOVA is appropriate. Both main effects and interactions between the factors may be estimated. The following example illustrate two way ANOVA analysis to demonstrate the effect of Reynolds number (or r.p.m) and temperature on the limiting current density without replication for the results given previously in Table (3.1) for two way ANOVA without replication.

The experiential data are obtained from Tables (4.11-4.13) as follows:

	30	40	50
50	1.88	2.2	1.3
200	4.97	5.1	3.3
300	6.6	6.7	5.8
400	8.1	8	7.4

The ANOVA calculations are presented in the following tables:

Table 4- 80 Two ways ANOVA

Source of Variation	SS	DF	MS	MSR	$F_{0.05}$	$F_{0.01}$
Columns (Temp.)	2.65875	2	1.329375	14.6053957	5.14	10.92
Rows(r.p.m)	61.26856	3	20.4228528	224.379009	4.76	9.78
Error	0.546117	6	0.09101944			
Total	64.47343	11				

This Table shows that Re (r.p.m) and temperature are both significant at 0.01 and 0.05 levels, but Re (r.p.m) is more effective than temperature.

4.7.2 Three Ways ANOVA

The following example illustrates three way ANOVA analysis to demonstrate the effect of Reynolds number (or r.p.m), temperature and heat flux on the limiting current density without replication for the method and procedure given previously in Table (3.3).The experimental data from Tables (4.2-4.7) leading to the following ANOVA :

Table 4-81 ANOVA results showing effect of each variable in the cathodic region under heat transfer conditions

Source of Variation	Sum of Square	DF	MS	MSR	$F_{0.05}$	$F_{0.01}$
Among Columns(Re)	16.799764	3	5.5999213	81.9555697	3.20	5.18
Among Rows(Q)	6.5271462	2	3.2635735	47.762893	3.59	6.11
Among Groups (Temp.)	0.55282176	1	0.55282176	8.0906302	4.45	8.4
Column-Row Interaction(Re*Q)	0.98577954	6				
Column-Group Interaction (Re*Temp.)	0.031751669	3				
Row-Group Interaction (Q*Temp.)	0.0451987	2				
Column-Row –Group Interaction (Re*Q*Temp.)	0.099053493	6				
Residual	1.161586889	17	0.06832864			

4.7.3 Higher Order Interactions

So far, the interactions that have been described are called "two-way" interactions. They are two-way interactions because they involve the interaction of two variables. A three-way interaction is an interaction among three variables. These interactions can not be determined because the experimental data were not repeated [63] .The purpose of this method is to show the mean effect of variables and interactions as in the following Table (4-82) .The remaining Tables are in Appendices (C.19-27)

Table 4.82 The mean effect of variables and their interactions using two level responses under heat transfer conditions (Limiting current density)[40].

	Response	Mean Effect	DF
1	2.4964		
H	3.2388	1.30152	1
T	2.2107	0.14963	1
HT	3.0201	0.14125	1
R	4.0257	2.04643	1
HR	6.1016	0.5256	1
TR	3.723	0.14963	1
HTR	5.3014	-0.14113	1
Total	30.1177		

Chapter Five
Discussion

5.1 Introduction

This chapter serves as an introduction for the effect of velocity, temperature and heat flux on the corrosion behavior of different metals. Specifically two systems are selected for the study: cylinder in cross flow and rotating cylinder electrode in order to show the effect of this variance on the corrosion and their interactions.

Corrosion and electrochemical materials wastage processes take on many different forms. Most of these forms are dramatically affected by the relative flow rates of the reactants in the corroding system. It is well known that relative electrolyte velocity can strongly influence rates and mechanisms of corrosion. One of the most important factors affecting corrosion reactions in the presence of a flowing liquid is the linear velocity of the flowing fluid at the interface of the metal or metal oxide surface. This linear velocity is not of necessity, equal to the bulk flow rate [69]. The other factors are temperature and heat flux which affect on corrosion .All of these factors will be discussed in this chapter.

Although it has been recognized for many years that hydrodynamic effects are often important in determining the rate of corrosive attack on metals, little attention has been paid to the influence of hydrodynamic factors on the analysis of the kinetics of materials degradation .Several approaches have been used to obtain some assessment of the magnitude of these hydrodynamic effects .These have included techniques such as pumping the corrosive fluid through tubular specimen or rotating the specimens [64].

This chapter presents a discussion of their significance under isothermal and heat transfer conditions as fellows:

5.2 Isothermal Conditions

5.2.1 Cathodic Region

5.2.1.1 Effect of Velocity

It was shown in Tables (4.1, 8, 9,10,14,15 and 16) that under isothermal conditions, increasing velocity at constant bulk temperature tends to increase cathodic current density. This is because that limiting current density increases with increasing r.p.m or (Re).This may be attributed to breakdown a hydrodynamic boundary layer and diffusion layer is formed. It is also observed that the higher the r.p.m or (Re), the higher the solution flows and thinner the diffusion layer [70], according to this equation:

$$i_{lm} = \frac{DnFC_b}{d_D} \qquad\qquad ..... \quad (5.1)$$

This would give a higher rate of transfer oxygen to the metal surface and, consequently enhances the rate of cathodic reaction.

The effect of the speed of rotation on the rate of cathodic reaction can also be used to determine whether the cathodic process is diffusion or chemically controlled process. If the rate of the process increases by increasing the speed of rotation, then the reaction is diffusion controlled. However, if the rate of the process is independent of the rotation, so the reaction is likely to be chemically controlled [16].

The effects of velocity and temperature on cathodic region were examined. Results were analysed using a two-way independent samples.i.e, ANOVA.

It is shown from Table (C.1) that velocity and temperature have significant effects because mean square ratio is higher than the tabulated F value at 95% and 99%, but the effect of velocity is more significant than

83

temperature. It is shown from table (C.2) that velocity has significant influence at value 95% and 99% while the temperature is significant at 95% and the effect of velocity is more significant. It is also shown from table (C.3) that temperature has significant influence because mean square ratio is higher than the tabulated F value at 95% and 99%, and velocity is less significant at both levels.

Flow affected only those corrosion processes which are controlled by transfer of reactants or/and and products to/from the metal surface, i.e., mass transfer controlled processes, but has no effect on activation controlled process. On mild steel and large number of other metals and alloys, transfer of the oxygen to the cathodic area is often rate controlling, whereas with relatively noble metals such as copper the rate of diffusion of metal ions away from the surface may be the controlling factor, in either case, flow is important. It is well known that velocity leads to increase the corrosion rate only if the process is under concentration polarization control [16, 1].

The corrosion of steel in neutral solution is process controlled by transfer of oxygen to the metal so it is concentration control [4]. This is shown in the analysis of variance in Tables (C.1, 2) where velocity is more significant.

The corrosion of copper in neutral solution is activation controlled because the corrosion resistance of copper is due to its being relatively noble metal. Its satisfactory service in water depends on formation of relatively thin adherent films of corrosion products (e.g., cuprous oxide and basic copper carbonate).It has only a weak tendency to passivation, and hence the effect of differential aeration is very sligh.However, the influence of copper ion concentration on the potential of copper solution is very marked. The reduction of copper ions takes place through two steps [71]:

$$Cu^{+2} + e \xleftarrow{\quad Slow \quad} Cu^{+} \quad \text{Step (1)}$$

$$Cu^{+} + e \xleftarrow{\text{Fast}} Cu \qquad\qquad\qquad \text{Step (2)}$$

It is assumed that the first step in this process occurred slowly and the rate is controlled by the equilibrium between Cu^{+2} and Cu^{+}. For this reason, when there are varying solution velocities over a copper surface (e.g., when the solution is stirred, the parts exposed to solution with the higher rate of movement becomes anode and not cathode as would be the case for iron [72, 16]. This is seen in the analysis of variance in Tables (C.3) where temperature is more significant.

5.2.1.2 Effect of Temperature

It is shown from Tables (4.1, 8, 9, 10, 14, 15 and 16) that current density increases with increasing bulk temperature at constant velocity. Temperature plays a significant role in the solubility of metal in water, particularly at neutral to acidic pH [1].

It is shown from Table (C.1) that velocity and temperature have significant effect, but the effect of velocity is more significant than temperature. It is shown from table (C.2) that velocity has significant influence at 95% and 99% levels while the temperature is significant at 95% so the effect of velocity is more significant. Also shown from table (C.3) that temperature has significant influence because mean square ratio is higher than the tabulated F value at 95% and 99% and velocity is significant at both levels. As the temperature of the environment increases, the rate of oxygen diffusion to the metal surface also increases; the viscosity of solution decreases and the electrical conductivity of the solution increases. All these factors can enhance the corrosion rate. This behavior can be interpreted as follows: the temperature increment accelerates both the cathodic reaction rate and diffusion rate of oxygen by increasing the molecular movement of the

ions. Additionally, one factor that plays an important role in determining the corrosion rate is Re number. The increment in the Re number enhances the eddy diffusion of oxygen ions, from the bulk of solution to the metal surface, leading to a higher corrosion rate. When Re increases, the amount of oxygen supplied to the surface from the bulk will also be increased. Then the combined effect of two variables, namely, hydrogen molecular diffusivity and solution velocity (eddy diffusion), will determine the trend of the corrosion rate with increasing temperature [73].

Iron is affected by velocity more significantly than temperature because it is activation controlled so it increases the solubility of oxygen and decreases the resistivity on iron surface [16].

Copper dissolution is under diffusion control, so it is affected by both temperature and velocity, the decrease in the diffusion coefficient (D) of Cu^{2+} ion in solution which is due to the increase in the interfacial viscosity (m) is in accordance with Stokes-Einstein equation as shown in [74]:

$$\frac{mD}{T} = Cons \tan t \qquad \qquad ..... (5.2)$$

The increase in interfacial viscosity is caused by the adsorption of surfactant molecules at the copper surface towards the solution.It has been observed for many metals that the magnitude of limiting current density increases with temperature and that the activation energy for dissolution is low, suggestive of diffusion – limited anode process when the migration of corrosion products away from the surface is rate controlling.

5.3 Heat Transfer Conditions

5.3.1 Cathodic Region

5.3.1.1 Effect of Velocity

It is shown from Tables (4.2 , 3, 4, 5, 6, 7, 11, 12, 13, 17- 25) that cathodic current density increases as heat transfer rate increases. This is because a decrease of diffusion boundary layer as the velocity increases. When the velocity increases, this will lead to increase the amount of oxygen arriving to the metal surface and decrease the fluid temperature and the temperature gradient. A third boundary layer, thermal boundary layer, is established under steady state heat flow conditions, the temperature in this layer is higher than bulk temperature [75]. The rate of heat flow is dependent on the temperature gradient across the layer and its thermal conductivity. The effects of velocity, temperature and heat flux were examined to visualize their effect on cathodic region. Results were analysed using two way and three-way independent samples ANOVA. It is shown from Table (C.4) that velocity and heat flux are significant because mean square ratio is higher than the tabulated F value at 95% and 99%, and temperature is significant only slightly at 95%. It is shown from Table (C.5) that velocity and temperature are significant because MSR is higher than the tabulated F value at 95% and 99% with temperature much less significant. And in Table (C.6) that velocity, heat flux and temperature are significant because mean square ratio is higher than the tabulated F value at 95% and 99%.In all three Tables (C.4, 5 and 6) show that velocity is more significant, followed by heat flux and then temperature because the interfacial temperature is higher than bulk temperature, thus leads to increase the diffusion coefficient and decrease the thermal boundary layer .

Mechanistic studies have revealed that electrochemical is a diffusion controlled reaction which takes place at the limiting current, being this

parameter attained most probably when the diffusion layer becomes saturated with Cu $^{2+}$. The limiting current depends on the rate of mass transfer of Cu^{2+} from the diffusion layer to the bulk of the solution. The rate of mass transfer depends on the relative movement of the anode and the electrolyte, physical properties of the electrolyte, temperature and geometry of the anode [74].Table (C.19) shows that the mean effect of the velocity (Re) is more significant than that heat flux and temperature, this agrees with the analysis of variance in Table (C.4).So the main effect (velocity and heat flux) is more significant than other. Table (C.19) indicates the presence of second order mean effects, i.e., HT, HR and TR. The third order effect interaction (HRT) is slightly negative. Table (C.20) shows that mean effect of the velocity (Re) is more significant than that heat flux and temperature .So the main effect (velocity) is more significant than other. Table (C.20) indicates the presence of second order mean effects, i.e., HT, HR and TR. The third order effect interaction (HRT) is slightly negative.

5.3.1.2 Effect of Temperature

Tables (4.2 , 3,4,5,6,7,11,12,13,17-25) shows the effect of temperature on cathodic region under heat transfer condition as that under isothermal conditions. At constant heat flux and velocity, increasing temperature will decrease the limiting current density
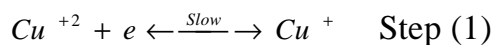
It is shown from Table (C.4) that velocity and heat flux have significant effect because mean square ratio is higher than the tabulated F value at 95% and 99%, and temperature is significant slightly only at 95% . It is shown from Table (C.5) that velocity and temperature are significant because mean square ratio is higher than the tabulated F value at 95% and 99%. The influence of velocity is much more than temperature. Table (C.6) shows that

velocity, heat flux and temperature are significant at 95% and 99% as the reaction is also activation controlled .In all three Tables (C.4, 5 and 6) it is clearly shown that velocity is more significant than heat flux and temperature.

The presence of heat transfer leads to form the thermal boundary layer near the electrode. Thus it may be expected that a temperature in this layer is ranging from surface temperature to solution temperature. The presence of this temperature will lead to increase the dissolution of the electrode by decreasing the surface concentration of this ion and enhancing their transfer to the bulk. Temperature also affects on the physical properties ν, and C_p [21].

Since the growth of magnetite involves diffusion of ions through the oxide layer into the solution, an increase in flow velocity will increase the rate of their removal as a result of the decrease in the thickness of the boundary layer. The increase in temperature increased the solubility of the magnetite that resulted in dissolution of the film [75].

The presence of heat transfer may lead to form thermal eddies adjacent to the metal surface. The thermal convection which depends on temperature gradient as the velocity increases the surface temperature decreases [59].

5.4 Mass Transfer Coefficient

5.4.1 Isothermal Conditions

Tables (4.26 - 34) show that mass transfer coefficient values increase as velocity increases at constant temperature.
Thus because increasing velocity will decrease the diffusion boundary layer and increase a concentration gradient according to this equation [73]:

$$k_m = \frac{D}{d_D} \qquad\qquad ..... (5.3)$$

The effects of velocity and temperature on mass transfer coefficient were examined. Results were analysed using a two-way independent samples

ANOVA .It is shown from Table (C.7) that velocity and temperature are significant because mean square ratio is higher than the tabulated F value at 95% and 99%. In Table (C.8) shows that velocity and temperature are significant effects because mean square ratio is higher than tabulated F value at 95% and 99%.Table (C.9) shows also that velocity and temperature are significant at the two levels. The tables show that velocity is more significant.

Mass transfer coefficient is flow dependent, because it increases as the rotation rate also increases. The effect of increasing velocity is to increase the surface concentration of the corroding metal or to decrease the surface concentration of the corrosion product. Therefore, the rate of corrosion increases with increasing velocity. At higher velocities, the rate of mass transfer is much faster than the rate of charge transfer reaction at the metal surface. Changing Sc by temperature leads to the change of many physical properties that have a direct influence on k_m. These physical properties are diffusivity, bulk concentration C_b and kinematic viscosity. The present results indicate that, at least for the higher Reynolds numbers, reduced dependence of k_m on the Reynolds number exists and, hence, k_m may no longer be diffusion limited (mass transfer will not influence reaction rate).Flow structure could be such that the diffusion layer of the whole of electrode surface may not be well within a laminar wall layer [64].

5.4.2 Heat Transfer Conditions

Tables (4.35 -4.52) show that mass transfer coefficient values, increase as velocity increase at constant temperature. Thus because increased velocity will decrease the diffusion boundary layer.

The effects of velocity, temperature and heat flux on mass transfer coefficient were examined. Results were analysed using a three-way independent samples ANOVA.

It is shown from Table (C.10) that velocity and heat flux have significance because mean square ratio is higher than the tabulated F value at 95% and 99%, and temperature is not significant. It is shown from Table (C.11) that velocity has significance because mean square ratio is higher than the tabulated F value at 95% and 99%, and temperature is not significant. Table (C.12) that velocity and temperature only at 95% are significant because mean square ratio is higher than the tabulated F value at 95% and 99% but the heat flux is not significant. In all Tables (C.10, 11 and 12) show that velocity is more significant than heat flux and temperature.

Corrosion rate dependence on mass transfer of a reactant to or a product from the surface is one of the most common causes for corrosion being sensitive to fluid motion. In the absence of films, the primary effect of flow on corrosion is through mass transfer of the species involved in the corrosion reaction at the metal surface. For mass transfer in turbulent liquid flow, due to very large Schmidt numbers, all the concentration changes occur in a very narrow layer adjacent to the metal surface, deep within the viscous sub layer in the so-called mass-transfer boundary layer. The thickness of this layer is a function of the flow rate (Reynolds number) and flow geometry. Mass transfer usually is associated with limiting currents (i.e., with situations where the electrochemical processes at the metal surface proceed so fast that it is difficult to transport enough reactants from the bulk). Conversely, sufficiently rapid removal of corrosion products from the surface also can become limiting, which can lead to accumulation, (super) saturation and precipitation of surface films. However, if the corrosion process is under charge transfer

(activation) or chemical reaction rate control, changes in the flow and associated mass transfer will have no effect on the corrosion rate [76].

Table (C.21) shows that mean effect of the velocity (Re) is more significant than that heat flux and temperature, this is which agrees with the analysis of variance in Table (C.10).So the main effect (velocity and heat flux) is more significant than other. Table (C.21) indicates the presence of second order mean effects, i.e., HT, HR and TR. The third order effect interaction (HRT) is slightly negative. Table (C.22) shows that mean effect of the velocity (Re) is more significant than that heat flux and temperature, this is which agrees with the analysis of variance in Table (C.12) .So the main effect (velocity and temperature) is more significant than heat flux. Table (C.21) indicates the presence of second order mean effects, i.e., HT, HR and TR. The third order effect interaction (HRT) is slightly negative.

5.5 Heat Transfer Coefficient

Tables (4.35 - 52) show that heat transfer coefficient increases as velocity increases at constant temperature. Thus because increasing velocity leads to increasing in temperature gradient and decrease a thermal boundary layer according to this equation:

$$h = \frac{k}{\Delta x} = \frac{k}{d_t}$$ ….. (5.4)

Changing temperature changes many physical properties, namely, k_T, v, and C_p.

The effects of velocity, temperature and heat flux on heat transfer coefficient were examined. Results were analysed using a three-way independent samples ANOVA.

It is shown from Table (C.13) that heat flux, velocity and temperature have significant effect because mean square ratio is higher than the tabulated F value at 95% and 99%, and heat flux is more significant. It is seen from Table (C.14) that velocity and temperature have significance at 95% and 99%, and temperature is more significant. Table (C.15) shows that velocity and temperature are significant at 95% and 99% with temperature more influential.

Heat transfer in production tubular, flow lines and pipelines generally is not sufficient to affect the corrosion process to the same degree as momentum transfer and mass transfer. Momentum transfer is the physical force within the fluid acting through turbulence at the solid material surface. When a fluid moves past a solid surface, the flow is characterized as laminar or turbulent. Fully developed turbulent flow consists of a turbulent core, where the mean velocity is essentially constant, and a boundary layer at the solid - interface. The majority of the changes in fluid stress characteristics, turbulence, mass transfer, and fluid interaction with the wall occur in the boundary layer.

Table (C.23) shows that mean effect of the heat flux is more significant than that velocity (Re) and temperature, this is which agrees with the analysis of variance in Table (C.13).So the main effect (velocity and heat flux) is more significant than temperature. Table (C.23) indicates the presence of second order mean effects, i.e., HT, HR and TR. The third order effect interaction (HRT) is slightly negative. Table (C.24) shows that mean effect of the temperature is more significant than that heat flux and velocity. So the main effect (temperature) is more significant than other. Table (C.21) indicates the presence of second order mean effects, i.e., HT, HR and TR. The third order effect interaction (HRT) is effect.

5.6 Effect of Heat Flux

Corrosion of heat exchangers in many cases is controlled by the rate of diffusion process. So far there is no common opinion about the influence of heat transfer on the corrosion rate in diffusion control. Thus, some authors consider that out of all the heat transfer parameters only the metal temperature affects corrosion .Ross attributes this effect to the increasing of diffusion coefficient with temperature gradient growth. According to Zarubin corrosion rate under heat transfer is consistent with that under isothermal conditions at some mean temperature of a given temperature drop. With the increasing liquid velocity this mean temperature shifts from the metal temperature to the solution temperature [59].

Corrosion under Heat Transfer provides accurate, on-line performance information for corrosion and fouling parameters within critical cooling water exchanger applications. Unique electrochemical measurement techniques, precise flow, heat input and temperature measurements coupled with innovative instrument design make this possible [21].

From the data it is shown that limiting current density increases as heat flux increases. It is shown from Table (C.4) that velocity and heat flux are significant because mean square ratio is higher than the tabulated F value at 95% and 99%, and temperature is significant only at 95%. It is shown from Table (C.5) that velocity and temperature are significant effects because mean square ratio is higher than the tabulated F value at 95% and 99%. In Table (C.6) velocity, heat flux and temperature are significant because mean square ratio is higher than the tabulated F value at 95% and 99%.All three Tables (C.4, 5 and 6) show that velocity is more significant that heat flux which is in turn more significant than temperature.

A number of reasons can be given why heat transfer is responsible for such accelerated corrosion:

94

1. The metal in this region will be hotter than in adjacent area and temperature may rise even further as corrosion product build up on the surface [77].
2. The presence of heat transfer leads to form the thermal eddies adjacent to the metal surface which leads to increase the rate of mass transfer of oxygen towards the electrode surface so limiting current density increases [77].
3. Water temperature has long been recognized an important influencing factor, largly used on theoretical consideration .It affected matter such as corrosion (ion) kinetic, oxygen concentration and diffusion[21].

There is an additional way in which thermal gradients over a metal surface immersed in an electrolyte can induce failure and this arises because of the possibility of a thermochemical cell being generated between the hot zone, acting as anode, and the colder regions acting catholically. The detailed mechanisms involved in thermochemical cells are complex and it should not be assumed that temperature variations over a metal surface will result invariably in corrosion from such a source, which is just as well in view of the impossibility of designing any heat exchanger without some temperature gradients. However, the problem does arise in some of the commonly used metals in certain environments, especially if the hot, anodic area is small in comparison with the colder, cathodic area [21, 77].

To investigation the influence of hydrodynamic factors on oxygen diffusion, the heat flux was so controlled that temperature of surface and solution did not change with the velocity, i.e., a constant temperature drop was maintained in the thermal boundary layer [77] .

5.7 Effect of Interfacial Temperature

It is shown from Tables (4.2, 3, 4, 5, 6, 7, 11, 12, 13, 17 - 25) that interfacial temperature decreases with increasing Reynolds number at a given temperature and heat flux.

The effects of velocity, temperature and heat flux on skin temperature were examined. Results were analysed using three - way independent samples ANOVA

It is clear from Table (C.16) that velocity, heat flux and temperature are significant at 95% and 99% and the effect of temperature is more significant. Table (C.17) shows that temperature and velocity are significant at both levels 95% and 90% and the temperature is more significant. Table (C.18) shows that velocity, heat flux and temperature are also significant at 95% and 99% and the effect of temperature is more significant. These Tables (C.16, 17 and 19) show clearly that significance of variables is in the following decreasing order: Bulk temperature > Heat Flux > Re or (velocity)

Although oxygen solubility tends to fall with a rise in temperature, the higher temperature tends to increase reaction rate. Evidence from work on steel in potable waters suggests that the temperature effect is more important and that corrosion, for steel, will increase with temperature. For copper alloys, increase in temperature accelerates film formation. For diffusion controlled corrosion reactions, the effect of temperature which increases diffusion rates, viscosity, diffusion coefficients and Schmidt No., changes the corrosion rate [78].

It is clear from Tables (4.2,3,4,5,6,7,11,12,13,17-25) that interfacial temperature of copper is higher than that iron, so Reynolds number is higher and also diffusion coefficient in the case of copper than iron.

Table (C.25) shows that mean effect of the temperature is more significant than that heat flux and velocity, this is which agrees with the

analysis of variance in Table (C.13).So the main effect (temperature and heat flux) is more significant than velocity. Table (C.25) indicates the presence of second order mean effects, i.e., HT, HR and TR. The third order effect interaction (HRT) is effect. Table (C.26) shows that mean effect of the temperature is more significant than that heat flux and velocity. So the main effect (temperature and heat flux) is more significant than other. Table (C.26) indicates the presence of second order mean effects, i.e., HT, HR and TR. The third order effect interaction (HRT) is slightly negative.

5.8 Boundary Layer

5.8.1 Isothermal Condition

When a fluid is flowing along the surface of a solid body where there is a mass transfer process, a boundary layer is formed known as diffusion boundary layer. This region is in the vicinity of an electrode where the concentrations are different from their value in the bulk solution. The definition of the thickness of the diffusion layer is arbitrary because the concentration approaches asymptotically the value C_o in the bulk solution [49]. Diffusion boundary layer decreases at Re (r.p.m) increases as seen in Fig. (5.1, 2 and 3).

In the Fig. (5.2 and 5.3), it found that the curves is so near to each other thus due to experimental work.

Tables (5.1, 2 and 3) show the ratio is almost constant and that there is no effect of Re at constant temperature, but the ratio is decreased by increasing temperature. The large Schmidt numbers normally encountered in liquids mean that the fully developed mass-transfer boundary layer for hydraulically smooth surfaces is much thinner than the fully developed hydrodynamic boundary layer. This relationship should exist in all situations

in which mass and momentum transfer are governed by the presence of fully developed boundary layers. Under turbulent flow conditions most of the change in velocity between the wall and free stream occurs over a fairly narrow distance from the wall. The hydrodynamic boundary layer on the rotating cylinder electrode is independent of position on its surface. This characteristic means that the rotating cylinder electrode would not be able to detect corrosion accelerated by regions of differential velocity or differential turbulence on the same surface causing one region to corrode differently from another [65].

Table 5-1 The ratio of δ_H/δ_D at different temperatures [40].

Re	δ_H/δ_D at 30 ℃	δ_H/δ_D at 40 ℃	δ_H/δ_D at 50 ℃
5000	6.964	6.015	
8000	6.964	6.015	5.378
10000	6.964	6.015	5.378
12000	6.964	6.015	5.378

Table 5-2 The ratio of δ_H/δ_D at different temperatures [67].

r.p.m	δ_H/δ_D at 30 ℃	δ_H/δ_D at 40 ℃	δ_H/δ_D at 50 ℃
50	6.732	5.695	5.201
200	6.732	5.695	5.201
300	6.732	5.695	5.201
400	6.732	5.695	5.201

Table 5-3 The ratio of δ_H/δ_D at different temperatures [41].

r.p.m	δ_H/δ_D at 30 ℃	δ_H/δ_D at 40 ℃	δ_H/δ_D at 60 ℃
100	9.055	7.318	6.096
200	9.055	7.318	6.096
300	9.055	7.318	6.096
400	9.055	7.318	6.096
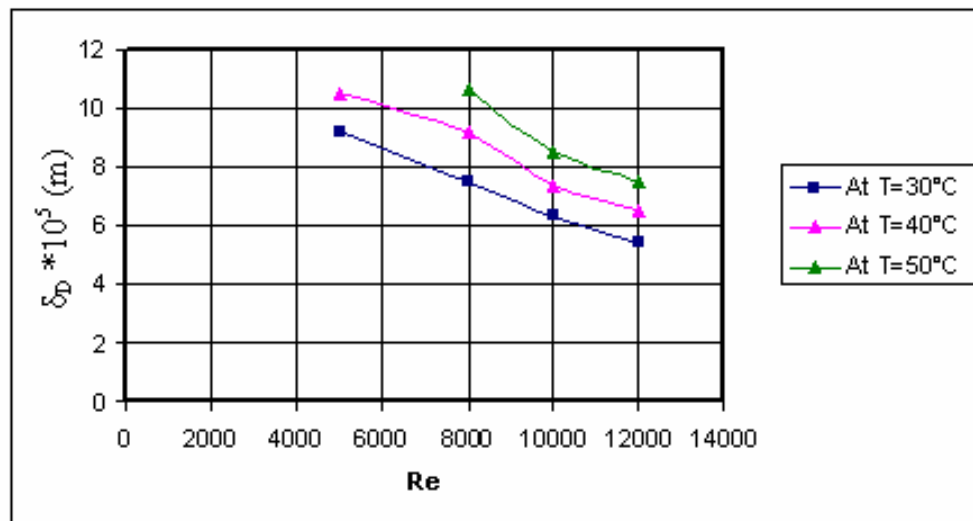
Fig.5-1 The relationship between Re and δ_D in different temperatures[40].
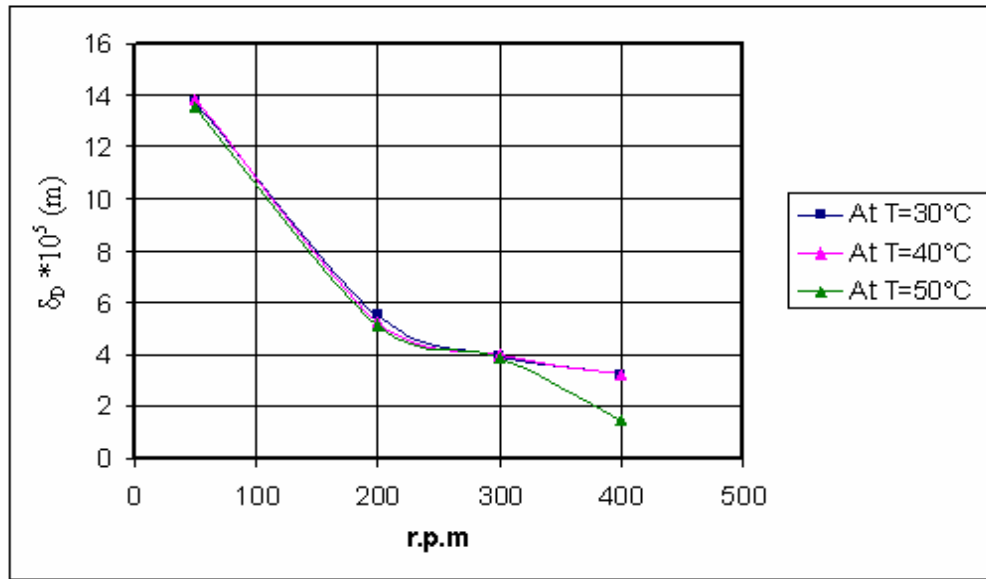
Fig.5-2 The relationship between r.p.m and δ_D in different temperatures[67].
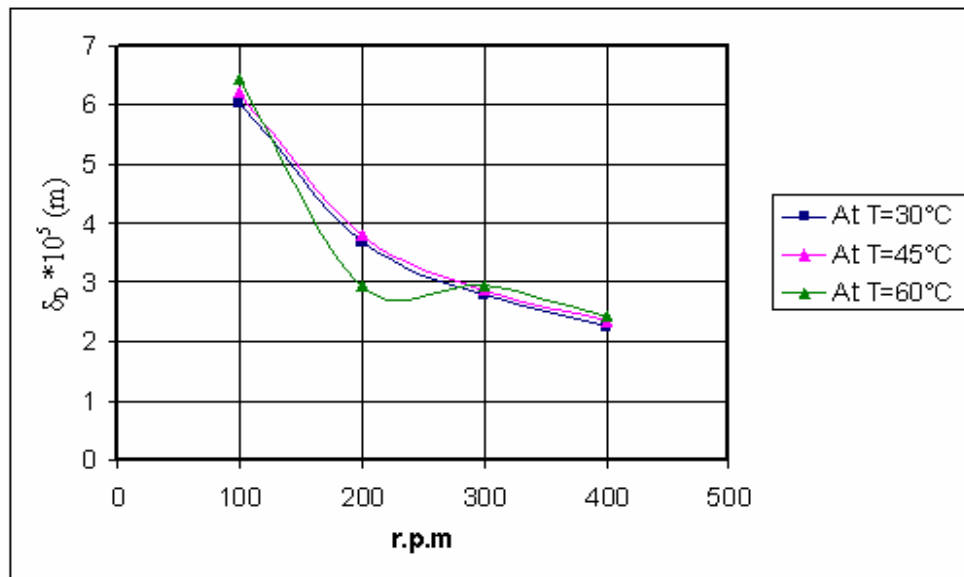
Fig. 5-3 The relationship between r.p.m and δ_D in different temperatures[41].

5.8.2 Heat Transfer Conditions

Stirring sets up a velocity gradient between the vessel wall and the bulk of the liquid and a hydrodynamic boundary layer, dependent upon the shear properties of the solution, is developed .In the region adjacent to the specimen/solution interface the concentration gradient for diffusion control extends for only a short distance from the surface and beyond this the concentration is essentially that in the bulk of the solution [21].

The thickness of thermal layer δ_t, in which the temperature is linear and heat transfer by conduction can be estimated using the following equation:

$$\delta_t = \frac{k_T}{h} \qquad \qquad \dots.. (5.5)$$

Tables (4.56-61, 65-67 and 71-79) show the values of d_t for the whole investigated range of Re and temperature. A comparison of the estimated boundary layer thickness show that d_D is much smaller than either d_t or d_H ,when considering thermal effects on the diffusion process, the process would be expected to depend basically on conditions at the specimen surface. That is, on the specimen surface temperature, not on the heat flux through the boundary layer or the solution bulk temperature.

The thickness of diffusion boundary layer depends upon the hydrodynamic flow conditions, while the rate of diffusion across the layer depends on the temperature concentration gradient and viscosity of the layer . Under steady heat flow conditions the rate of heat flux is dependent on the temperature gradient across the thermal boundary layer and the thermal conductivity of this layer [21]. Tables (5.4, 5, 6, 7, 8, 9 and 10) show also that the ratio of thermal boundary layer to diffusion boundary layer is higher than one, this shows that thermal boundary layer is greater than diffusion boundary layer. Figures (5.4, 5, 6, 7, 8, 9 and 10) show the variation of d_D with Re at

different temperatures. It is obvious that as Re increases d_D decreases for all temperatures due to the increased turbulence near the wall causing increasing thermal eddies reaching to the surface. In the Fig. (5.7, 8, 9 and 10), it found that the curves are so near to each other thus due to experimental work.

Table 5-4 The ratio of boundary layers at different temperatures at Q =10 kW/m^2 [40]

Re	Temp.(℃)	d_H/d_D	d_H/d_T	d_T/d_D
5000	30	6.599	1.673	5.325
8000	30	6.698	1.649	4.761
10000	30	6.747	1.704	5.069
12000	30	6.799	1.718	4.513
5000	40	5.794	1.573	4.050
8000	40	5.868	1.582	3.656
10000	40	5.897	1.593	3.797
12000	40	5.973	1.604	3.065

Table 5-5 The ratio of boundary layers at different temperatures at Q =30 kW/m^2 [40]

Re	Temp.(℃)	d_H/d_D	d_H/d_T	d_T/d_D
5000	30	6.363	1.6729	3.124
8000	30	6.491	1.6862	3.000
10000	30	6.598	1.7043	3.335
12000	30	6.698	1.7915	2.936
5000	40	5.652	1.573	2.384
8000	40	5.722	1.582	2.473
10000	40	5.794	1.593	2.655
12000	40	5.869	1.604	2.301

Table 5-6 The ratio of boundary layers at different temperatures at Q =50 kW/m^2 [40]

Re	Temp.(℃)	d_H/d_D	d_H/d_T	d_T/d_D
5000	30	6.231	1.656	2.574
8000	30	6.319	1.668	3.056
10000	30	6.455	1.686	2.719
12000	30	6.550	1.699	2.892
5000	40	5.550	1.555	1.917
8000	40	5.562	1.573	1.851
10000	40	5.723	1.582	2.153
12000	40	5.767	1.590	2.069

Table 5-7 The ratio of boundary layers at different temperature and Q =20 kW/m^2 [40]

r.p.m	Temp.(℃)	d_H/d_D	d_H/d_T	d_T/d_D
50	30	5.528	1.596	0.649
200	30	5.583	1.606	1.657
300	30	5.695	1.627	1.798
400	30	5.699	1.636	2.107
50	40	5.200	1.525	5.346
200	40	5.377	1.531	1.167
300	40	5.384	1.567	1.179
400	40	5.404	1.581	1.394
50	50	4.533	1.454	4.588
200	50	4.626	1.464	1.137
300	50	4.806	1.480	1.104
400	50	4.915	1.486	1.176

Table 5-8 The ratio of boundary layers at different temperatures at Q =15.6 kW/m^2 [41]

Re	Temp.(℃)	d_H/d_D	d_H/d_T	d_T/d_D
100	30	6.949	1.547	2.367
200	30	7.044	1.549	3.750
300	30	7.166	1.561	4.608
400	30	7.367	1.583	4.969
100	45	5.906	1.402	2.019
200	45	6.077	1.444	3.135
300	45	6.173	1.453	3.824
400	45	6.262	1.462	4.272
100	60	5.270	1.349	1.652
200	60	5.304	1.353	2.582
300	60	5.331	1.355	3.314
400	60	5.407	1.365	3.620

Table 5-9 The ratio of boundary layers at different temperatures at Q =18.75 kW/m^2 [41]

r.p.m	Temp.(℃)	d_H/d_D	d_H/d_T	d_T/d_D
100	40	6.561	1.495	2.572
200	40	6.659	1.505	4.010
300	40	6.774	1.519	4.991
400	40	6.819	1.524	5.991
100	45	5.812	1.411	2.088
200	45	5.888	1.421	3.222
300	45	5.989	1.432	3.904
400	45	5.997	1.436	4.739
100	60	5.259	1.349	1.464
200	60	5.289	1.351	2.270
300	60	5.380	1.360	2.589
400	60	5.441	1.366	2.294

Table 5-10 The ratio of boundary layers at different temperatures
and Q =21.75 kW/m^2 [41]

r.p.m	Temp.(°C)	d_H/d_D	d_H/d_T	d_T/d_D
100	40	6.297	1.466	2.545
200	40	6.345	1.472	5.519
300	40	6.387	1.476	5.321
400	40	6.477	1.486	6.256
100	45	5.642	1.391	2.011
200	45	5.687	1.396	3.194
300	45	5.743	1.402	4.060
400	45	5.854	1.416	4.616
100	60	5.139	1.335	1.436
200	60	5.206	1.342	2.161
300	60	5.243	1.346	2.754
400	60	5.332	1.356	2.965
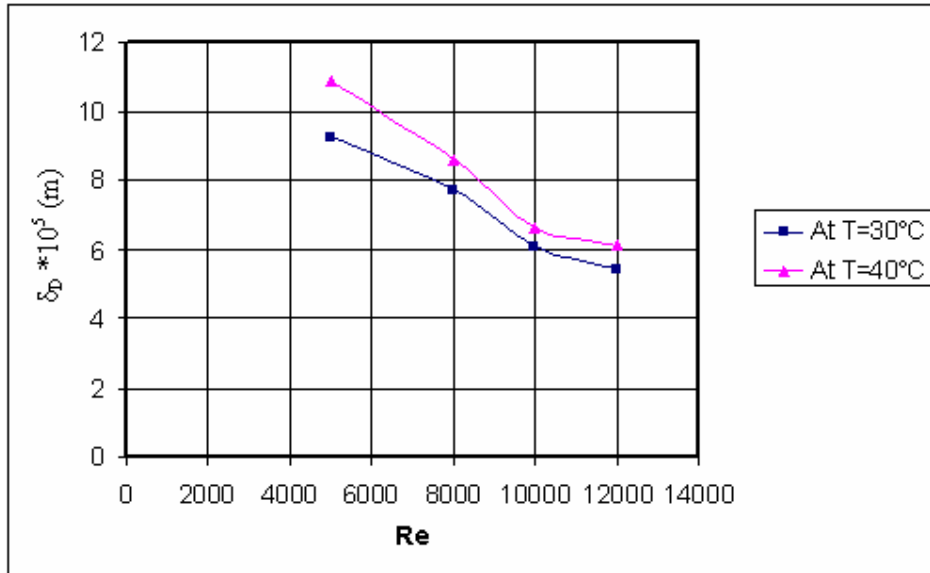
Fig. 5.4 The relationship between Re and δ_D at different temperatures at Q =10kW/m^2[40]
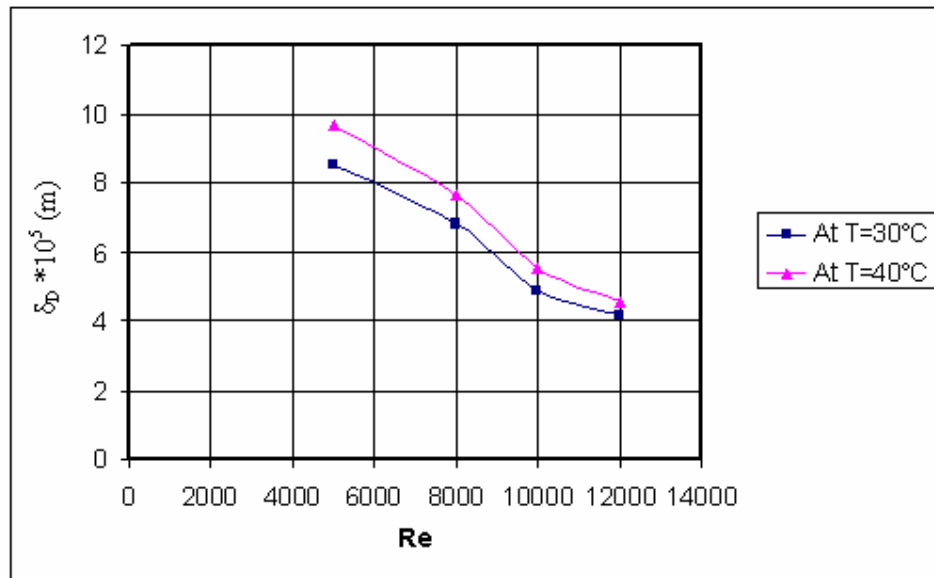
Fig. 5.5 The relationship between Re and δ_D at different temperatures at Q =30kW/m^2[40]

.
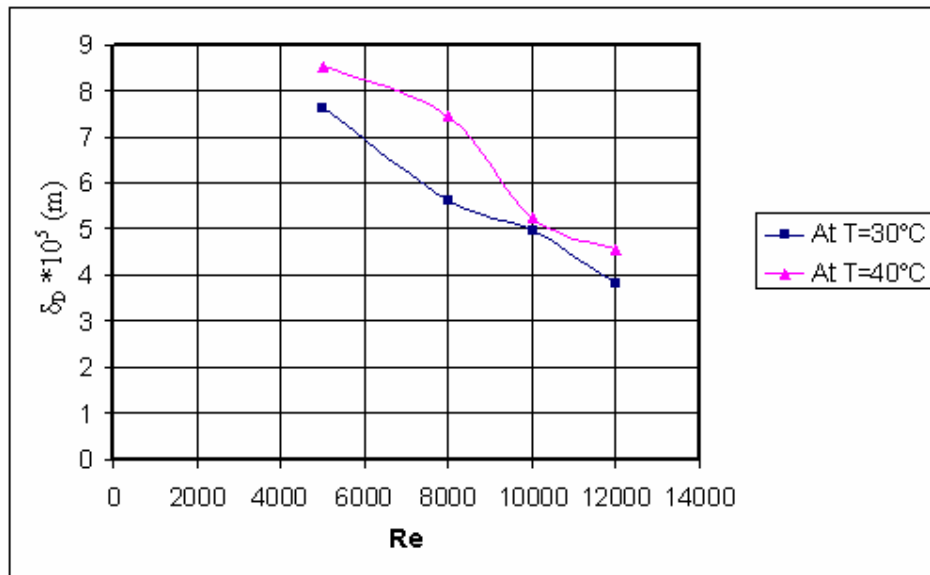
Fig. 5.6 The relationship between Re and δ_D at different temperatures at Q =50kW/m^2[40]
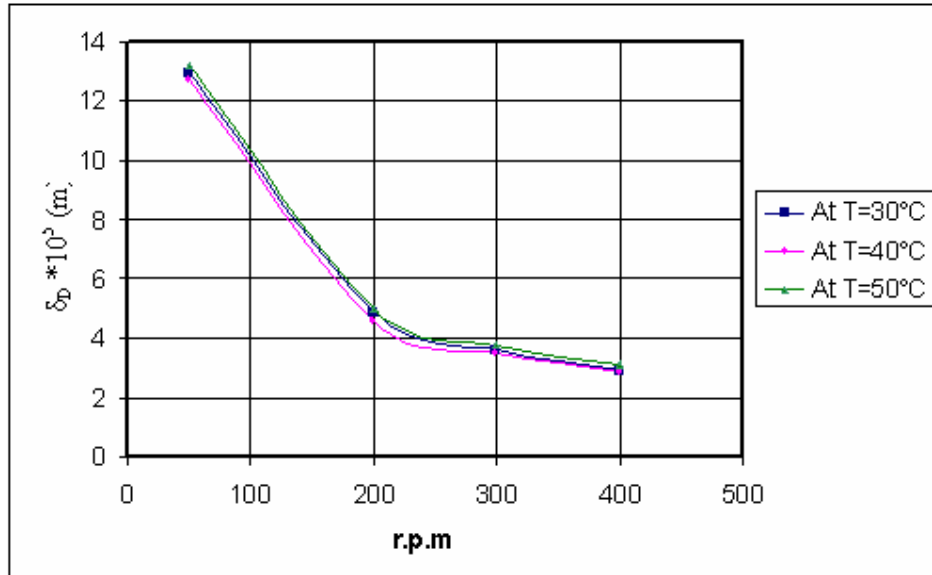
Fig. 5.7 The relationship between r.p.m. and δ_D at different temperatures at Q =20 kW/m^2 [68]
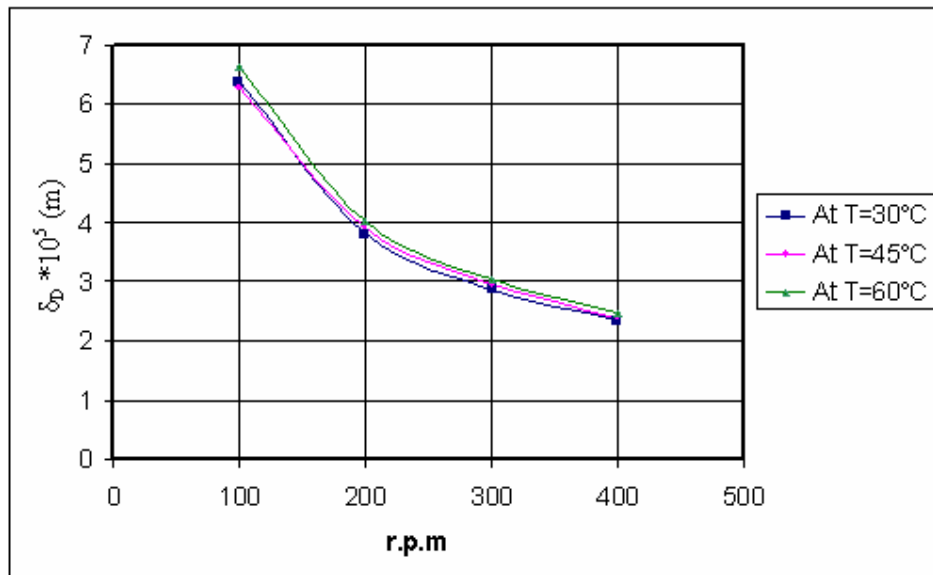
Fig. 5.8 The relationship between r.p.m and δ_D in different temperatures at Q=15.65kW/m^2 [41]
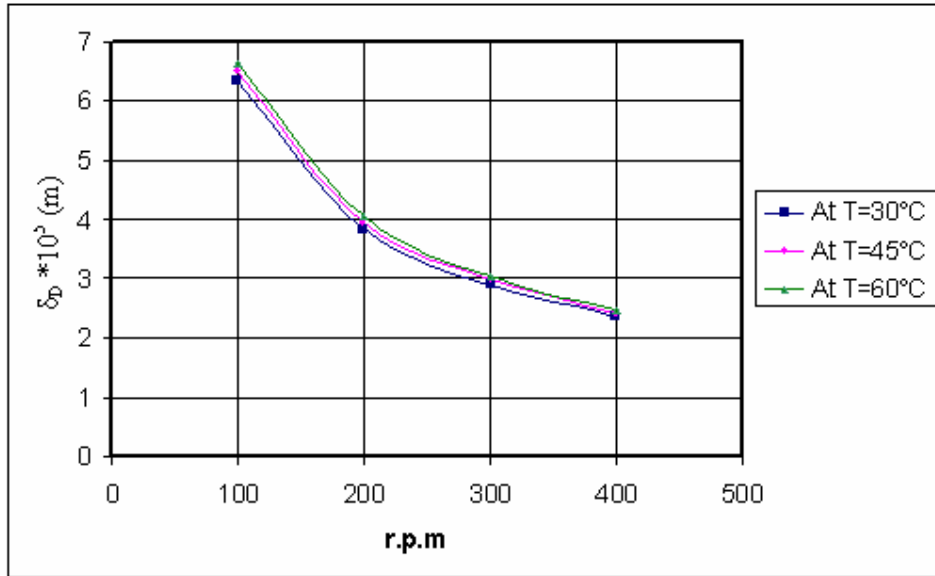
Fig. 5.9 The relationship between r.p.m and δ_D in different temperatures at Q=18.75kW/m^2 [41]
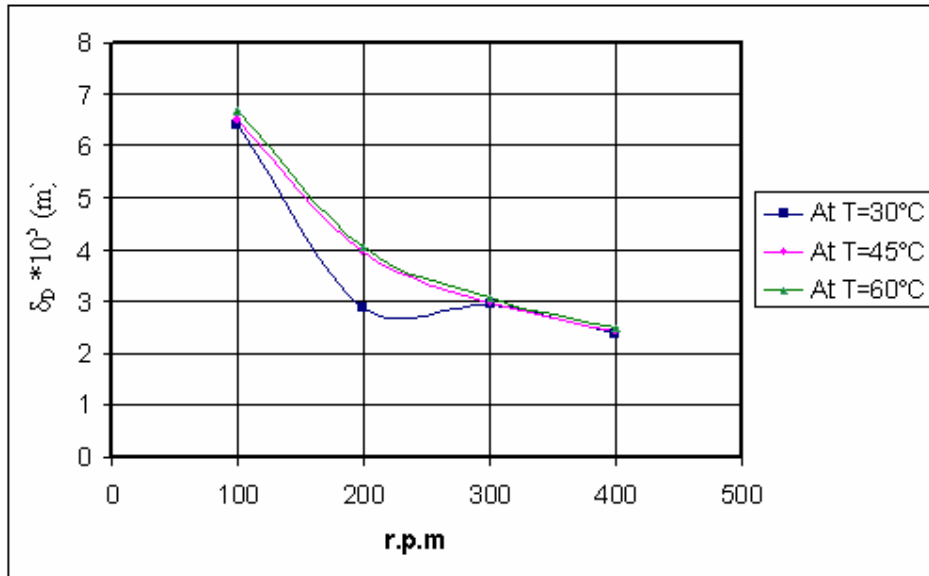
Fig. 5.10 The relationship between r.p.m and δ_D in different temperatures at Q=21.65 kW/m^2 [41]

This review examines several important areas by the analysis of variance as related to corrosion:

From the analysis of data of carbon steel cylinder under cross flow [40] and carbon steel rotating cylinder [67], it is found that limiting current density under isothermal conditions is significantly affected by velocity than temperature while copper rotating cylinder [41] shows that temperature is more significant than velocity. Mass transfer coefficient under isothermal conditions is affected by velocity more than temperature.

Under heat transfer conditions, the limiting current density on carbon steel cylinder under cross flow [40], carbon steel rotating cylinder [68] and copper rotating cylinder [41] show that velocity is more significant followed by heat flux and temperature. Mass transfer coefficients are also dependent on velocity and then heat flux and temperature. Heat flux and Re or (r.p.m.) are the more effective.

And below there are a summary of all ANOVA tables under isothermal and heat transfer conditions.

Table 5.11 ANOVA for limiting current density under isothermal conditions

Ref.	Source of Variation	MSR	$F_{0.05}$	$F_{0.01}$
40	Columns (Temp.)	91.29334	5.14	10.92
	Rows(Re)	293.3482	4.76	9.78
67	Columns (Temp.)	8.0727959	5.14	10.92
	Rows (r.p.m)	162.48408	4.76	9.78
41	Columns (Temp.)	54.324759	5.14	10.92
	Rows(r.p.m)	28.016502	4.76	9.78

Table 5.12 ANOVA for mass transfer coefficients under isothermal conditions

Ref.	Source of Variation	MSR	F $_{0.05}$	F $_{0.01}$
40	Columns (Temp.)	32.60304	5.14	10.92
	Rows(Re)	500.4345	4.76	9.78
67	Columns (Temp.)	22.86808	5.14	10.92
	Rows (r.p.m)	178.0944	4.76	9.78
41	Columns (Temp.)	21.34109	5.14	10.92
	Rows (r.p.m)	24.52144	4.76	9.78

Table 5.13 ANOVA for limiting current density under heat transfer conditions

Ref.	Source of Variation	MSR	F $_{0.05}$	F $_{0.01}$
	Among Columns(Re)	81.9555697	3.20	5.18
40	Among Rows(Q)	47.762893	3.59	6.11
	Among Groups (Temp.)	8.0906302	4.45	8.4
68	Columns (Temp.)	14.6053957	5.14	10.92
	Rows(r.p.m)	224.379009	4.76	9.78
	Among Columns(Re)	79.555	2.95	4.57
41	Among Rows(Q)	70.6667	3.34	5.54
	Among Groups (Temp.)	59.5556	3.34	5.54

Table 5.14 ANOVA for mass transfer coefficients under heat transfer conditions

Ref.	Source of Variation	MSR	F $_{0.05}$	F $_{0.01}$
	Among Columns(Re)	17.820237	3.20	5.18
40	Among Rows(Q)	10.464548	3.59	6.11
	Among Groups (Temp.)	1.9309152	4.45	8.4
68	Columns (Temp.)	3.70923684	5.14	10.92
	Rows(r.p.m)	23.9727517	4.76	9.78
	Among Columns(Re)	13.967198	2.95	4.57
41	Among Rows(Q)	0.713667	3.34	5.54
	Among Groups (Temp.)	5.0182721	3.34	5.54

Table 5.15 ANOVA for heat transfer coefficients under heat transfer conditions

Ref.	Source of Variation	MSR	$F_{0.05}$	$F_{0.01}$
40	Among Columns(Re)	5.7068148	3.20	5.18
	Among Rows(Q)	123.42833	3.59	6.11
	Among Groups (Temp.)	23.380943	4.45	8.4
68	Columns (Temp.)	23.14892	5.14	10.92
	Rows(r.p.m)	14.55659	4.76	9.78
41	Among Columns(Re)	5.4125261	2.95	4.57
	Among Rows(Q)	3.9663922	3.34	5.54
	Among Groups (Temp.)	110.20107	3.34	5.54

Table 5.16 ANOVA for Interfacial temperature under heat transfer conditions

Ref.	Source of Variation	MSR	$F_{0.05}$	$F_{0.01}$
40	Among Columns(Re)	69.66407	3.20	5.18
	Among Rows(Q)	148.18644	3.59	6.11
	Among Groups (Temp.)	861.66253	4.45	8.4
68	Columns (Temp.)	417.7431	5.14	10.92
	Rows(r.p.m)	91.02562	4.76	9.78
41	Among Columns(Re)	6.8258	2.95	4.57
	Among Rows(Q)	42.3752	3.34	5.54
	Among Groups (Temp.)	44.6421	3.34	5.54

Chapter Six

Conclusions and Recommendations

6.1 Conclusions

The present work analyzed the effect of two and three variables on corrosion under isothermal and heat transfer conditions using the statistical technique, ie, Analysis Of Variance (ANOVA) and using matlab program to check the results .The following conclusions are drawn from this analysis:

1. The limiting current density of dissolved oxygen on carbon steel under isothermal conditions are affected by rotation rate or Re of the electrode more than the solution bulk temperature because the mean square ratio of velocity and temperature are higher than the tabulated F value at 95% and 99% but the effect of velocity or (r.p.m) is more significant than temperature.

2. The limiting current density of copper rotating cylinder under isothermal conditions is affected by temperature more than Re or (r.p.m) because mean square ratio of temperature is higher than the tabulated F value at 95% and 99%, and velocity is less significant at both levels.

3. The limiting current density of carbon steel and copper under heat transfer conditions are significantly affected by Re or (r.p.m) of the electrode followed by heat flux and then temperature because mean square ratio of Re or (r.p.m) is higher than the tabulated F value at 95% and 99%.

4. The mass transfer coefficient is dependent on flow, because it increases as the rotation rate or Re increases, followed by temperature, under isothermal conditions because mean square ratio Re and temperature are higher than the tabulated F value at 95% and 99% but the velocity is more significant

5. The mass transfer coefficients under heat transfer conditions are affected by flow more than heat flux followed by temperature because mean square ratio of velocity is higher than the tabulated F value at 95% and 99%.

6. Heat transfer coefficients are significantly affected by temperature followed by heat flux and then Re or (r.p.m) because mean square ratio of temperature is higher than the tabulated F value at 95% and 99%.

7. Interfacial temperature is affected by bulk temperature more significantly than heat flux, followed by Re or (r.p.m) because mean square ratio of velocity, heat flux and temperature are significant at 95% and 99% and the effect of temperature is more significant more than other .

8. Under isothermal conditions, hydrodynamic boundary layer decreases as temperature increases at constant Re or (r.p.m) ,also decreases with increasing Re or (r.p.m) with constant temperature. Diffusion boundary layer increases with increasing temperature at constant Re or (r.p.m) and at constant temperature, it increasing with Re or (r.p.m) increasing.

9. Under heat transfer conditions, hydrodynamic and thermal boundary layer decreases as temperature increases as constant Re or(r.p.m) ,also decreases with increasing Re or (r.p.m) with constant temperature and diffusion boundary layer increases with increasing temperature at constant Re or (r.p.m) and it increasing with Re or (r.p.m) decreasing at constant temperature.

6.2 Recommendations

1. Application of ANOVA in the anodic region of various corrosion processes under isothermal and heat transfer conditions.

2. Application of ANOVA in order to investigate the influence of inhibitors on corrosion processes under isothermal and heat transfer conditions.

3. Using ANOVA to show the effect of pH, various salts and acids concentrations on different corrosion processes.

4. A four ways ANOVA to show concurrently the effect of temperature, hydrodynamics, various aggressive solutions concentrations and heat flux.

5. Study the effects of metallurgical factor on corrosion.

References

1. Uhlig H.H, Corrosion and Corrosion Control, 3rd Edition. Wiley Interscience publication, New York, 1985.

2. Henry S.D and Scott W.M Corrosion in petrochemical industry ,1st Edition ASM international ,USA 1999.

3. NACE International, Date Revised: 09/10/2003; Date Accessed: 10/06/2005,   Cost of Corrosion.

   http://nace.org/nace/content/publicaffairs/cocorrindex.asp

4. Fontana M.G, N.D Green, Corrosion Engineering, 2nd Edition, London, 1984.

5. Shreir L.L., Corrosion Handbook, 2nd Edition. Part 1, Newness-Butter., London, 1976.

6. Bulter and Ison "Corrosion and its prevention waters" Chemical and process engineering series, Leonard Hill Book Co. ,1966.

7. Francis L.La Que   "Marine Corrosion Causes and Preventation" Awilely inter science publication Co ,1975.

8. Polan, N. W. "Copper and Copper Alloy" in ASM handbook - Corrosion, Ed., 1987.

9. Tretheway K.R and Chamberlian J., Corrosion Science and Engineering, 2nd Edition, Longman, London, 1996.

10. Fundamentals of Electrochemical corrosion ,ASM international (2000), www.asminternational.org.

11. Steigewald R.F ,Corrosion NACE,vol.24 p.1 to 10 ,1968.

12. Peabody A.W., Control of pipeline corrosion,2nd Edition ,2001.

13. Kruger J.,Electrochemistry of Corrosion ,The John Hopknis University, Baltimore,USA April 2001.

14. The Effect And Economic Impact of Corrosion ,ASM International ,Materials Park,Ohio,USA.

15. West J.M . ,Electrode Deposition and Corrosion Processed, 1976.

16. Shreir L.L.Corrosion ,Vol. 1 ,Metal/Environment Reactions ,Newnes-Butler Worths Book,1994.

17. Pierre R.Roberge "Handbook of Corrosion Engineering",MC Grew-Hill ,1999.

18. Adam R. N.,"Electrochemistry of solid electrodes", Morcel Dekkev, Inc., 1969.

19. Poulson B.,Corrosion Science,Vol.23, No.1391 ,P.391,1983.

20. Stern M., "Corrosion-NACE", Vol. 13, P.97, 1957.

21. Porter D.T , Donimirska M. and Wall R.,Corrosion.Science, Vol.8, P.833-843,1968.

22. Fisher A. O. and Whitney F. L. , Corrosion, Vol. 15,P.257t, 1959

23. Zurubin P.I and Zasita Metallov,No. 3, P. 279, 1965. (cited in 157).

24. Kerst H., Corrosion J., Vol. 16, P. 523t, 1960.

25. Ross T. K., Br. Corrosion J., No. 2, P.131, 1967.

26. Kreysztof K.,Nauk Pr. Inst. Tech.,Nieros Nawzow Miner Pollitch Warcaw ,Poland,No.16,P.153, 1979.

27. Ross T. K., The Chem. Eng. J., No. 247, P.95, 1971.

28. WarrgA.A, Nasiruddin A. K., Electrochem. Acta., Vol. 18, P. 619, 1973.

29. Ashford J. H., Garsy R., and Mann G. M., Corrosion Science, Vol. 14, P. 515, 1974.

30. Alwash S. H., Ph. D. Thesis, UMIST, 1977.

31. Jaralla A .A., Ph.D.Thesis, UMIST, 1984.

32. Kolotyrkin M., Pakhomov V. S., Parshin A. V., and, Chelkhovski A. V., Conf. Int. Congr. On Metalic Corrosion, Vol. 3, P.1, 1984.

33. Pakhamov S., Chekovsky A.V., and Kotolykin Y.A.M., Corrosion Sci., Vol.22, P.845, 1982.

34. Andon VR., Pembeton R. C., G.N. Thomos, J. M. Harrison S. E. Worrthington, and R.D. Shaw, Br. Corrosion J., Vol. 21, No.2, P.119, 1986.

35. Alwash and Ashworth V., Corrosion Science,Vol. 27, No.12, P.383 and P. 1301, 1987.

36. Jaralla A.A.,Proc.11th Int.Corrosion Congr.,Vol.3 ,P.489 ,Florence , 1990.

37. Samh S. A., Ph. D. Thesis, Dept. of Chem. Eng., University of Technology, Baghdad, 1994.

38. Al-Tal M. M.., Ph. D. Thesis, Dept. Chem. Eng., University of Technology, Baghdad, 1995.

39. Atia M. A., Ph.D. Thesis, Dept. Chem. Eng., Saddam University, Baghdad, 1996.

40. Al-Mashta S. E., M. Sc. Thesis, Chem. Eng. Dept., Saddam University, Baghdad, 1996.

41. Wathiq, Ph.D Thesis, Chem.Eng.Dept. Technology University, Baghdad, 2007.

42. Arzola -Peralta S., Mendoza- Flores J., R.Duran- Romero and . Genesca , Corrosion Eng.,Science and Technology,Vol. 41,No 4, 2006

43. Gabe D.R., Wilcox G.D., Journal of Applied Electrochemistry ,Vol 28 ,P.759-780 ,1998.

44. Hydrodynamic of a smooth cylinder from the site: www. Argentum solutions.com.

45. Holman J.P., "Heat Transfer ",Mc-Grew Hill International Editions,8th edition ,1999.

46. Koichi Asano "Mass Transfer. From Fundamentals to Modern Industrial Applications" Wiley-Vch Verlag Gmbh&Co.KGaA, 2006.

47. Bagotsky V.S.,"Fundemental of Electrochemist",2nd Edition, Wiley Interscience publication, 2006.

48. Perez N.,"Electochemistry and Corrosion Science",Nework,2004

49. Wu B. Q., Liu z Z., A. Keigler, and J. Harrell, Journal of The Electrochemical Society, Vol. 152 (5) ,P.C272-C276 ,2005 .

50. Low C.T.J., Roberts E.P.L., Walsh F.C., Electrochimica Acta 52,P. 3831–3840 ,2007.

51. Macial J.M. and Agostinto S.M.L. "J.applied of Electro.",1999

52. Brodkey R. S. and Hershey H. C., Transport Phenomena, 2nd Printing, Mc Graw Hill, New York, 1989.

53. Eisenberg M., Tobias C.W. and, Wilke C.R. J.Electrochem.Soc , 106, 306 ,1954.

54. Pang J.and Ritchi I.M, Electrochem. Acta,Vol. 26, P.1345,1981

55. Gabe D.R and Walsh F.C , J.Appl. Electrochem. Vol.14 , NO.555 , 1984 .

56. Christopher Depcik and Dennis Assains"University Michigan ,P.1 , 372 ,2002.

57. Karmers H.,Physics,Vol.12,P.61-80,1946.

58. Churchill S.W. and Brenstein M. Tran.ASME,J.Heat Transfer,Vol 99,P.300-306, 1977.

59. Parshin A.G., Pakhomou V.S.,"Corrosion " Vol. 27,No 4 P.642, 1982.

60. Green J.R. and Margerison D.,"Statistical treatment of experimental data, Amsterdam,1978.

61. Lipson J. R., and Sheth N., Statistical Design and Analysis of Engineering Experiments, 1975.

62. Lin Z.C. and Ho C.Y., "International J.Adv.Tech.",P.10-14 ,2003.

63. Analysis of Variance,www.statgraghics.com.

64. Chen T.Y., Moccari A.A., and D.D. Macdonald, Corrosion Engineering"Vol. 48, No. 3,1992.

65. Silverman D.C. , COorrosion,Vol. 60, No. 11,2004.

66. Ricardo Galván-Martínez,Juan Mendoza-Flores,Rubén Durán-Romero. 62 (519), 448-454,2005.

67. Sameh,Sh.A.,Alwash,S.H.,Eng.&Technoogy,Vol.18,No.5,P.490 , 1999.

68. Sameh,Sh.A.,Alwash,S.H.,Eng.&Technoogy,Suppl.of No.3 , Vol.19 , 2000.

69. Kim J.-G., Choi Y.-S., Lee H.-D., and Chung W.-S. , Corrosion,Vol. 59, No. 2, S2003.

70. Howaida M. El-Kashlan,"American Journal Of Applied Sciences" ,Vol 5, P.347-354,2008.

71. Soliman H.M.A. and Abdel Rahman H.H.."J.Braz. Chem. Soc.Vol 17,No. 4,P.705-714 ,2006.

72. Michael R. Schock and Darren A. Lytle , P.312-317.

73. Arzola Peralta S. and Mendoza J. , Duran R. and Genesca J., Corrosion Eng.,Science and Technology" Vol 41,No4 ,2006.

74. Gehan M. El-Subruiti and A. M. Ahmed, Portugaliae Electrochimica Acta 20 ,2002, 151-166.

75. Perez-Herranz V., Montanes M.T., Garcia-Anton J. and Guion J.L. ,Corrosion Vol,57,No.10,2001.

76. Nesic S., Solvi G.T., and J. Enerhaug,Corrosion,Vol. 51, No. 10,1995

77. Bremhorst K., Kear G., Keating A.J., and Huang S.-H. Corrosion,October 2005.

78. Ashford J.H., Garnsey R. and Mann G.M.W. ,"Corrosion Science",Vol.14,P.515-525, 1974.

79. Perry R.H. and Chilton C.H., Chem Eng. Hand-Book, 6th Ed., Mc Graw Hill, 1998.

80.Audin and L. John, J. Chem. Eng. Data, Vol.17, No.3, P.789, 1972.

81.Maisel D.S. and Sherwod T.K.,Chem Eng.Prog.,Vol.46,P. 131-138, 1950.

82.Bedingfield C. and Drew M.,Ind.Eng.Chem.,Vol 42 , P. 1164-1173, 1950.

83.Winding C.C and Cheney A.J.,Ind.Eng.Chem.,Vol 40,No. 6 ,P 1087-1093 ,1948.

84.Sarma C.B.,Gopichand T. and Raju G.J.,Ind Tech.,Vol 24,P.580-586 1986.

Appendix A

Table A-1 Physical Properties of Water at Atmospheric Pressure [79]

T (^{o}C)	Cp (KJ/Kg. ^{o}C)	ρ (Kg/m^3)	$\mu \times 10^4$ (Kg/m.sec)	k_T (W/m. ^{o}C)
0.00	4.225	999.8	17.9	0.566
4.44	4.208	999.8	15.5	0.575
10.0	4.195	999.2	13.1	0.585
15.56	4.186	998.6	11.2	0.595
21.11	4.179	997.4	9.80	0.604
26.67	4.179	995.8	8.60	0.614
32.22	4.174	994.9	7.65	0.623
37.78	4.174	993.0	6.82	0.630
43.33	4.174	990.6	6.16	0.637
54.44	4.179	985.7	5.13	0.649
60.0	4.179	983.3	4.71	0.654
65.55	4.183	980.3	4.30	0.659
71.11	4.186	977.3	4.01	0.665
82.22	4.195	970.2	3.47	0.673
93.33	4.204	963.2	3.06	0.678

A.2 Diffusivity of Oxygen

Many workers showed that the diffusivity of the electrolyte is lower than that in water, and it proportionally decreased with increasing electrolyte concentration according to this equation [80]:

$$D = D_o (1-K \sqrt{C})$$

where D_o: diffusivity of pure water.

D: diffusivity of electrolyte.

K: is an empirical constant.

C= concentration of the electrolyte solution (mol/l).

Table A.2 Values of oxygen diffusivity

T(^{o}C)	$D_o \times 10^9$ (m^2/sec) (pure water)	$D \times 10^9$ (m^2/sec) (0.1N NaCl)	$D \times 10^9$ (m^2/sec) (in 600ppm Cl$^-$)
20	2.01	2.3714	2.034
40	3.55	3.0194	3.563
50	4.20	3.5571	3.938
60	5.70	4.8276	5.345

Table A.3 Oxygen Solubility at atmospheric Pressure

T (^{o}C)	Solubility (mg/l) Distilled Water
30	7.559
35	6.625
40	6.401
45	6.001
50	5.477
60	4.501

A.3 Diffusivity and Solubility of CuCl$_2$

To calculate the diffusion coefficient of the CuCl$_2$ from the following relationship:

$$D = D_o e - (E_D / RT)$$

where E$_D$: is the activation energy for diffusion and equals to 4.5 Kcal/mole.

D$_o$: is the diffusivity and equals to 1.9×10^{-6} m^2 /s .

While the concentration of CuCl$_2$ is calculated from limiting current density from the equation:

$$i_l = \frac{nF(CuCl_2)}{d_D}$$

Where the $d_D = 12.64 \dfrac{d^{0.3} n^{0.344} D^{0.356}}{V^{0.7}}$

Table A.4 Values of copper diffusivity and solubility at 30^0C

r.p.m	$D*10^9$(m² /s)	Concentration of $CuCl_2$ *10^2 (mole/m³)
100	1.12	8.78
200	1.12	5.89
300	1.12	5.22
400	1.12	7.42

Table A.5 Values of copper diffusivity and solubility at 45^0C

r.p.m	$D*10^9$(m² /s)	Concentration of $CuCl_2$ *10^2 (mole/m³)
100	1.6	13
200	1.6	9.4
300	1.6	9.6
400	1.6	10.0

Table A.6 Values of copper diffusivity and solubility at 60^0C

r.p.m	$D*10^9$(m² /s)	Concentration of $CuCl_2$ *10^2 (mole/m³)
100	2.2	10.1
200	2.2	7.85
300	2.2	7.63
400	2.2	7.12

Table A.7 Values of copper diffusivity and solubility at 30^0C and Q=15.6kW/m^2

r.p.m	D*10^9(m² /s)	Concentration of CuCl$_2$ *10² (mole/m³)
100	1.74	12
200	1.70	8.96
300	1.65	8.56
400	1.58	8.23

Table A.8 Values of copper diffusivity and solubility at 45^0C and Q=15.6kW/m^2

r.p.m	D*10^9(m² /s)	Concentration of CuCl$_2$ *10² (mole/m³)
100	2.86	8.41
200	2.81	6.42
300	2.79	6.16
400	2.72	5.49

Table A.9 Values of copper diffusivity and solubility at 60^0C and Q=15.6kW/m^2

r.p.m	D*10^9(m² /s)	Concentration of CuCl$_2$ *10² (mole/m³)
100	1.92	11.8
200	1.86	8.84
300	1.82	8.64
400	1.80	7.84

Table A.10 Values of copper diffusivity and solubility at 30^0C and Q=18.75kW/m^2

r.p.m	D*10^9(m² /s)	Concentration of CuCl$_2$ *10² (mole/m³)
100	2.38	10
200	2.33	7.68
300	2.27	7.47
400	2.24	6.86

Table A.11 Values of copper diffusivity and solubility at 45^0C and Q=18.75kW/m^2

r.p.m	D*10^9(m^2 /s)	Concentration of CuCl$_2$ *10^2 (mole/m^3)
100	2.22	10.2
200	2.20	7.79
300	2.15	7.24
400	2.10	6.72

Table A.12 Values of copper diffusivity and solubility at 60^0C and Q=18.75kW/m^2

r.p.m	D*10^9(m^2 /s)	Concentration of CuCl$_2$ *10^2 (mole/m^3)
100	2.86	8.81
200	2.71	6.84
300	2.73	6.54
400	2.70	6.32

Table A.13 Values of copper diffusivity and solubility at 30^0C and Q=21.87kW/m^2

r.p.m	D*10^9(m^2 /s)	Concentration of CuCl$_2$ *10^2 (mole/m^3)
100	2.07	11.6
200	2.02	8.49
300	2	7.77
400	1.98	7.63

Table A.14 Values of copper diffusivity and solubility at 45^0C and Q=21.87kW/m^2

r.p.m.	D*10^9(m^2 /s)	Concentration of CuCl$_2$ *10^2 (mole/m^3)
100	2.51	10.1
200	2.45	7.4
300	2.43	6.72
400	2.35	6.51

Table A.15 Values of copper diffusivity and solubility at 60^0C and $Q=21.87kW/m^2$

r.p.m.	$D*10^9(m^2/s)$	Concentration of $CuCl_2$ $*10^2$ (mole/m³)
100	2.98	10.6
200	2.91	7.2
300	2.87	6.28
400	2.47	6.43

Appendix B

Table B-1 Mass transfer Correlation rotating cylinder [44]

$Sh = a\,\mathrm{Re}^b\,Sc^c$	Experimental Conditions
$Sh = 0.0791\,\mathrm{Re}^{0.7}\,Sc^{0.356}$	Ferricyanide-ferrocyanide on nickel electrode $10^3 \leq \mathrm{Re} \leq 10^5$
$Sh = 0.0964\,\mathrm{Re}^{0.7}\,Sc^{0.356}$	Ferricyanide-ferrocyanide on platinum electrode $10^3 \leq \mathrm{Re} \leq 2\mathrm{x}10^4$
$Sh = 0.0791\,\mathrm{Re}^{0.67}\,Sc^{0.356}$	Theoretical calculation with constant assumed to be 0.0791
$Sh = 0.0791\,\mathrm{Re}^{0.69}\,Sc^{0.41}$	Cathodic deposition of copper from copper sulfate $10^4 \leq \mathrm{Re} \leq 5\mathrm{x}10^5$
$Sh = 0.217\,\mathrm{Re}^{0.6}\,Sc^{0.333}$	Copper-copper sulfate deposition on copper electrode $10^3 \leq \mathrm{Re} \leq 1.9\mathrm{x}10^4$
$Sh = 0.127\,\mathrm{Re}^{0.66}\,Sc^{0.333}$	Copper-copper sulfate deposition on copper electrode $10^3 \leq \mathrm{Re} \leq 1.9\mathrm{x}10^4$
$Sh = 0.165\,\mathrm{Re}^{0.674}\,Sc^{0.333}$ $Sh = 0.144\,\mathrm{Re}^{0.654}\,Sc^{0.356}$	Oxygen reduction in sodium chloride on monel and sodium sulfate on steel $2\mathrm{x}10^3 \leq \mathrm{Re} \leq 1.2\mathrm{x}10^5$
$Sh = 0.0489\,\mathrm{Re}^{0.748}\,Sc^{0.356}$	Derived from curve-fit of Theodorsen and Regier over range $2\mathrm{x}10^2 \leq \mathrm{Re} \leq 4\mathrm{x}10^6$

Table B-2 Mass transfer Correlation cylinder in cross flow

$Sh = a\,\mathrm{Re}^b\,Sc^c$	Experimental Conditions
$Sh = 0.322\,\mathrm{Re}^{0.57}\,Sc^{0.333}$	Evaporation of water into gases [81] $1\mathrm{x}10^3 \leq \mathrm{Re} \leq 30\mathrm{x}10^{30}$
$Sh = 0.281\,\mathrm{Re}^{0.6}\,Sc^{0.333}$	Liquids [82] $1 \leq \mathrm{Re} \leq 4\mathrm{x}10^3$
$Sh = 0.16\,\mathrm{Re}^{0.67}$	Sublimation naphthalene in air [83] $4\mathrm{x}10^3 \leq \mathrm{Re} \leq 33\mathrm{x}10^3$
$Sh = 0.3\,\mathrm{Re}^{0.59}\,Sc^{0.333}$	Electrochemical reduction of ferric ions [84] $10 \leq \mathrm{Re} \leq 10^4$

Appendix C
Analysis of Variance

The ANOVA procedure is one of several procedures available in for analysis of variance. The ANOVA procedure is designed to handle balanced data .ANOVA help researchers to design an experiment properly and analyzed the data it produces in correctly way and using Matlab program to check the results.

There are two method of ANOVA were discussed in (3.11). In this section find the detailed calculation of ANOVA for two ways ANOVA and three ways ANOVA.

The two ways ANOVA calculation of the experiential data are obtained from Tables (4.11-4.13) as fellows:

	30	40	50
50	1.88	2.2	1.3
200	4.97	5.1	3.3
300	6.6	6.7	5.8
400	8.1	8	7.4

The detailed calculations are shown below:

No. of rows =4, No. of columns =3

N=total no. of observation=12

On completion of the 2-way ANOVA the results will look something like this

SUMMARY	Count	Sum
Row 1	3	5.38
Row 2	3	13.37
Row 3	3	19.1
Row 4	3	23.5
Column 1	4	21.55
Column 2	4	22
Column 3	4	17.8

The ANOVA tables are shown below

Source of Variation	SS	DF	MS	MSR	$F_{0.05}$	$F_{0.01}$
Columns (Temp.)	2.65875	2	1.329375	14.6053957	5.14	10.92
Rows(r.p.m)	61.26856	3	20.4228528	224.379009	4.76	9.78
Error	0.546117	6	0.09101944			
Total	64.47343	11				

And three ways ANOVA are from the experimental data from Tables (4.2-4.7):

		5000	8000	10000	12000
10	30	2.4964	2.9060	3.6657	4.2057
	40	2.21107	2.7448	3.5290	3.723
30	30	2.8768	3.4605	4.7091	5.3733
	40	2.5862	3.2155	4.3535	5.1969
50	30	3.2388	4.3956	4.8053	6.1016
	40	3.0201	3.9466	4.5786	5.3014

r= number of rows=3, c= number of columns=4, g= number of groups=2, n=1, N=24

T= $\sum x$ =92.4551, T^2=8547.945516

1.Among Column:

$$= \frac{\sum {T_C}^2}{nrg} - \frac{T^2}{N}$$

$$= \frac{(16.423)^2 + (20.669)^2 + (25.6412)^2 + (29.7219)^2}{1 \times 3 \times 2} - \frac{8547.945516}{24} = 16.799764$$

2. Among rows

$$= \frac{\sum {T_r}^2}{ncg} - \frac{T^2}{N}$$

$$= \frac{(25.3013)^2 + (31.7658)^2 + (35.388)^2}{1 \times 4 \times 2} - \frac{8547.945516}{24} = 6.5271462$$

3. Among Groups

$$= \frac{\sum Tg^2}{ncr} - \frac{T^2}{N}$$

$$= \frac{(48.0488)^2 + (44.4063)^2}{1 \times 4 \times 3} - \frac{8547.9455.16}{24} = 0.55282176$$

4. Column-Row Interaction

$$= \frac{\sum {T_{Cr}}^2}{ng} - \frac{T^2}{N} - SS_C - SS_r$$

$$= \frac{(47.071)^2 + (5.6508)^2 + (7.1947)^2 + (7.7477)^2 + (5.457)^2 + (6.676)^2 + (9.0626)^2 + (10.5702)^2 + (6.2589)^2}{1 \times 2}$$

$$+ \frac{(8.3422)^2 + (9.3839)^2 + (11.4030)^2}{1 \times 2} - \frac{8547.945516}{24} - 16.799764 - 6.5271469$$

$$= 0.985779545$$

5. Column-group Interaction

$$= \frac{\sum Tcg^2}{nr} - \frac{T^2}{N} - SS_C - SSg$$

$$= \frac{(8.606)^2 + (10.76.1)^2 + (13.1801)^2 + (15.5006)^2 + (7.817)^2 + (9.9069)^2 + (12.4611)^2 + (14.22.3)^2}{1 \times 2} - \frac{8547.945516}{24}$$

$$-16.799664 - 0.5528.1708 = 0.317516692$$

6. Row-Group Interaction

$$= \frac{\sum T_{rg}^2}{nc} - \frac{T^2}{N} - SS_r - SS_g$$

$$= \frac{(13.0938)^2 + (12.2075)^2 + (16.4137)^2 + (15.3521)^2 + (18.5413)^2 + (16.8467)^2}{1 \times 2} - \frac{8547.945516}{24}$$

$$-6.5271469 - 0.5528.2176 = 0.450021817$$

7. Column-Row-Group Interaction:

$$= \frac{\sum T_{crg}^2}{nc} - \frac{T^2}{N} - SS_c - SS_r - SS_g - SS_{cr} - SS_{cg} - SS_{rg}$$

$$= \frac{(2.4964)^2 + (2.906)^2 + (3.6657)^2 + (4.0257)^2 + (2.2107)^2 + (2.7448)^2 + (3.529)^2 + (3.723)^2}{1}$$

$$+ \frac{(2.8708)^2 + (3.4605)^2 + (4.7091)^2 + (5.3733)^2 + (2.5862)^2 + (3.2155)^2 + (4.3535)^2 + (5.1969)^2}{1}$$

$$+ \frac{(3.2388)^2 + (4.3956)^2 + (4.8053)^2 + (6.1016)^2 + (3.0201)^2 + (3.9466)^2 + (4.5786)^2 + (5.3014)^2}{1}$$

$$- \frac{8547.945516}{24} - 16.799764 - 6.5271462 - 0.55282176 - 0.985779545 - 0.317516692$$

$$- 0.450021817 = 0.0990534933$$

8. Total :

$$SS_{total} = \Sigma x^2 - \frac{T^2}{N}$$

$$= (2.4964)^2 + (2.906)^2 + (3.6657)^2 + (4.0257)^2 + (2.2107)^2 + (2.7448)^2 + (3.529)^2$$

$$+ (3.723)^2 + (2.8708)^2 + (3.4605)^2 + (4.7091)^2 + (5.3733)^2 + (2.5862)^2 + (3.2155)^2$$

$$+ (4.3535)^2 + (5.1969)^2 + (3.2388)^2 + (4.3956)^2 + (4.8053)^2 + (6.1016)^2 + (3.0201)^2$$

$$+ (3.9466)^2 + (4.5786)^2 + (5.3014)^2 - \frac{8547.945516}{24} = 25.04151955$$

9. Residual and errors:

$$SS_{residual} = SS_{total} - \text{all previous SS}$$

$$= 2.504151955 - [16.799764 + 6.5271462 + 0.55282176 + 0.98577954$$

$$+ 0.031751669 + 0.0451987 + 0.099053493] = \text{zero}$$

The ANOVA tables are shown below

Source of Variation	SS	DF	MS	MSR	$F_{0.05}$	$F_{0.01}$
Among Columns(Re)	16.799764	3	5.5999213	81.9555697	3.20	5.19
Among Rows(Q)	6.5271462	2	3.2635735	47.762893	3.59	6.11
Among Groups (Temp.)	0.55282176	1	0.55282176	8.0906302	4.45	8.4
Column-Row Interaction(Re*Q)	0.98577954	6				
Column-Group Interaction (Re*Temp.)	0.031751669	3				
Row-Group Interaction (Q*Temp.)	0.0451987	2				
Column-Row –Group Interaction (Re*Q*Temp.)	0.099053493	6				
Residual	1.161586889	17	0.06832864			

Cathodic Region
Isothermal Conditions

Table C-1 ANOVA for limiting current density in cylinder of a cross flow under isothermal conditions [40]

Source of Variation	SS	DF	MS	MSR	$F_{0.05}$	$F_{0.01}$
Columns (Temp.)	0.767687	2	0.383844	91.29334	5.14	10.92
Rows(Re)	3.700154	3	1.233385	293.3482	4.76	9.78
Error	0.025227	6	0.004205			
Total	4.493068	11				

Table C-2 ANOVA for limiting current density of a rotating cylinder under isothermal conditions [67]

Source of Variation	SS	DF	MS	MSR	$F_{0.05}$	$F_{0.01}$
Columns (Temp.)	2.317116667	2	1.158558333	8.0727959	5.14	10.92
Rows (r.p.m)	69.95616667	3	23.31872222	162.48408	4.76	9.78
Error	0.861083333	6	0.143513889			
Total	73.13436667	11				

Table C-**3** ANOVA for limiting current density of a rotating cylinder under isothermal conditions [41]

Source of Variation	SS	DF	MS	MSR	$F_{0.05}$	$F_{0.01}$
Columns (Temp.)	0.155819	2	0.0779093	54.324759	5.14	10.92
Rows(r.p.m)	0.120539	3	0.0401796	28.016502	4.76	9.78
Error	0.008605	6	0.0014341			
Total	0.284962	11				

Heat Transfer Conditions

Table C-4 ANOVA for limiting current density of a cylinder in cross flow cylinder under heat transfer conditions [40]

Source of Variation	Sum of Square	DF	MS	MSR	F_{0.05}	F_{0.01}
Among Columns(Re)	16.799764	3	5.5999213	81.9555697	3.20	5.19
Among Rows(Q)	6.5271462	2	3.2635735	47.762893	3.59	6.11
Among Groups (Temp.)	0.55282176	1	0.55282176	8.0906302	4.45	8.4
Column-Row Interaction(Re*Q)	0.98577954	6				
Column-Group Interaction (Re*Temp.)	0.031751669	3				
Row-Group Interaction (Q*Temp.)	0.0451987	2				
Column-Row –Group Interaction (Re*Q*Temp.)	0.099053493	6				
Residual	1.161586889	17	0.06832864			

Table C-5 ANOVA for limiting current density of a rotating cylinder under heat transfer conditions [68]

Source of Variation	SS	DF	MS	MSR	F_{0.05}	F_{0.01}
Columns (Temp.)	2.65875	2	1.329375	14.6053957	5.14	10.92
Rows(r.p.m)	61.26856	3	20.4228528	224.379009	4.76	9.78
Error	0.546117	6	0.09101944			
Total	64.47343	11				

Table C-6 ANOVA for limiting current density of a rotating cylinder under heat transfer conditions [41]

Source of Variation	SS	DF	MS	MSR	$F_{0.05}$	$F_{0.01}$
Among Columns(r.p.m)	0.0053816	3	0.00179	79.555	2.95	4.57
Among Rows(Q)	0.0031721	2	0.00159	70.6667	3.34	5.54
Among Groups (Temp.)	0.0026802	2	0.00134	59.5556	3.34	5.54
Column-Row Interaction(r.p.m*Q)	0.000213	6				
Column-Group Interaction (r.p.m*Temp.)	0.00011	6				
Row-Group Interaction (Q*Temp.)	0.0001221	4				
Column-Row –Group Interaction (r.p.m*Q*Temp)	0.00018	12				
Residual	0.0006251	28	0.00002			

Mass Transfer Coefficients
Isothermal Conditions

Table C-7 ANOVA for mass transfer coefficient of a cylinder in cross flow under isothermal conditions [40]

Source of Variation	SS	DF	MS	MSR	$F_{0.05}$	$F_{0.01}$
Columns (Temp.)	$2.44075*10^{-11}$	2	$1.22*10^{-11}$	32.60304	5.143249	10.92485
Rows(Re)	$5.61958*10^{-10}$	3	$1.87*10^{-10}$	500.4345	4.757055	9.779569
Error	$2.24588*10^{-12}$	6	$3.74*10^{-13}$			
Total	$5.88611*10^{-10}$	11				

Table C-8 ANOVA for mass transfer coefficient of a rotating cylinder under isothermal conditions [67]

Source of Variation	SS	DF	MS	MSR	$F_{0.05}$	$F_{0.01}$
Columns (Temp.)	$9.27938*10^{-8}$	2	$4.64*10^{-8}$	22.86808	5.14	10.92
Rows (r.p.m)	$1.084*10^{-06}$	3	$3.61*10^{-07}$	178.0944	4.76	9.78
Error	$1.21734*10^{-8}$	6	$2.03*10^{-09}$			
Total	$1.18897*10^{-06}$	11				

Table C-9 ANOVA for mass transfer coefficient of a rotating cylinder under isothermal conditions [41]

Source of Variation	SS	DF	MS	MSR	$F_{0.05}$	$F_{0.01}$
Columns (Temp.)	$1.61563*10^{-9}$	2	$8.07817*10^{-10}$	21.34109	5.14	10.92
Rows (r.p.m)	$2.78461*10^{-9}$	3	$9.28202*10^{-10}$	24.52144	4.76	9.78
Error	$2.27116*10^{-10}$	6	$3.78527*10^{-11}$			
Total	$4.62736*10^{-9}$	11				

Table C -10 ANOVA for mass transfer coefficient of a cylinder in cross flow under heat transfer conditions [40]

Source of Variation	SS	DF	MS	MSR	$F_{0.05}$	$F_{0.01}$
Among Columns(Re)	$3.45342*10^{-5}$	3	$1.15114*10^{-5}$	17.820237	3.20	5.19
Among Rows(Q)	$1.35196*10^{-5}$	2	$6.7598*10^{-6}$	10.464548	3.59	6.11
Among Groups (Temp.)	$1.24732*10^{-6}$	1	$1.24732*10^{-6}$	1.9309152	4.45	8.4
Column-Row Interaction(Re*Q)	$9.83639*10^{-6}$	6				
Column-Group Interaction (Re*Temp.)	$6.520898*10^{-7}$	3				
Row-Group Interaction(Q*Temp.)	$3.5464*10^{-7}$	2				
Column-Row-Group Interaction (Re*Q*Temp.)	$1.38429*10^{-7}$	12				
Residual	$10.98155*10^{-6}$	17	$6.4597*10^{-7}$			

Table C-11 ANOVA for mass transfer coefficient of a rotating cylinder under heat transfer conditions [68]

Source of Variation	SS	DF	MS	MSR	$F_{0.05}$	$F_{0.01}$
Columns (Temp.)	$1.3583*10^{-7}$	2	$6.79*10^{-8}$	3.70923684	5.14	10.92
Rows(r.p.m)	$1.3168*10^{-6}$	3	$4.39*10^{-7}$	23.9727517	4.76	9.78
Error	$1.09858*10^{-7}$	6	$1.83*10^{-8}$			
Total	$1.56249*10^{-6}$	11				

Table C-12 ANOVA for mass transfer coefficient of a rotating cylinder under heat transfer conditions [41]

Source of Variation	SS	DF	MS	MSR	$F_{0.05}$	$F_{0.01}$
Among Columns(Re)	$2.77707*10^{-5}$	3	$9.2569*10^{-6}$	13.967198	2.95	4.57
Among Rows(Q)	$9.45988*10^{-7}$	2	$4.7299*10^{-7}$	0.713667	3.34	5.45
Among Groups (Temp.)	$6.65183*10^{-6}$	2	$3.3259*10^{-6}$	5.0182721	3.34	5.45
Column-Row Interaction(Re*Q)	$1.96208*10^{-6}$	6				
Column-Group Interaction (Re*Temp.)	$1.40852*10^{-5}$	6				
Row-Group Interaction(Q*Temp.)	$8.5734*10^{-7}$	4				
Column-Row-Group Interaction (Re*Q*Temp.)	$1.65266*10^{-6}$	12				
Residual	$18.55728*10^{-6}$	28	$662.76*10^{-9}$			

Heat Transfer Coefficients:

Table C-13 ANOVA for heat transfer coefficient of a cylinder in cross flow under heat transfer conditions [40]

Source of Variation	SS	DF	MS	MSR	$F_{0.05}$	$F_{0.01}$
Among Columns(Re)	19284262.9	3	642807.6	5.7068148	3.20	5.19
Among Rows(Q)	27805588	2	13902794	123.42833	3.59	6.11
Among Groups (Temp.)	2633596.5	1	2633596.5	23.380943	4.45	8.40
Column-Row Interaction(Re*Q)	1355834.4	6				
Column-Group Interaction (Re*Temp.)	247651.8	3				
Row-Group Interaction(Q*Temp.)	267339.5	2				
Column-Row-Group Interaction (Re*Q*Temp.)	44030.4	6				
Residual	1914856.1	17	112638.59			

Table C-14 ANOVA for heat transfer coefficient of a rotating cylinder under heat transfer conditions [68]

Source of Variation	SS	DF	MS	MSR	$F_{0.05}$	$F_{0.01}$
Columns (Temp.)	639264.9	2	319632.4	23.14892	5.14	10.92
Rows(r.p.m)	602977.1	3	200992.4	14.55659	4.76	9.78
Error	82845.95	6	13807.66			
Total	1325088	11				

Table C-15 ANOVA for heat transfer coefficient of a rotating cylinder under heat transfer conditions [41]

Source of Variation	SS	DF	MS	MSR	$F_{0.05}$	$F_{0.01}$
Among Columns(Re)	48515	3	16171.7	5.4125261	2.95	4.57
Among Rows(Q)	23701.7	2	11850.9	3.9663922	3.34	5.45
Among Groups (Temp.)	658523.7	2	329261.9	110.20107	3.34	5.45
Column-Row Interaction(Re*Q)	1418.9	6				
Column-Group Interaction (Re*Temp.)	8470.3	6				
Row-Group Interaction(Q*Temp.)	69271.9	4				
Column-Row-Group Interaction (Re*Q*Temp.)	4498.1	12				
Residual	83659.2	28	2987.8286			

Interfacial Temperature:

Table C-16 ANOVA for interfacial temperature of a cylinder in cross flow under heat transfer conditions [40]

Source of Variation	SS	DF	MS	MSR	$F_{0.05}$	$F_{o.01}$
Among Columns(Re)	104.115	3	34.705	69.66407	3.20	5.19
Among Rows(Q)	147.646	2	73.823	148.18644	3.59	6.11
Among Groups (Temp.)	429.26	1	429.26	861.66253	4.45	8.40
Column-Row Interaction(Re*Q)	5.104	6				
Column-Group Interaction (Re*Temp.)	0.615	3				
Row-Group Interaction (Q*Temp.)	2.146	2				
Column-Row –Group Interaction (Re*Q*Temp.)	0.604	6				
Residual	8.469	17	0.4981764			

Table C-17 ANOVA for interfacial temperature of a rotating cylinder under heat transfer conditions [68]

Source of Variation	SS	DF	MS	MSR	$F_{0.05}$	$F_{0.01}$
Columns (Temp.)	326.0717	2	163.0358	417.7431	5.14	10.92
Rows (r.p.m)	106.5758	3	35.52528	91.02562	4.76	9.78
Error	2.341667	6	0.390278			
Total	434.9892	11				

Table C-18 ANOVA for interfacial temperature of a rotating cylinder under heat transfer conditions [41]

Source of Variation	SS	DF	MS	MSR	$F_{0.05}$	$F_{0.01}$
Among Columns(r.p.m)	187.03	3	62.344	6.8258	2.95	4.57
Among Rows(Q)	773.07	2	387.037	42.3752	3.34	5.45
Among Groups (Temp.)	815.48	2	407.742	44.6421	3.34	5.45
Column-Row Interaction(r.p.m*Q)	4.6	6				
Column-Group Interaction (r.p.m*Temp.)	1.3	6				
Row-Group Interaction (Q*Temp.)	242.57	4				
Column-Row-Group Interaction (r.p.m*Q*Temp.)	7.27	12				
Residual	255.74	28	9.13357			

Table C-19 The mean effect of variables and their interactions using two level responses under heat transfer conditions (limiting current density) [40]

	Response	Mean Effect	DF
1	2.4964		
H	3.2388	1.30152	1
T	2.2107	0.14963	1
HT	3.0201	0.14125	1
R	4.0257	2.04643	1
HR	6.1016	0.5256	1
TR	3.723	0.14963	1
HTR	5.3014	-0.14113	1
Total	30.1177		

Table C-20 The mean effect of variables and their interactions using two level responses under heat transfer conditions (limiting current density) [41]

	Response	Mean Effect	DF
1	0.325		
H	0.368	0.062	1
T	0.353	0.055	1
HT	0.459	0.0025	1
R	0.553	0.24	1
HR	0.629	-0.0125	1
TR	0.630	-0.0045	1
HRT	0.653	-0.029	1
Total	3.97		

Table C-21 The mean effect of variables and their interactions using two level responses under heat transfer conditions (mass transfer coefficients) [40]

	Response	Mean Effect	DF
1	$2.76*10^{-5}$		
H	$3.58*10^{-5}$	$0.27*10^{-5}$	1
T	$2.89*10^{-5}$	0	1
HT	$3.94*10^{-5}$	$2.45*10^{-5}$	1
R	$4.45*10^{-5}$		1
HR	$6.74*10^{-5}$	$0.62*10^{-5}$	1
TR	$4.86*10^{-5}$	$0.025*10^{-5}$	1
HRT	$6.92*10^{-5}$	$-0.115*10^{-5}$	1
Total	$3.614*10^{-5}$		

Table C-22 The mean effect of variables and their interactions using two level responses under heat transfer conditions (mass transfer coefficients) [41]

	Response	Mean Effect	DF
1	$2.627*10^{-5}$		
H	$3.125*10^{-5}$	$0.7005*10^{-5}$	1
T	$4.126*10^{-5}$	$2.4795*10^{-5}$	1
HT	$4.72*10^{-5}$	$-0.2885*10^{-5}$	1
R	$6.523*10^{-5}$	$5.3195*10^{-5}$	1
HR	$8.003*10^{-5}$	$0.1545*10^{-5}$	1
TR	$10.56*10^{-5}$	$0.9325*10^{-5}$	1
HRT	$10.79*10^{-5}$	$-0.3365*10^{-5}$	1
Total	$5.0474*10^{-5}$		

Table C-23 The mean effect of variables and their interactions using two level responses under heat transfer conditions (heat transfer coefficients) [40]

	Response	Mean Effect	DF
1	1250		
H	3125	2670.37	1
T	1428.57	711.04	1
HT	3846.15	205.09	1
R	2500	2101.46	1
HR	5555.56	524.08	1
TR	3333.33	261.18	1
HRT	6666.67	-66.2	1
Total	27705.28		

Table C-24 The mean effect of variables and their interactions using two level responses under heat transfer conditions (heat transfer coefficients) [41]

	Response	Mean Effect	DF
1	408.42		
H	400.07	65.665	1
T	590.11	292.515	1
HT	696.47	90.015	1
R	477.11	105.95	1
HR	436.34	16.45	1
TR	700	53.26	1
HRT	905	32.87	1
Total	4613.1		

Table C-25 The mean effect of variables and their interactions using two level responses under heat transfer conditions (interfacial temperature) [40]

	Response	Mean Effect	DF
1	38		
H	46	5.875	1
T	47	8.375	1
HT	53	-0.625	1
R	34	-5.125	1
HR	39	-1.125	1
TR	43	0.375	1
HRT	47.5	0.375	1
Total	347.5		

Table C-26 The mean effect of variables and their interactions using two level responses under heat transfer conditions (interfacial temperature) [41]

	Response	Mean Effect	DF
1	68		
H	84.59	11.19	1
T	86.3	12.91	1
HT	91.3	-7.455	1
R	59.1	-6.44	1
HR	79.8	0.395	1
TR	81.53	0.405	1
HRT	84	-1.66	1
Total	634.62		

Analysis of Variance:

A significant difference between treatments is suggested if the calculated F value exceeds the tabulated F value. But this significant differences between the treatments as a whole. There are two Tables below to show the F-distribution at 0.01 and 0.05 [61].

Table C.27 F-distribution at 0.01 [61]

df2\df1	1	2	3	4	5	6	7	8	9	10	11	12	13
3	34.12	30.82	29.46	28.71	28.24	27.91	27.67	27.49	27.35	27.23	27.13	27.05	26.98
4	21.20	18.00	16.69	15.98	15.52	15.21	14.98	14.80	14.66	14.55	14.45	14.37	14.31
5	16.26	13.27	12.06	11.39	10.97	10.67	10.46	10.29	10.16	10.05	9.96	9.89	9.82
6	13.75	10.92	9.78	9.15	8.75	8.47	8.26	8.10	7.98	7.87	7.79	7.72	7.66
7	12.25	9.55	8.45	7.85	7.46	7.19	6.99	6.84	6.72	6.62	6.54	6.47	6.41
8	11.26	8.65	7.59	7.01	6.63	6.37	6.18	6.03	5.91	5.81	5.73	5.67	5.61
9	10.56	8.02	6.99	6.42	6.06	5.80	5.61	5.47	5.35	5.26	5.18	5.11	5.05
10	10.04	7.56	6.55	5.99	5.64	5.39	5.20	5.06	4.94	4.85	4.77	4.71	4.65
11	9.65	7.21	6.22	5.67	5.32	5.07	4.89	4.74	4.63	4.54	4.46	4.40	4.34
12	9.33	6.93	5.95	5.41	5.06	4.82	4.64	4.50	4.39	4.30	4.22	4.16	4.10
13	9.07	6.70	5.74	5.21	4.86	4.62	4.44	4.30	4.19	4.10	4.02	3.96	3.91
14	8.86	6.51	5.56	5.04	4.70	4.46	4.28	4.14	4.03	3.94	3.86	3.80	3.75
15	8.68	6.36	5.42	4.89	4.56	4.32	4.14	4.00	3.89	3.80	3.73	3.67	3.61
16	8.53	6.23	5.29	4.77	4.44	4.20	4.03	3.89	3.78	3.69	3.62	3.55	3.50
17	8.40	6.11	5.19	4.67	4.34	4.10	3.93	3.79	3.68	3.59	3.52	3.46	3.40
18	8.29	6.01	5.09	4.58	4.25	4.01	3.84	3.71	3.60	3.51	3.43	3.37	3.32
19	8.19	5.93	5.01	4.50	4.17	3.94	3.77	3.63	3.52	3.43	3.36	3.30	3.24
20	8.10	5.85	4.94	4.43	4.10	3.87	3.70	3.56	3.46	3.37	3.29	3.23	3.18
22	7.95	5.72	4.82	4.31	3.99	3.76	3.59	3.45	3.35	3.26	3.18	3.12	3.07
24	7.82	5.61	4.72	4.22	3.90	3.67	3.50	3.36	3.26	3.17	3.09	3.03	2.98
26	7.72	5.53	4.64	4.14	3.82	3.59	3.42	3.29	3.18	3.09	3.02	2.96	2.90
28	7.64	5.45	4.57	4.07	3.75	3.53	3.36	3.23	3.12	3.03	2.96	2.90	2.84
30	7.56	5.39	4.51	4.02	3.70	3.47	3.30	3.17	3.07	2.98	2.91	2.84	2.79
35	7.42	5.27	4.40	3.91	3.59	3.37	3.20	3.07	2.96	2.88	2.80	2.74	2.69
40	7.31	5.18	4.31	3.83	3.51	3.29	3.12	2.99	2.89	2.80	2.73	2.66	2.61
45	7.23	5.11	4.25	3.77	3.45	3.23	3.07	2.94	2.83	2.74	2.67	2.61	2.55
50	7.17	5.06	4.20	3.72	3.41	3.19	3.02	2.89	2.79	2.70	2.63	2.56	2.51

Table C.28 F-distribution at 0.05 [61]

df2\df1	1	2	3	4	5	6	7	8	9	10	11	12	13
3	10.13	9.55	9.28	9.12	9.01	8.94	8.89	8.85	8.81	8.79	8.76	8.74	8.73
4	7.71	6.94	6.59	6.39	6.26	6.16	6.09	6.04	6.00	5.96	5.94	5.91	5.89
5	6.61	5.79	5.41	5.19	5.05	4.95	4.88	4.82	4.77	4.74	4.70	4.68	4.66
6	5.99	5.14	4.76	4.53	4.39	4.28	4.21	4.15	4.10	4.06	4.03	4.00	3.98
7	5.59	4.74	4.35	4.12	3.97	3.87	3.79	3.73	3.68	3.64	3.60	3.57	3.55
8	5.32	4.46	4.07	3.84	3.69	3.58	3.50	3.44	3.39	3.35	3.31	3.28	3.26
9	5.12	4.26	3.86	3.63	3.48	3.37	3.29	3.23	3.18	3.14	3.10	3.07	3.05
10	4.96	4.10	3.71	3.48	3.33	3.22	3.14	3.07	3.02	2.98	2.94	2.91	2.89
11	4.84	3.98	3.59	3.36	3.20	3.09	3.01	2.95	2.90	2.85	2.82	2.79	2.76
12	4.75	3.89	3.49	3.26	3.11	3.00	2.91	2.85	2.80	2.75	2.72	2.69	2.66
13	4.67	3.81	3.41	3.18	3.03	2.92	2.83	2.77	2.71	2.67	2.63	2.60	2.58
14	4.60	3.74	3.34	3.11	2.96	2.85	2.76	2.70	2.65	2.60	2.57	2.53	2.51
15	4.54	3.68	3.29	3.06	2.90	2.79	2.71	2.64	2.59	2.54	2.51	2.48	2.45
16	4.49	3.63	3.24	3.01	2.85	2.74	2.66	2.59	2.54	2.49	2.46	2.42	2.40
17	4.45	3.59	3.20	2.96	2.81	2.70	2.61	2.55	2.49	2.45	2.41	2.38	2.35
18	4.41	3.55	3.16	2.93	2.77	2.66	2.58	2.51	2.46	2.41	2.37	2.34	2.31
19	4.38	3.52	3.13	2.90	2.74	2.63	2.54	2.48	2.42	2.38	2.34	2.31	2.28
20	4.35	3.49	3.10	2.87	2.71	2.60	2.51	2.45	2.39	2.35	2.31	2.28	2.25
22	4.30	3.44	3.05	2.82	2.66	2.55	2.46	2.40	2.34	2.30	2.26	2.23	2.20
24	4.26	3.40	3.01	2.78	2.62	2.51	2.42	2.36	2.30	2.25	2.22	2.18	2.15
26	4.23	3.37	2.98	2.74	2.59	2.47	2.39	2.32	2.27	2.22	2.18	2.15	2.12
28	4.20	3.34	2.95	2.71	2.56	2.45	2.36	2.29	2.24	2.19	2.15	2.12	2.09
30	4.17	3.32	2.92	2.69	2.53	2.42	2.33	2.27	2.21	2.16	2.13	2.09	2.06
35	4.12	3.27	2.87	2.64	2.49	2.37	2.29	2.22	2.16	2.11	2.08	2.04	2.01
40	4.08	3.23	2.84	2.61	2.45	2.34	2.25	2.18	2.12	2.08	2.04	2.00	1.97
45	4.06	3.20	2.81	2.58	2.42	2.31	2.22	2.15	2.10	2.05	2.01	1.97	1.94
50	4.03	3.18	2.79	2.56	2.40	2.29	2.20	2.13	2.07	2.03	1.99	1.95	1.92

الخلاصـة

إنّ الهدفَ من العمل الحالي هو اَستعمالَ التحليلَ الاحصائي لِدراسَة تأثيراتِ عِدّة متغيّرات على تآكل المعادن تحت تاثير عوامل مختلفة عند ثبوت وانتقال الحرارةِ . ان هذه الدراسة نُفذتْ للكشف عن تأثير المتغيّراتِ الهايدروديناميكيةِ بالإضافة إلى درجةِ الحرارةً وجريان الحرارة على تآكلِ النحاس والحديد.

يوجد ـ إثنان من الاشكال الهندسية المستخدمة وهي : الإسطوانة في التدفق المتقاطع ونظامِ الإسطوانةِ الدائري عندِدرجات حرارة مختلفة ، وعدد رينولدز وجريان الحرارة.التحليلَ الاحصائي المستخدمُ يَتضمّنُ المقارنةً بين عِدّة متغيرات مختلفة أو تأثير إثنان أو ثلاثة عوامل في نفس الوقت.

ان البياناتُ التي تم الحصول عليها مِنْ التقنياتِ الكهروكيميائيةِ المختلفةِ قد حُللتْ لتعيين تاثير عددِ رينولدز، درجة الحرارةً و جريانَ الحرارة على المنطقةِ الكاثودية . إنّ التحليل يتضمن كثافة التيار المحددَ، معامل انتقال الكتلة و الحرارةِ، ودرجة حرارة المحلول.

وقد وُجِدَ ان كثافة التيارَ المُحدّد لصلب الكاربون تُتأثرُ بالسرعة أكثر مِنْ درجة الحرارة و بالتالي يؤثر ذلك على انتشارجزيئات الأوكسجين بينما على القطب الموجب للنحاس تتأثرُ بدرجةِ الحرارة أكثر مِنْ السرعة عند ثبوت الحرارة. وقد تبين أيضا بأنّ كثافةِ التيار المُحدّد لصلبا الكاربون والنحاس تحت شروطِ انتقال الحرارةِ تُتأثرُ بالسرعةِ يليها جريان الحرارةِ وبعد ذلك درجة حرارة عند المستويات المختلفة 0.01 و0.05.

إنّ معاملَ انتقال الكتلة يعتمد بالاساسُ على السرعة، لأنه يَزدادُ عند زيادة عدد رينولدز أو (rpm) تحـت ثبـوت الحـرارة.حيـث أن النحـاس فـي القطـبِ الموجـب يتـأثر بالتسـاوي بالهدروديناميكية ودرجةِ الحرارة. ولوحظ أن معامل انتقال الكتلةِ تحت شروط انتقال الحرارةِ تتأثر ايضا بالسرعة اكثر من المتغيرات الاخرى .

انّ معامل انتقال الحرارةَ يَتأثرُ بدرجةِ حرارة السطحِ يليها جريان الحرارةِ وبعد ذلك عدد رينولدز (rpm) ؛ حيث انه يزداد بزيادة درجة الحرارة .و عليه فان درجة حرارة المحلول تتأثرُ أساساً بدرجةِ حرارة السطح أكثر مِنْ المتغيّرات الأخرى كجريان الحرارةِ والسرعةِ حيث ان هذه التأثيراتِ هي من قبل التحليل الاحصائي.

تحت ثبوت درجة الحرارة،فان سُمك الطبقةِ الهايدروديناميكيةِ يَنْقصُ مع زيادة عدد رينولدز او (rpm) و أيضاً يَنْقصُ بزيَادَة درجةِ الحرارةِ عند ثبوت عدد رينولدزاو (rpm).ان سمك

طبقة الانتشار يَنْقصُ بزيادة عدد رينولدز او (rpm) عند درجةِ الحرارة الثابتةِ. ومن الناحية الأخرى يَزدادِ بزيَادَة درجةِ الحرارة عند ثبوت عدد رينولدز أو (rpm). ان النسبة ما بين الهايدروديناميكيةِ و سمك طبقة الحرارة لا تتاثربعدد رينولدز أو (rpm) وانما تقل بزيَادَة درجةِ الحرارة. تحت شروطِ انتقال الحرارة، فان الهايدروديناميكية وسمك طبقة الحرارة يقل بزيادةُ درجةالحرارة عند ثبوت عدد رينولدز أو(rpm) وأيضاً يقل بزيادة عدد رينولدز أو(rpm) عند درجةِ الحرارة الثابتةِ. سمك طبقةُ الإنتشاريزداد بزيَادَة درجةِ الحرارة عند ثبوت عدد رينولدز أو (rpm) و يَنْقصُ مَع زيَادَة عدد رينولدز او (rpm) عند درجةِ الحرارة الثابتةِ.ان نسبة سمك طبقةِ الحرارة الى سمك طبقةِّ الإنتشارتكون أعلى مِنْ واحد والتي يُتبين بأنّ سمك طبقةِ الحرارةِ تكونُ دائماً اكبر مِنْ سمك طبقةِ الإنتشار.

ان سمك طبقةِ الإنتشارَيمكن ان تقدر على انها أصغر مِنْ سمك الطبقةِ الهايدروديناميكيةِ،مما يؤدي إلى اهمـال الانتقال الحراري ضـمن طبقةِ الإنتشارَ.و هذا يَعْني أنّ الجزء الرئيسي من الطبقةِ الهايدروديناميكيةِ توثر على حركة السائل ومعدل التركيزَالتي من المحتمل ان توثر على سمك الطبقةِ الحراريةِ والتي بدورها توثر على سمك طبقةِ الإنتشار ونسَبِ التآكل الأعلى.

شكر وتقدير

دراسه تحليل متغيرات التاكل تحت تاثير الحرارة

رسالة

مقدمة الى كلية الهندسة في جامعة النهرين

وهي جزء من متطلبات نيل درجة ماجستير علوم

في الهندسة الكيمياوية

من قبل

لينا نائل سليم

(بكالوريوس علوم في الهندسة الكيمياوية ٢٠٠٥)

محرم ١٤٣٠

كانون الثاني ٢٠٠٩